Financial System Stability

Inaugural-Dissertation
zur Erlangung des akademischen Grades eines Doktors
der Wirtschafts- und Sozialwissenschaften
der Wirtschafts- und Sozialwissenschaftlichen Fakultät
der Christian-Albrechts-Universität zu Kiel

vorgelegt von
M.A., Christian Freund
aus Stuttgart

Kiel, Mai 2017

Gedruckt mit Genehmigung der
Wirtschafts- und Sozialwissenschaftlichen Fakultät
der Christian-Albrechts-Universität zu Kiel

Dekan: Prof. Dr. Till Requate
Erstbegutachtung: Prof. Dr. Thomas Lux
Zweitbegutachtung: Prof. Dr. Stefan Reitz

Tag der Abgabe der Arbeit: 11. Mai 2017
Tag der mündlichen Prüfung: 21. Juni 2017

Table of contents

List of figures

List of tables

Chapter 1

Introduction

1.1 A short note on methodology in economics

Many economists and historians consider the eighteenth century writings of David Humes, Adam Smith and others as the beginning of economics. In their work the idea gains hold that individual actions and interactions might yield systematic outcomes even without the imposition of processes and goals by governments or administrations. This represents a very early concept of self-organization in economics, that is, the emergence of regularities from a bottom-up perspective instead of a top-down imposition. This interaction-based approach stayed the focus of economics until the discipline responded to the Great Depression in the 1930s by evolving into two increasingly distinct branches, micro- and macroeconomics. The latter aimed exclusively at analyzing the dynamics and relations of aggregate economic quantities while the former continued to extend the formalistic framework of interactions of a very limited number of agents. As the gap between these two disciplines widened, unease among economists grew. How were micro and macro related, the individual and the aggregate, the agent and the economy? The answer that dominates economics to this day emerged after World War II. Economists such as Arrow, Debreu and von Neumann formalized the idea that rational, fully informed agents who participate in a free exchange can indeed arrive at a Pareto-efficient equilibrium. And it did not take long for these newly developed tools to be exploited for the reconciliation of micro- and macroeconomics. The solution came in the form of the representative agent. Some economist such as Robert E. Lucas even went as far as postulating that the distinction between micro- and macroeconomics should be abolished since all economics was essentially based on the preferences and decisions of the individual

(Hausman 1994). The most widely used models of economic and financial systems have been based on representative agents ever since.

A second way to look back at this early history of economics is to examine it against the background of larger scientific and educational[1] trends that took place alongside developments in economic theory. Mirowski (1991), Weintraub (2002) and many others point out that at the time when the foundations were laid for modern economics in the eighteenth century, economists looked up to mathematics and physics as prime examples of a "hard science." Caldwell (1993) states: "There are a number of reasons why methodology took this path. Most fundamentally, economics like many of the other social sciences was very eager to establish its scientific credentials." In particular, the Newtonian paradigm which at the time not only seemed to be universally applicable to problems involving force and motion but also was seen as the constituting physical framework of the universe, was considered by many economists as the archetype of an ideal science. The struggle and frustration of early failures to obtain a similarly well structured foundation of economics is described in Mirowski (1991). The author states that is was only with the influx of scientists ranging from Jevons to Walras, specifically educated in physics, that the efforts bore fruit. These early economists transfered the concept of equilibrium from physics to economics and "[...]copied the physical mathematics literally *term for term* and dubbed the result mathematical economics" (Mirowski (1991), italics in the original).

Before I entered my undergraduate studies in economics, I had spent some years pursuing a degree in engineering. Unbeknown to me at the time, this put me in the privileged position to notice these striking parallels myself very early on. I still remember the day in my first year when I was introduced to the two fundamental theorems of welfare economics. I was

[1] As in every science, the education of scientists formed their future research. A great account of the impact of university education on early economics is given by Weintraub (2002). In Cambridge, the cradle of many fundamental discoveries and theories during the early years of economics, graduates had to pass a tedious series of exams in applied mathematics and physics called *Tripos* that covered differential equations, optics, conic sections and other fields. Passing these exams required the fast and error-free applications of a standard set of mathematical tools to problems that were so far abstracted from reality as to be completely meaningless. Examples can be found in Weintraub (2002). I took the liberty and showed a few of the example questions along with characterizations of the *Tripos* institution to some Master students and PhD candidates in economics. Without exception, they all noted the similarity to modern day exams in macroeconomics. Following the path of various eminent economists from the days of their university education throughout their research career, Weintraub (2002) goes as far to state "The cause of the backwardness of English mathematics was the backward-looking Tripos examination."

struck by it. The arguments and the presentation[2] were nearly identical to the exposition of the first two fundamental theorems of thermodynamics, which I had been taught less than a year ago![3] As my education in economics progressed, the mechanical, physics-inspired nature of many economic models became more and more evident. At the same time though, doubts arose as to whether this "modeling by analogy" was justified and could be reconciled with everyday observations. In order to shed light on this question, let us first take a look at a concrete example of how physics arrived at consistent microfoundations. The example I present here is adapted from Hausman (1994). In a slightly varied form, it can also be found in Hofstadter (1980). I chose this particular one because it is closely related to that first analogy between economics and physics that I noted in my undergraduate days.

One of the elementary natural laws in thermodynamics links the main features of an ideal gas. In particular, the relation between pressure p, volume V and temperature T of an ideal gas is given by

$$pV = nRT$$

where n is the number of moles, and R is a universal constant. While this law, formulated in the eighteenth century, was confirmed experimentally time and again, physicists were unsatisfied with the lack of an explanation rooted in the known laws of physics, in particular Newtonian mechanics. In other words, they looked for plausible *microfoundations* of the law. And they succeeded. Under some not too strict simplifying assumptions, the above law was derived from two ingredients. The first were the well-known Newtonian mechanisms governing the movement of individual gas particles. The second one was the assumption that the distribution over the directions of movements of the gas particles is uniform, i.e. each direction of movement has the same probability. From this model, temperature emerges as the average energy of the gas particles, and pressure emerges as the average momentum that is transferred by gas particles bumping into the walls of the containing vessel. Two points

[2] The rhetorics of economics should not be underestimated, McCloskey (1998).

[3] This is not without a certain irony. Despite the superficial similarity, the two are in a way diametrically opposed. The main message of the fundamental theorems in welfare economics states reassures first year students that everything will be fine since market efficiency and thus order can be considered the default outcome. In contrast, the second fundamental theorem in thermodynamics results in $dS/dt \geq 0$, that is, bare the injection of energy, the entropy S will never decrease in a system. To put it in sloppy terms, the natural way of things is to go from order to disorder.

about this derivation are worth mentioning. First, it is not completely microfounded since the distribution of directions only exists on the macro level; a single particle moves only into one particular direction. Second, temperature and pressure are themselves emergent properties. An individual particle can be ascribed neither of those. That is, the aggregate develops qualitatively new properties which are nevertheless rooted in the properties of the individual constituents.

To sum up, it is the combination of detailed information on mechanisms on the microscopic level, together with statistical assumptions that are relevant for the interaction of entities on the micro-level, that give rise to emergent regularities on the macroscopic level. In the words of Hausman (1994): "Yet, it also underscores the connection between the micro and the macro: no macro state exists unless an appropriate micro state exists."

It is clear that the most general form of microfoundation in economics, the individual agent, does not follow this equation. Here, instead of explicitly taking into account the large number of agents interacting, they are simply assumed away and replaced with one example of an agent. Hausman (1989) states: "The claim that representative-agent models provide micro-foundations succeeds only when we steadfastly avoid the fact that representative-agent models are just as aggregative as old-fashioned Keynesian macroeconometric models. They do not solve the problem of aggregation; rather they assume that it can be ignored." It is as if physicists tried to model the behavior of gas with a representative molecule.

While the majority of models in macro- and financial economics still embraces the representative agent, a growing number of economists voices concerns over this approach. Kirman (1992) reviews the pitfalls, shortcomings and inconsistencies of the representative agent. First of all, usually no trade takes place in representative agent models. This notion provides the most striking contrast to the complex world of business and finance with its continuous interactions that surrounds us on a daily basis. Second, any distributional aspects are excluded a priori in representative agent models. This point, in my view, has become even more important in recent years due to the perceived and factual widening in the income and wealth distributions, especially in many developed nations. On a more technical note, Kirman (1992) continues, it is far from clear whether the actions of the representative agent are equivalent to the aggregate actions of many agents in each state of the world. Finally, imposing the sometimes complex aggregate behavior of a collective of entities may yield highly implausible behavior for the representative agent. Kirman (1992) also points out

that the long cherished property of most representative agent models, that of unique stable equilibria, disappears in many agent-based models.

Given these criticisms, it is quite surprising to still see that the majority of macroeconomic models embraces the representative agent. Rather cynically, Caldwell (1993) points out that "[...] many economists are indifferent to economic methodology, and most of the rest are openly hostile to it." More differentiated, Hausman (1989) discusses the various approaches that can be taken to evaluating economic research. From an eclectic perspective, put forward among others by McCloskey (1998), the quality of economic research is primarily determined by its acceptance by other economists. This viewpoint is certainly mirrored in the incentive system of academic economics and may thus provide a reasonable explanation of the current landscape in macroeconomic modeling.

However, a few economists have followed the tradition of transferring models, methods and formalisms from other sciences into economics. A simple example of such a transfer from physics is the Ising model. It provides a mathematical description of a system of many particles that interact locally with their neighbors on a fixed structure such as a lattice. The model has proven useful in various fields, from quantum physics to the analysis of crystallization processes and in recent years also as a test bed for random number generators (Coddington 1996). In economics, adaptations have been developed with varying success[4] in order to account for phenomena such as financial market crashes. The particles in the original model gain interpretation as market participants, and the bonds between particles represent the extent to which the participants influence each other's opinion or sentiment. When agents synchronize their behavior due to increasing interaction strength past a critical threshold, the market is increasingly susceptible to sudden changes of sentiment sweeping through the model. This may then result in sudden, drastic price movements, or crashes. While the model consists of many interacting agents, analytical results for the model behavior can be obtained, and the emergent properties can be estimated from data (Sornette et al. 1996; 2001).

Biology has been another source of inspiration for those looking to overcome the inadequacy of the standard micro-macro link in economics. In particular models of swarm formation such as those of Ballerini et al. (2008) and Hemelrijk and Hildenbrandt (2011) can be seen as examples demonstrating that individual agents with simple heuristics are often

[4]Chang and Feigenbaum (2006), Brée et al. (2013)

sufficient to generate complex aggregate behavior. Both papers contribute to the literature of modeling the dynamics of flocks of birds from the ground up. That is, simple rules for bird behavior give rise to realistic dynamics of complete flocks. These simple rules are grounded in the local orientation of the birds, such as the position relative to its nearest neighbors and its velocity and orientation relative to those neighbors. Ballerini et al. (2008) present the results of detailed measurement of actual bird behavior in large flocks and contribute thus to a more accurate microfoundation of these models. This demonstrates the need for high-quality microlevel data on agent behavior in most agent-based models. Hemelrijk and Hildenbrandt (2011) extend the models to incorporate more realistic environmental conditions such as specific movements arising from aerodynamic constraints, and flocking over specific points on the ground. This highlights the need not only for data on agent behavior, but also for a detailed knowledge of the environment in which the agents operate. In both papers the models are no longer tractable, but can easily be analyzed computationally and visually.

Baianu (1986) provide a detailed review of the limits of computational models and automata for biological models. The authors discuss the core questions of this approach such as the simplest structures possible needed for biological organisms, and the network structures of neural and genetic networks. In particular their discussion of fundamental differences between biological organisms and automatons and its implications on modeling are highly recommended for any agent-based modeler.

Finally, also in the social sciences, the bottom up approach has received increased interest in the past years. Traffic jams have been analyzed and simulated with the help of cellular automata, for example by Nagel and Schreckenberg (1992). Their work underlies the assumption that all drivers exhibit small imperfections in their behavior, such as tiny delays in adjusting the speed due to a change in the distance to the leading car. This is sufficient to generate traffic jams without an obvious obstacle on the road. Instead, jams spontaneously emerge once the vehicle density on the road exceeds a critical threshold. This work highlights how small imperfections on the agent level that one might be tempted to abstract from can give rise to sizable effects on the aggregate. Another illustrative example is provided by Helbing et al. (2000) who analyze human movement patterns in crowds in order to analyze past and prevent future mass panics. The strand of the literature they represent constructs models of human behavior in broad analogy to the models of bird flocks discussed above.

The approach has since been used to inform planning decisions at large events as well as architectural design processes.

The inadequacy of the representative agent approach and the potential of transfer from other disciplines have both received increasing support in the wake of the Global Financial Crisis that started to unravel in 2007. The self-praise of macroeconomists after years of celebrating the Great Moderation turned into defensive arguments against the attacks launched from the general public, politicians and monarchs as to why nobody had seen the crisis coming. At the same time, funding for and interest in alternative approaches increased. In the context of the crisis, in particular the stability of the financial system and the connection between financial system health and economic growth received increased attention. Most definitions of systemic risk entail the notion that one institution failing may drag others with it. Yet this part-endangers-whole situation is exactly what cannot be described if the system is described by a single representative agent. Moreover, the notion of financial contagion also required the analysis of the topology of the interactions between economic entities. Mapping the paths between institutions and providing meaningful statistical summaries of those topologies required the adaptation of network theory to economics. As a consequence, agent-based modeling and network theory both have gained more and more popularity in economics.

Agent-based modeling, i.e. the construction of economic or financial systems from the bottom up, can roughly be divided into two approaches. In what I deem *numerical* agent-based modeling, the proportions of a finite number of different strategies or agent types in an otherwise homogeneous population evolve endogenously based on a fitness function such as the past success of each strategy. An overview in the context of financial markets can be found in Hommes (2006). These models do not represent each individual agent individuals explicitly. Instead, they model the evolution of the proportions in the population that follow distinct strategies. In contrast, *computational* agent-based models employ modern programming techniques and paradigms in order to represent each agent in the system explicitly. System-level results are obtained by simply letting the agents interact and then collecting the aggregate statistics, for example by summing up, in close analogy to how aggregate statistics such as GDP or unemployment are obtained in the real world. A recent example of a full-scale model of the U.S. private sector can be found in Axtell (2016).

It should be noted that agent-based modeling has proven helpful in explaining economic phenomena also outside macro- and financial economics. A prominent example can be found in Axelrod (1981). The authors evaluated a wide range of strategies for the well-known prisoner's dilemma in the context of a tournament. Among other results, their research showed that cooperative strategies result on average in higher scores than non-cooperative strategies. This stands in stark contrast to the results taught in most microeconomics courses that base the result of non-cooperation on the backward induction of rational agents. Their research is one of the cornerstones of today's literature of evolutionary game theory. It is particular interesting in the light of the recent surge of of behavioral economics. While the picture of human-decision making gets more detailed and richer with every new experimental study, the above examples show that the aggregate impact of many of these imperfections[5] may not easily be deduced from agent-level results.

Network theory in its simplest form amounts to a statistical summary of the – mostly pairwise – connections between nodes. In our case, these can be economic agents such as countries, banks, firms or households. However, also individual securities or portfolios of securities lend themselves to this representation. These pairwise connections may take various forms. On the country level, the most prominent application is the analysis of the world trade web as discussed by Squartini et al. (2011a) and Squartini et al. (2011b). In this case, the links amount to trade relations between countries, and the weight indicates the trade volume. Between banks and firms, the links may represent credits granted by banks, for example in the work by Boss et al. (2004). Between firms, they may represent production chains (Lu and Wang 2008). In the case of securities as nodes, the links may have a less tangible interpretation such as the correlation between prices. Similarly in the case of security portfolios, the links may indicate the extent to which two portfolios overlap. The contribution of network theory in its simplest form can best be explained by comparing it to conventional statistics. These statistics, such as, for example, the mean of a variable over a population, allow us to condense in a meaningful way information that is dispersed over the sample. In contrast to this summary of *entity attributes*, network theory thus explicitly summarizes the *relations between entities* and thus allows to quantify, summarize and analyze interactions between a large number of agents.

[5] Imperfections here is to be interpreted as deviations from the standard model of rational decision making.

While both agent-based models and network theory have appeared in economics independent from each other, increasingly research makes use of both techniques simultaneously due to their complementary nature. In computational agent-based models, one of the unresolved challenges so far is the at times large number of degrees of freedom in the algorithm design and the choice of parameters. In order to evaluate the model performance, the resulting aggregate and agent-level statistics are often compared to their empirical counterparts. Here, network theory can add value by providing a possibility to evaluate the model performance also on the meso level. That is, it enables the modeler to judge as to whether the structure of interactions in the model resembles the structure of interactions in reality, and to use this information to calibrate or even estimate the model accordingly. These insights can in turn inform the design of agents' strategies for choosing interaction partners in future iterations of model development. In the narrow sense used so far, network theory is rather static. Here, agent-based modeling can add value by providing richer node behavior. This is in particular relevant in the social sciences such as economics. As a consequence, agent-based modeling can bring otherwise static models of economic topologies to life, or increase the space of possible temporal evolutions of simple dynamic network models.

1.2 Overview

The methodological considerations discussed above have given rise to this thesis. My contributions are all applications of network theory or agent-based modeling or both to problems in macroeconomics and financial economics. The focus on financial stability was due to the fact that when this thesis was started, the economic discipline (and economies around the world) were still digesting the impact of the Global Financial Crisis. Unless explicitly mentioned, the contributions presented herein have all been developed by myself.

1.2.1 Stability of Core-Periphery Interbank Networks

In chapter 2 we explore the stability of core-periphery interbank networks in a static simulation framework. The overnight interbank market virtually disappeared overnight at the height of the financial crisis in 2007/8. This provoked a surge in interest in the nature and the functioning of these markets. On the empirical side, a number of papers found that these

markets are organized around a small number of banks, the "core", who redistribute liquidity in the system. We combine this class of networks with a simple simulation framework from the literature. It is classified as static because banks cannot adapt their behavior to the market situation by opening new credit lines or other measures. Consequently, the topology of the network is fixed a priori and does not evolve endogenously. Instead, our simulation takes the network structure and thus the bilateral credit exposures as given and then evolves the system in a mechanical way after an initial default of one or several banks. Our work contributes to the literature in two ways. First, we extend the analysis from an existing model that employs primarily random networks to a more realistic network topology that is more in line with empirical findings. On the way, we also examine the implications of the simulation set-up itself on the simulation outcome. The results exhibit similarities between our model and the random network baseline, and new aspects that are due to the core-periphery structure. The dependence of system stability as measured as the number of default banks on the amount of interbank credit in the system is comparable in the two cases. Both for random and core-periphery networks, the number of defaults is low for small and large amounts of interbank assets in the system. For medium values, the number of defaults rises. In the specific case of core-periphery networks, we show that the extremely low connectivity in the periphery is a strong contributor to instability. This has no equivalent in the random network case since there the connectivity is the same across the whole system. We also demonstrate that the difference between core and periphery banks in our model is only partially due to the parameterization. Additionally, the particular algorithm that initializes the simulation contributes to the heterogeneity by allocating assets disproportionately to core banks. This insight demonstrates the sensitivity of outcomes in agent-based models to even subtle aspects of model design.

In a second step, we compare the results of the full-scale simulation to an analytical approximation. This mean-field approach has been successfully demonstrated in the case of random networks in the literature. It works by modeling the average bank and calculating its average transactions with its neighbors. When we adapt the method to account for core-periphery networks, we find that it provides good approximations to the full-scale dynamics right after the initial default. However, as the simulation unfolds over time, the results of the approximation differ more and more from the simulation results. This serves as tentative

evidence that mean-field approximation is less useful for heterogeneous networks such as the ones that we employ.

1.2.2 Bipartite Clustering in Bank-Firm Networks

Chapter 3 contributes to the empirical literature on real-world economic and financial networks. We explore the topology of the Spanish bank-firm credit network over the years 1999-2007. This network has two distinct sets of nodes, banks and firms. Links in the network always connect nodes of the two sets, never two nodes that belong to the same set. These types of networks are called bipartite. As mentioned above, statistical descriptions of empirical networks can, among other things help in the calibration of agent-based macroeconomic models in the future. In particular we analyze the bipartite clustering between banks and firms with several different statistics. Under bipartite clustering we subsume all network statistics that are a function of the degree[6] distributions of both, banks and firms. The paper has two intertwined goals. First, we aim at describing the internal linking structure between banks and firms. In particular we ask whether the bipartite clustering coefficients that we calculate from the empirical data are random or whether they exhibit significant deviations from randomness. For this purpose, we compare them with bipartite clustering coefficients that we obtain from random variations of the empirical networks. These random variations are generated by keeping all the nodes and their degrees in the original network, but randomly connecting them. Our comparison finds strong evidence that the bipartite clustering in the empirical data cannot be explained solely by the degree distributions of banks and firms, but that it is a particular feature of the data. Our calculations also indicate slight temporal trends in bipartite clustering over time.

Second, we compare the performance of a range of measures that have been developed to capture bipartite clustering. Here, the picture that emerges is mixed. While some measures succeed at identifying the non-randomness of bipartite clustering in the data, other measures fail to detect this difference. Similarly, the temporal trend can be found in some statistics but not in others.

[6]The degree of a node is the number of links that start or end at this node. Precise definitions are provided in the chapter itself.

1.2.3 Interactions of Macroprudential and Monetary Policy in Housing Markets

In chapter 4, we explore the interaction of monetary and macroprudential policy in a simple agent-based model of the housing market. Housing booms and busts are an integral part of the economic history of almost all developed nations. Due to financial innovations such as securitization, housing credit has permeated even more through the financial system in the run-up to the 2007 crisis in the U.S., increasing its importance for financial stability even further. Regulatory agencies have responded to this development by crafting policies aimed in particular at stabilizing the housing market, both in the boom and the bust period. These measures are part of the recent evolution of so-called macroprudential regulation. Among the most popular policy measures are caps on loan-to-value (LTV) ratios and caps on debt-service-to-income (DSTI) ratios. In our model, we examine the combined effects of these measures and monetary policy on the housing market. We show that the impact of monetary policy on housing market dynamics is smaller than the impact of macroprudential regulation, thus reinforcing the call for macroprudential regulation. While both maximum LTV ratios and maximum DSTI ratios are shown to have a significant impact on the market outcome, the impact of these measures are strongly interdependent. Moreover, their performance also depends on the state of monetary policy, that is, the interest rate. The main message from our model is that the effectiveness of individual macroprudential policy measures must not be evaluated in isolation, but against the full background of monetary policy and other macroprudential regulations in place.

Chapter 2

Stability of Core-Periphery Interbank Networks

2.1 Introduction

Interbank markets allow banks to share liquidity risk. Similar to standard models of insurance, they allow banks to trade the concrete yet a priori unknown realization of a liquidity shock against the expected value over the whole system. Their importance has been highlighted by the interbank market freeze in 2008, which lead to unprecedented liquidity injections by central banks. In the aftermath of the crisis, interbank market structure has come under increased scrutiny by researchers and policy makers alike. One important strand of research aims at describing real world interbank markets from a network perspective. Representing interbank markets as complex networks allows for the use of established tools and statistics from network theory in order to quantify key characteristics of the topology of real-world interbank markets. The use of network theory in financial economics is not restricted to interbank markets. Overviews can be found in Allen and Babus (2008), Jackson et al. (2008) and Galati and Moessner (2013).

At the same time, research has started to examine the link between interbank market structure and systemic risk. Systemic risk is here defined as the risk that a shock to an individual institution propagates through the banking system, leading to an amplification of the initial losses. In many cases, this question of shock propagation does not lend itself to an analytical answer. This stands in contrast to other areas of applied network theory such as epidemiology, where analytical results of dynamic processes on networks can sometimes be

obtained (Allen et al. 2008). One of the reasons is that interbank networks exhibit nontrivial shock transmission behavior and heterogeneous nodes. As an example, in the susceptible-infected-recovered (SIR) model in epidemiology, agents cant take only one of these three states. If the agent is susceptible and the infection reaches him from one of his neighbors, he becomes infected. If he is already infected, the renewed infection has no effects. If he is recovered, depending on the model specification, he may be either immune to renewed infection, or he may be susceptible again.

In comparison, the question of whether a bank goes default, or "gets infected" due to a loss, is less trivial to answer. In other words, the transition between the agent states is not as straightforward as in the above example. Some banks may be resilient to defaults of one or several of their debtors. This can be due to those debtors only making up a small part of the loan portfolio, and to sufficiently large capital buffers to accommodate the shock. For other banks, the defaults of these very same debtors may pose an existential risk due to a higher portfolio concentration or lower capital buffers. As a consequence of this added complexity, full-scale simulations of interbank networks are often used in order to analyze systemic stability.

This paper adds to the literature by examining the stability of core-periphery interbank networks. These networks are characterized by a small number of densely connected core banks, and a large number of sparsely connected periphery banks. Originally developed for the analysis of social networks, the concept has successfully been applied to financial networks in recent years. Models of core-periphery networks have been shown to provide a very good description for a variety of interbank market topologies. The most common interpretation is to see core banks as money center banks, redistributing liquidity in the banking system. Compared to periphery banks, their health is disproportionally essential for the unimpaired flow of liquidity through the banking system. This may give rise to moral hazard since regulators and policy makers might be inclined to bail out core banks that come under distress.

In a second step, I compare the results of the numerical simulations with an analytical approximation. This mean-field approach allows to derive approximate results by treating all core banks and all periphery banks as identical. This reduces not only the computational costs of making statements about the resilience of a given interbank market. Additionally, it

enables us to gain further analytical insights into the behavior of the system, and to determine the key drivers of systemic stability.

The paper is structured as follows. Section 2.2 reviews the literature. In section 2.3 we introduce the network terminology and the core-periphery model. Section 2.4 describes the simulation set-up and the simulation routine. Section 2.5 presents the simulation results. Section 2.6 presents the mean-field approach, and section 2.7 concludes.

2.2 Literature Review

Allen and Gale (2000) and Freixas et al. (2000) mark the cornerstones of the recent surge in interbank market research. They analyze the role of the network structure in a game theoretic context with four banks. In both models, banks lend cash among themselves in order to provide mutual insurance against liquidity shocks, thereby reducing the individual bank's need to hold large amounts of liquid assets. Allen and Gale (2000) provide a model where individual banks are exposed to uncertainty with respect to its customers' temporal preferences. The authors show that financial system stability is highest with a fully connected network, where each bank acts as liquidity insurance for all other banks. In contrast, Freixas et al. (2000) model the banking system with traveling depositors and thus induce uncertainty about the location of deposit withdrawal. Customers prefer to withdraw at the destination of their journey since taking cash with them implies foregone investment returns as opportunity costs. In their setting, the fully connected banking system is less resilient as opposed to credit chains. Both papers highlight the two faces of interbank markets. On the one hand they can provide insurance against individual bank's liquidity shortage. But on the other hand, they also serve as potential contagion channels in case of initial financial distress of one bank, propagating it throughout the system when it would otherwise be contained locally.

The empirical literature on interbank networks has focused on describing different network characteristics of real-world interbank markets. Often used statistics are the number of nodes N in the network, the number of links Z in the network, the resulting density $D = \frac{Z}{N(N-1)}$ and a small number of commonly accepted network statistics. The *degree distribution* gives the distribution of the number of links that a node participates in. If the network is directed, that is if each link has a clearly defined start and a clearly defined end, the in- and out-degree can be distinguished, and correspondingly the in-degree distribution and

the out-degree distribution. Another common statistic is the average shortest path length. It gives the mean length of the shortest paths between all pairs of nodes. Clustering coefficients measure the extent to which the neighbors of a node are connected among themselves. Finally, assortativity gives the correlation between the degree of a node and the average degree of its neighbors.

Boss et al. (2004) examine the Austrian interbank market and find scale-free degree distributions. Furthermore, the interbank market network exhibits low clustering and short average path lengths. Bech and Atalay (2010) explore the network topology of the federal funds market and find short average path lengths. Furthermore, they characterize the network as disassortative, i.e. small banks tend to be linked to large banks and vice versa. Soramäki et al. (2007) explore the network structure of the fedwire funds service. They too find a scale-free degree distribution and classify the network as a small-world network. However, they also find significant clustering in the network, and a structural break coinciding with the terror attacks in September 2001. Cocco et al. (2009) examine the Portuguese interbank market and look at the determinants of lending behavior, i.e. relationship lending. They find that banks make use of established lending relationships in case of larger liquidity needs. These relationships are usually found between institutions whose liquidity shocks are less strongly correlated.

Craig and Von Peter (2014) identify core-periphery structures in the German interbank market. A small proportion of about two percent of all banks forms a core of money center banks who act as liquidity re-distributors in the system. Craig and Von Peter (2014) also find that balance sheet characteristics are a good predictor of core membership. Fricke and Lux (2015) identify a core-periphery structure in the Italian overnight interbank market. In both markets, the core exhibits little turnover and little variation in size over time. Similar results are obtained for the Dutch banking system by van Lelyveld et al. (2014), and by Langfield et al. (2014) for the UK interbank market.

A key problem for researchers trying to link interbank network topology to financial stability is the lack of available bank-level data on interbank exposures. Apart from very few exceptions, this data is only available in regulatory institutions. Some researchers have thus resorted to inferring the bilateral credit exposures from boundary information in the form of bank balance sheets. Upper and Worms (2004) use individual balance sheet information for Germany including maturity categories to estimate interbank exposures. They perform

stability analyses based upon entropy-based estimates of the network structure. In their model, interbank lending is very closely related to the institutional structure of the banking landscape with most of the borrowing and lending taking place between banks and their respective head institutions, such as savings banks and their Landesbanken. Individual bank failures may in some cases lead to contagion, but widespread waves of defaults do not occur. Sheldon et al. (1998) also use entropy-based methods to infer the network structure of the swiss interbank network. Using it as input for stability simulations, they conclude that default contagion via the interbank market may not be an important source of financial stability risk, given the small number of defaults that results from direct interbank exposures. Mistrulli (2011) compare real interbank networks to approximations derived by maximum entropy methods. They show that entropy-based methods may underestimate the heterogeneity of real-world networks, resulting in significantly different implications for interbank market stability.

A second way to deal with the lack of bank level data on bilateral interbank exposures is to assume that the interbank market topology can be approximated by a well-defined class of networks.[1] Cifuentes et al. (2005) examine the effect of direct contagion and fire sales in a homogeneous interbank markets structured as random networks. Within their model, fire sales may lead to widespread defaults while direct contagion is less likely to do so. Thurner et al. (2003) provide a dynamic model with banks interacting on predefined network structures. They find that connectivity, free capital and external risk govern the stability of their system. Nier et al. (2007) provides the benchmark for this paper. The authors develop a simulation framework with a small number of network and balance sheet parameters. They use a random network, where a link between any two banks in the system is equally likely. Their work highlights the non-monotonic relation between network parameters and system stability. For sparsely connected networks, an increase in connectivity decreases system stability. However, for denser networks, a further increase in connectivity results in less defaults.

May and Arinaminpathy (2010) provide a mean-field approximation to the model of Nier et al. (2007). This analytical approach calculates the average interaction of an average

[1] Though *well-defined* has to be taken with caution. For example, so-called scale-free networks are defined via the degree distribution following a power law. This, however, does not necessarily fix other network statistics such as assortativity.

bank with its neighbors. They show that for random networks, the analytical results are well in line with the full-scale simulation. Moreover, the analytical solutions obtained in the approximation allow to calculate thresholds in the network parameters where the system behavior changes significantly. These insights contribute to a better understanding of the strongly nonlinear relation between network topology and systemic stability.

An overview over the state of counterfactual simulations of interbank markets is given by Upper (2007). The author finds that while contagion may arise in most models, it does so only with small probabilities. Whenever it is realized, however, it inflicts significant damage on the system at hand, driving a large share of institutions into bankruptcy. Given the strong underlying assumptions in these models as well as the lack of behavioral foundations, the author concludes that the current generation of these models is less suited for stress testing and the analysis of policy options.

2.3 Core-Periphery Networks

2.3.1 Networks: Definitions

A *network* consists of a set $\{n_i\}$ of N nodes, and a set $\{z_i\}$ of Z edges or links between these nodes. The *adjacency matrix* $A_{N\times N}$ represents links and nodes: entry a_{ij} is equal to the number of links from node i to node j. In our case $a_{ij} \in \{0;1\}$, i.e. banks can be connected by at most one link in each direction. In the *weighted adjacency matrix* $W_{N\times N}$, the entry w_{ij} equals the link weight between node i and node j if there is a link between node i and j, and zero otherwise. In this paper, all networks are *directed*, that is each link has a clearly defined start node and end node. As a consequence, neither the adjacency matrix nor the weighted adjacency matrix are necessarily symmetric. Furthermore, we exclude self loops. These are links where the starting point and the end point are one and the same node. As a consequence the elements on the main diagonal of both the adjacency matrix and the weighted adjacency matrix are zero by definition. In our specific case of interbank networks, a link from bank i to bank j exists if bank i has lent money to bank j, and the weight on this link equals the nominal amount of the loan.

The *out-degree* z^i_{out} of a node i is the number of links starting at node i. The *in-degree* z^i_{in} of a node i is the number links ending at node i. In our context, z^i_{out} represents the number of

debtors to bank i, and z_{in}^{i} is the number of creditors to bank i. The *total degree* of a node is the sum of in- and out-degree. For each of the three degree types,[2] the *degree distribution* can be specified over all nodes of the network.[3] The *density* d of a network is the proportion of possible links that are realized, $d = \frac{Z}{N(N-1)}$.

2.3.2 Core-Periphery Networks

Core-periphery networks are a specialization of more general block networks that were developed for the analysis of social networks (Wasserman and Faust 1994). The underlying idea is that the linking behavior of actors (banks, in our case) depends on actor attributes. In the simplest setting actors are partitioned into distinct classes, depending on the role they take in the system. The number of distinct classes is smaller than the number of actors, and most roles are adopted by more than one actor. In a deterministic model, the classes two actors belong to are sufficient to determine whether these two actors share a link or not (Lorrain and White 1971). As an example, if we have a network where each actor belongs to exactly one class A,B or C, we can state for every pair[4] of classes whether two actors that belong to these two classes are connected or not. For example, each actor of class A is connected to each actor of class B but to none of class C. Two actors whose sets of direct neighbors are identical are said to be structurally equivalent (White et al. 1976).

Fienberg and Wasserman (1981) and Holland et al. (1983) generalized these models to pair-dependent stochastic models. Here, the authors introduced stochastic equivalence: all actors within the same class have the same probabilities for links to actors of all other classes. In analogy to the above example, now we can make stochastic statements on links between actors based on their classes. For example, the probability that an actor of class A and an actor of class B are linked may be $p_{AB} = 0.5$, and the probability that an actor of class A and an actor of class C are linked may be $p_{AC} = 0.2$. For a detailed introduction into stochastic block models, see Anderson et al. (1992). An extensive analysis of simple stochastic block models with two classes can be found in Snijders and Nowicki (1997).

[2]The distinction between in-, out- and total degree exists only for directed networks. For undirected networks, in-, out- and total degree are identical.

[3]Or in our case, also over subsets of nodes.

[4]If the network is directed, for every ordered pair. If the network is undirected, for every unordered pair.

Core-periphery networks are a further specialization of stochastic block models with only two classes. In a network of N nodes, we will adopt the notation that the nodes are ordered such that nodes $1...m$ belong to the core (C), while the remaining nodes $m+1...N$ belong to the periphery (P). We denote the class membership of node i as $b_i \in \{C,P\}$. The adjacency matrices this class of core-periphery networks can then be described stochastically as

$$A = \begin{pmatrix} d_{cc} & d_{cp} \\ d_{pc} & d_{pp} \end{pmatrix}. \tag{2.1}$$

where $d_{b_i b_j}$ denotes the linking probability between nodes i and j.[5] Realizations of the adjacency matrix are then generated by drawing a random realizations from a uniform distribution for each element of the adjacency matrix, $u_{ij} \sim U(0,1)$, and a_{ij} is equal to one if $u_{ij} \leq d_{b_i b_j}$ and equal to zero otherwise. Core nodes are assumed to be highly interconnected among each other, while periphery nodes are hardly connected among each other. Thus, $d_{cc} \approx 1$ and $d_{pp} \approx 0$. The specification of d_{cp} and d_{pc} differ in the literature. Borgatti and Everett (2000) postulate the off-diagonal densities $d_{cp} = d_{pc} = 1$ for the idealized core-periphery structure. In the application to interbank markets, Craig and Von Peter (2014) only require that the *CP*-block be row-regular and the *PC*-block be column-regular. This means that each core node must have at least one outgoing link to and at least one incoming link from a periphery node. Row and column regularity thus translate into the following constraints:

$$\begin{array}{lll} \sum_{j=m+1}^{N} a_{ij} \geq 1 & \forall & i = 1,...,m \\ \sum_{j=m+1}^{N} a_{ji} \geq 1 & \forall & i = 1,...,m. \end{array} \tag{2.2}$$

In this paper, we follow this definition of Craig and Von Peter (2014). A stochastic description of core-periphery networks is thus given by the parameter set $\{N, m, d_{cc}, d_{cp}, d_{pc}, d_{pp}\}$.

2.4 Simulation set-up and process

The simulation setup follows very closely the one employed by Nier et al. (2007). There are two main differences between their approach and ours. First, we employ core-periphery

[5] Note that this is *not* equal to the density of the subgraph created by all nodes in b_i and b_j, which is given by the average of $d_{b_i b_j}$ and $d_{b_j b_i}$.

market topologies while Nier et al. (2007) analyze random networks. Second, we increase the number of banks by one order of magnitude.

Our interbank markets have $N = 200$ participating banks. The asset side of each bank's balance sheet consists of external assets e_i and interbank assets in the form of loans provided to other banks, iba_i. Each bank's liabilities consist of interbank liabilities ibl_i, equity eq_i and deposits d_i. Total external assets in the banking system are denoted by E. The system-wide proportion of interbank assets IBA to system-wide total assets A is held fixed and denoted as $\theta = \frac{IBA}{A}$. Since E is exogenously determined, and total assets are the sum of interbank assets and external assets $A = IBA + E$, the absolute amount of interbank assets is given by

$$IBA = \frac{\theta}{1-\theta} E. \tag{2.3}$$

Each bank's equity is a fixed proportion η of its total assets,

$$eq_i = \eta \cdot (e_i + iba_i). \tag{2.4}$$

The interbank market is created as follows. In a first step, a random realization of the core-periphery network structure is generated as described in section 2.3, resulting in a fully specified adjacency matrix. The next step is to determine the link weight, corresponding to the credit amount on each link. Total interbank assets are then evenly distributed across the $|Z|$ realized links, yielding the links weight $w = \frac{IBA}{|Z|}$. The link weight together with each bank's in- and out-degree determine each bank's interbank assets and liabilities. After this step, some banks may end up with more interbank liabilities than interbank assets. Since all links carry the same weight, this is equivalent to saying that for some banks the in-degree exceeds the out-degree. The external assets are used to close any existing positive gaps between interbank liabilities and interbank assets,

$$e_i = max(0, ibl_i - iba_i). \tag{2.5}$$

The remaining external assets

$$\tilde{E} = E - \sum_{i=1}^{N} e_i \tag{2.6}$$

are evenly distributed across the banks,

description	parameter	default value
total number of banks	N	200
number of core banks	m	16
number of realizations	g	500
shock size	s	1
external assets	E	800000
net worth	η	0.005
proportion interbank assets	θ	0.3
density CC block	d_{cc}	1
density CP block	d_{cp}	0.5
density PC block	d_{pc}	0.5
density PP block	d_{pp}	0

Table 2.1 Default parameters used in the simulation.

$$e_i := e_i + \tilde{E}/N. \tag{2.7}$$

With the asset side fully specified, each bank's net worth is then calculated according to equation 2.4. Finally, deposits are used to ensure the balance sheet identity. Table 2.1 shows the default values for the model parameters.

For the given parameters, the size of balance sheets is primarily driven by the size of a bank's interbank assets and liabilities. Since all links in the network have the same weight, interbank assets and liabilities are directly proportional to a bank's out- and indegree. On average, core banks have higher in- and out-degrees under the default parameters in table 2.1. Core banks have an average in-degree of 107 and an average out-degree of 107, while periphery banks arrive on average only at 8 outgoing and 8 incoming links. Consequently, core bank interbank assets and liabilities are on average one order of magnitude larger than their corresponding periphery counterparts, resulting in a sizable difference between the average total assets of a core bank and the average total assets of a periphery bank. Our model setup thus confirms the empirical correlation documented by Craig and Von Peter (2014) between bank size as measured by total assets, and bank core membership.

The simulation process starts in round 1 with an exogenous shock to a bank i that wipes out a fraction s of that bank's external assets. The bank adjusts its liabilities in the following way. First, the bank's net worth is used to accommodate the shock. If the size of the shock

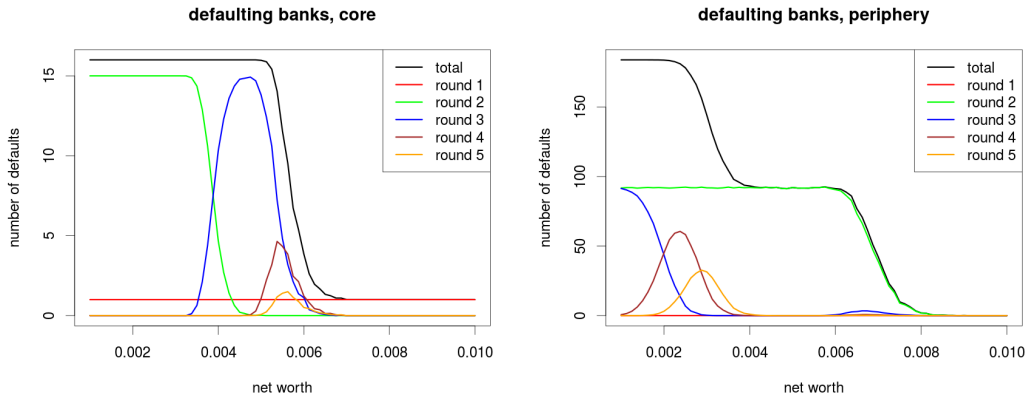

(a) defaults, core **(b)** defaults, periphery

Fig. 2.1 Number of defaults for varying net worth.

exceeds the net worth, $e_i \cdot s > eq_i$, the bank starts defaulting on its interbank liabilities on a pro rata basis. That is, it transmits a shock of $min(w, \frac{e_i \cdot s - eq_i}{z^i_{in}})$ to each of its creditors. If the total shock to the bank is larger than net worth and interbank liabilities combined, $e_i \cdot s > eq_i + ibl_i$, the deposits absorb the remaining shock.

In round 2 and all subsequent rounds, each bank calculates its decrease in total assets due to the sum of incoming shocks from its neighbors from the previous round. It then adjusts its liabilities along the same steps described above. First, equity absorbs the shock. If that does not suffice, banks default on their interbank liabilities. Once these are depleted, any remaining shock will be absorbed by deposits. The simulation stops if there are no more defaults.

2.5 Simulation results

Throughout the simulations, we initially shocked a randomly chosen core bank. We also ran the simulations with an initially defaulting periphery bank. Since this did not lead to any significant defaults, it is omitted here.

Figure 2.1 shows the number of defaults for varying values of the net worth η, averaged over 500 simulations. The overall number of defaulting core banks stays constant up to a net worth of around 0.6% before decreasing to zero. The time of default, however, changes

over this range: for low net worth, all core banks go default in round 2. This is due to direct contagion from the initially defaulting bank and the fact that the core is fully connected ($d_{cc} = 1$). For the net worth increasing from 0.3% to 0.6%, the total number of core bank defaults stays at the maximum, but the time of default gradually changes to later rounds. Beyond $\eta = 0.7\%$, no core banks apart from the initial one go default.

Figure 2.1b shows the number of defaulting periphery banks. For a net worth up to 0.7%, 92 periphery banks go default in the first round, i.e. all direct peripheral creditors of the initially defaulting core bank. This threshold of 0.7% for direct periphery neighbors is higher than the corresponding threshold of 0.3% for direct core neighbors. The reason is that while both core and periphery neighbors experience the same shock, core neighbors have, due to larger total assets, a larger absolute net worth. Consequently, a shock that leads to periphery bank defaults may not default any core banks. However, a shock that is large enough to default a core bank is guaranteed to be large enough to default a periphery bank. Round two periphery defaults occur only for a net worth up to 0.4%. Similar to the behavior of core banks, the total number of defaults stays constant at 184 over this range while the time of default gradually shifts to later rounds.

The threshold for the net worth beyond which the system does not exhibit any defaults is significantly lower than in the similar model by Nier et al. (2007). The primary reason is that the system analyzed here is far less concentrated. Under the default parameters in table 2.1, the shock emitted by the initially defaulting core bank is already divided evenly among an average of 107 counterparties. In contrast, in the small system with 25 banks, even if the system is fully connected, the initial shock is only divided among 24 counterparties. Thus, if the proportion between the total shock emitted by the initially defaulting bank and the average net worth of its direct neighbors stays the same, an increase in the number of banks tends to stabilize the system.

Figure 2.2 shows the total number of defaults for a varying share θ of interbank assets. Although the number of simulations per value of θ stays the same, the average number of defaults becomes slightly more erratic with increasing θ. Up to $\theta \approx 0.17$, the amount of interbank assets and the resulting nominal amount of each loan is not sufficient to trigger any defaults beyond the initially defaulting core bank. The number of core bank defaults then jumps sharply to the maximum of $m = 16$, with all defaults occurring in round 2. From $\theta \approx 0.35$ on, the number of core bank defaults slowly starts to decrease again and reaches

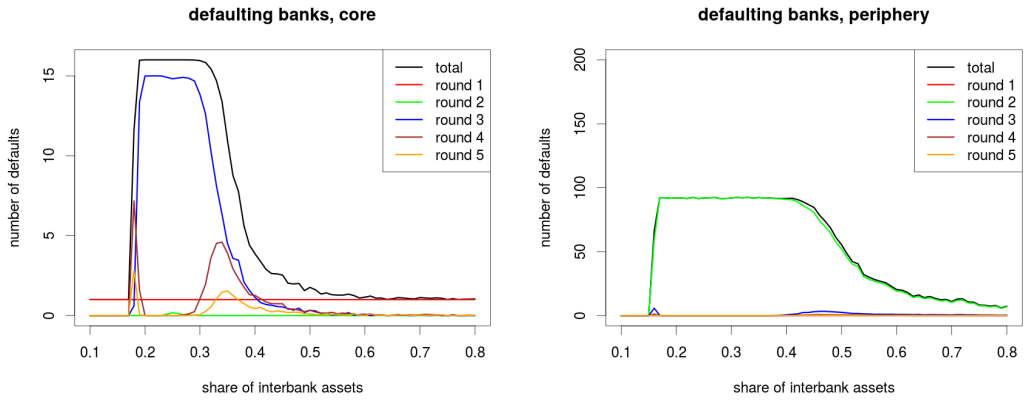

(a) defaults, core

(b) defaults, periphery

Fig. 2.2 Number of defaults for varying share of interbank assets.

1 for $\theta \approx 0.6$. Before the core defaults decrease to 1, they again shift from round 2 to later rounds. A similar picture emerges for periphery banks in figure 2.2b. The number of defaults increases sharply from 0 to 184 already for $\theta \approx 0.15$ and decreases slowly starting around $\theta \approx 0.45$ to an average of 10 for $\theta = 0.8$.

Figure 2.3 shows the simulation results for varying the core size m between 1 and 50. For a core size up to $m \approx 40$, the full core defaults. For core sizes above 40, the number of defaults suddenly collapses, and only the initial bank defaults. Similar to previous simulations, as we increase the core size, the collapse in the number of defaults is preceded by a shift of defaults to later rounds. Up to $m \approx 25$, all core banks default in round 3. For $m > 25$, core defaults gradually shift to rounds 4 and 5. Similar to the core bank defaults, the defaults in the periphery mirror primarily the constraints of the network structure. The slow decrease in the number of round 2 periphery defaults corresponds directly to the slowly decreasing number of direct periphery neighbors of the initially defaulting core bank. With the total number of banks being constant, an increase in the number of core banks is equivalent to a decrease in the number of periphery banks. Since d_{PC} is constant as well, the average number of creditors of the initially defaulting core bank decreases with an increasing core size, too. There are no periphery defaults in later rounds.

The reason for the sudden decrease in core bank defaults is as follows. From the graphics, we see that (1) no core banks go default in round 2, and (2) all direct periphery neighbors of

the initially defaulting core bank go default in round 2. In round 1, the initially defaulting core bank sends out an initial shock. This shock is divided evenly among all direct neighbors of that bank. Part of it is sent to its core neighbors, and part of it ends up at its peripheral neighbors. The peripheral neighbors, who are not connected among themselves due to $d_{pp} = 0$, buffer a part of the shock with their net worth. They then sent back the minimum of the remaining shock and their interbank liabilities back to the core.

Thus, in round three the core has received a total shock of

$$s_c(1) - d_{cp}(N-m)\left[n\bar{w}_p - min(0, i\bar{bl}_p - \frac{s_c(1)}{z_c^{in}} - n\bar{w}_p)\right]. \tag{2.8}$$

$s_c(1) = min(e\bar{a}_c - n\bar{w}_c, i\bar{bl}_c)$ is the shock emitted by the initially defaulting bank. Each of its $d_{cp}(N-m)$ periphery neighbors reduces the shock on average by $n\bar{w}_p$ before sending it back into the core. The term $min(\cdot)$ captures the fact that periphery banks can emit at most a shock in size equal to their outstanding interbank liabilities ibl_p. This shock is larger than the combined net worth of all core banks, $(m-1)n\bar{w}_c$, up to a value of $m \approx 43$, leading to a complete core default. Beyond this value, the total shock received by the core does no longer exceed the total core net worth. Remarkably, at no time are there any core defaults in round 2. This corresponds to stating that the shock that is emitted by the initially defaulting bank is not large enough to threaten other core banks. It is only when the default periphery banks send the remainder of their round 2 shocks back to the core in round 3 that the remaining core banks go default.

Figure 2.4 shows the simulation results for varying the density of the CC block of the adjacency matrix from 0.5 to 1. The number of core bank defaults linearly increases up to 16, representing the average number of direct core neighbors of a core bank. Apart from the initially defaulting core bank, all core defaults take place in round 3. Only for $d_{cc} \approx 1$ does a small proportion of core defaults shift to round 4. The picture for periphery banks remains unchanged for all values of d_{cc}: the direct creditors of the initially defaulting core bank go bust in round 2, and we do not observe any periphery defaults beyond that.

Figure 2.5 shows the results for varying the density of the CP block of the adjacency matrix. Overall, the total number of core defaults slightly decreases for large values of d_{cp}. Starting from $d_{cp} \approx 0.5$, the number of core defaults comes down from the full core size of $m = 16$, reaching 11 for $d_{cp} = 1.0$. Again, before the overall number of defaults decreases,

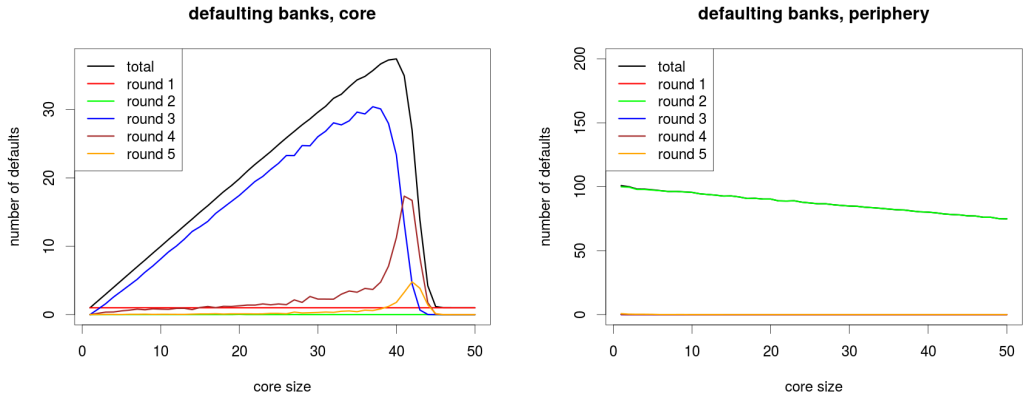

(a) defaults, core **(b)** defaults, periphery

Fig. 2.3 Number of defaults for varying core size.

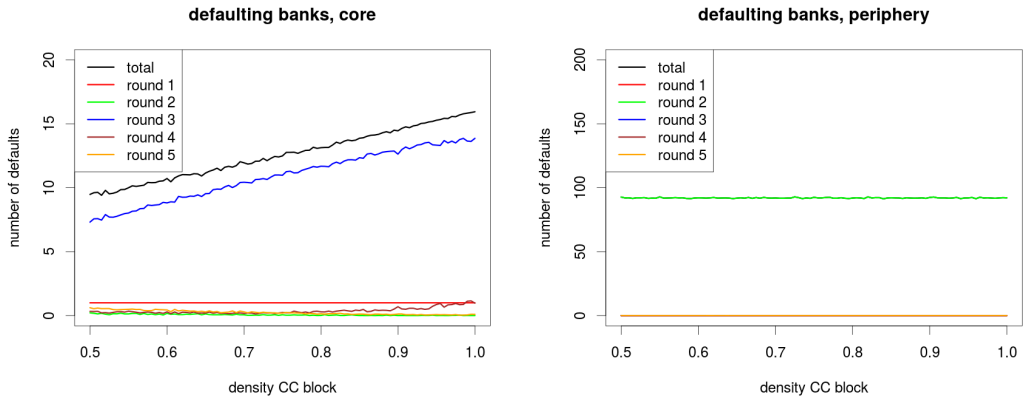

(a) defaults, core **(b)** defaults, periphery

Fig. 2.4 Number of defaults for varying CC block density.

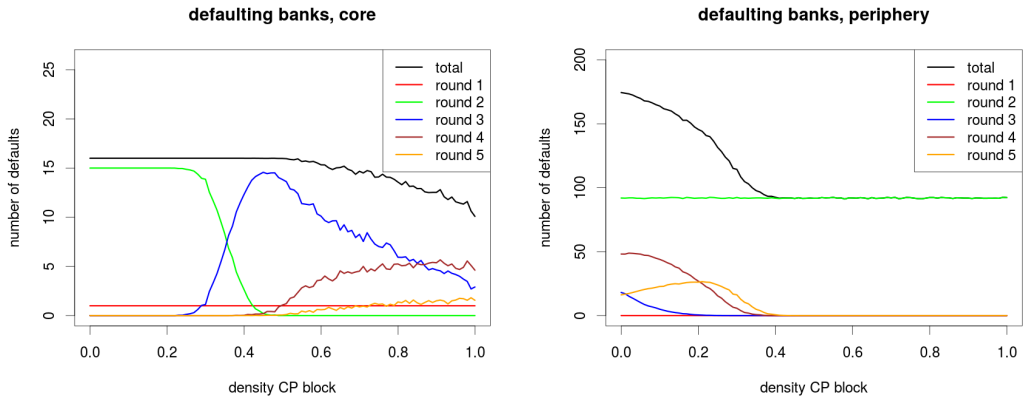

(a) defaults, core

(b) defaults, periphery

Fig. 2.5 Number of defaults for varying CP block density.

the defaults begin to shift from round 2 to round 3. Later on the defaults shift to rounds 4 and 5, although slower than the transition from round 2 to 3. The slight increase in core stability can be shown to be a pure balance sheet effect. With an increase in d_{cp}, the average core bank out-degree increases. Consequently, also average core bank interbank assets and thus also total assets increase. Since net worth is a function of total assets, the average absolute net worth of core banks also increases, making them more resilient. At the same time the initial shock, being only a function of external assets, stays the same.

Round 2 periphery defaults remain constant at 92 for all values of d_{cp}. These are again the direct periphery neighbors of the initially defaulting core bank. Total periphery defaults continuously decrease for d_{cp} increasing from 0 to 0.4, and for $d_{cp} > 0.4$, there are no periphery defaults beyond the direct creditors of the initially defaulting core bank. The decrease in later round defaults of periphery banks stems again from the increase in core stability. This leads core banks to send less and less residual shocks to the periphery with the increase in d_{cp}.

Figure 2.6 shows the results for varying the density of the PC block of the adjacency matrix. Except for a small dent around $d_{pc} \approx 0.6$, the total number of core defaults stays constant at $m = 16$. Core defaults shift from round 2 to round 3 starting from $d_{pc} \approx 0.2$, and for $d_{pc} > 0.4$ hardly any core defaults occur in round 2 any more. For d_{pc} between 0.5 and 0.6, a few core defaults shift from round 3 to round 4. The picture for periphery

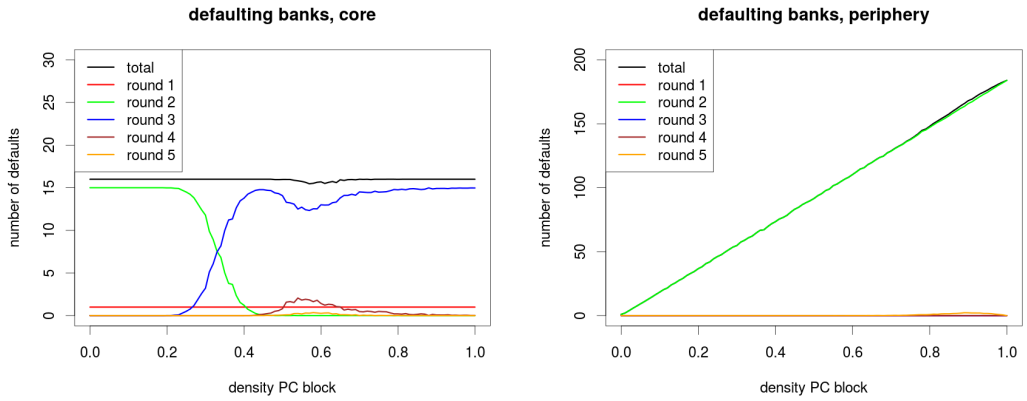

(a) defaults, core **(b)** defaults, periphery

Fig. 2.6 Number of defaults for varying PC block density.

defaults varies drastically from the corresponding results for d_{cp}. Since d_{pc} directly impacts the number of shock transmission channels from the initially defaulting core bank to the periphery, the number of its periphery creditors and thus of the round 2 defaulting periphery banks increases linearly with d_{pc}. We do not observe any periphery defaults in later rounds.

For the Italian interbank market as represented by the e-MID dataset, Fricke and Lux (2015) find a pronounced asymmetry between the densities of the two off-diagonal blocks. The density of the *CP* block varies between 0.4 and 0.5 while the *PC* block is far less dense, with d_{pc} varying between 0.1 and 0.2. For simulation results regarding this asymmetric structure the reader is referred to Karimi and Raddant (2016) who employ a simulation algorithm similar to ours on the original e-MID data.

Figure 2.7 shows the simulation results for varying the periphery density. For $d_{pp} > 0.3$, we do not observe any defaults at all after round 1. Core bank defaults already disappear at $d_{pp} \approx 0.25$. Shortly before the number of defaults drops to zero, both core and periphery defaults partially shift from round 3 (core) and round 2 (periphery) to later rounds. In contrast to the balance sheet argument we gave for the previous graphs, here it is a function of the transmission. To see this, note that an increase in d_{pp} leads to an increase in the total number of links and thus a reduction in the link weight. Since the increase in links only concerns periphery banks, core banks face the same average degree and decreased link weights. This results in a reduction in interbank assets. In analogy to the argument before, from a balance

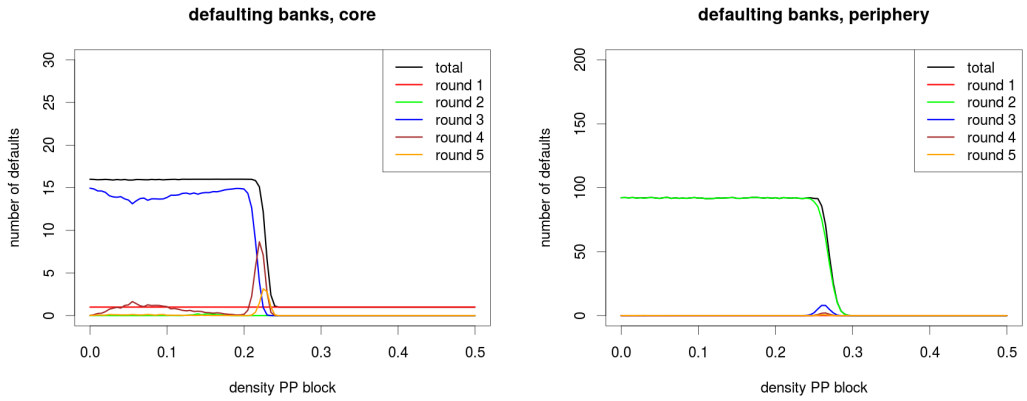

(a) defaults, core **(b)** defaults, periphery

Fig. 2.7 Number of defaults for varying PP block density.

sheet perspective this decreases the absolute net worth of core banks while keeping the initial shock as a function of the external assets constant. Thus, if at all, from the balance sheet perspective core banks would have to become increasingly unstable as d_{pp} increases. Clearly, this is not what we find in the results. What happens instead is that, as the periphery becomes more and more connected, it is increasingly capable of buffering the shock by itself instead of sending it back to the core. It is this increased absorption capability by the periphery that leads to the transition to stability.

2.6 Mean-field approach

Having explored the behavior of the full-scale simulation along the most important parameter axes, we now examine whether we can approximate those results reasonably well with an established analytical approach. The mean-field approach is an analytical approximation to the behavior of the system. It serves two purposes. First, as compared to the full-scale simulation, it greatly reduces computational costs. Approximations even to large systems are calculated quickly. This is especially useful in mapping out the parameter space of the model. Second, by tracing the behavior of the system analytically, we can gain insight into the main factors that govern the dynamics of the system. The mean-field approach presented here follows in broad strokes the one May and Arinaminpathy (2010) applied to random

networks. The authors provided approximations to the model by Nier et al. (2007) and in the process, gave explanations for the nonlinear behavior observed in the original model. The main difference to our approach is that from the very beginning, we need to track two types of nodes, core and periphery banks. In section 2.6.1 we will first discuss the balance sheet mechanics before comparing the simulation results and the mean-field approximations in section 2.6.2.

2.6.1 Balance sheet construction

The balance sheets are initialized as described in section 2.4. However, instead of drawing a realization of the network structure in the first step, and gather bank degrees from that realization, the mean-field approach takes the average in- and out-degree of core and periphery banks as a starting point.

The average number of links in the network is given by the sum of the average of the number of links in each of the four blocks of the adjacency matrix in equation 2.1,

$$Z = Z_{CC} + Z_{CP} + Z_{PC} + Z_{PP}, \tag{2.9}$$

where

$$\begin{aligned} Z_{CC} &= m(m-1)d_{cc} \\ Z_{CP} &= m(N-m)d_{cp} \\ Z_{PC} &= m(N-m)d_{pc} \\ Z_{PP} &= (N-m)(N-m-1)d_{pp} \end{aligned} \tag{2.10}$$

The size of each individual interbank loan is then calculated as $w = \frac{IBA}{Z}$. The in- and out-degree of each bank can be split into the number of links to/from core banks, and the number of links to/from periphery banks. As an example, the average core bank has $\bar{z}_{out}^{cc} = d_{cc}(m-1)$ outgoing links to other core banks, and $\bar{z}_{out}^{cp} = d_{cp}(N-m)$ outgoing links to periphery banks. The average in- and out-degrees of core and periphery banks are thus given by

$$\begin{array}{rcll} \bar{z}^c_{in} & = & \bar{z}^{cc}_{in} + \bar{z}^{pc}_{in} & = d_{cc}(m-1) + d_{pc}(N-m) \\ \bar{z}^c_{out} & = & \bar{z}^{cc}_{out} + \bar{z}^{cp}_{out} & = d_{cc}(m-1) + d_{cp}(N-m) \\ \bar{z}^p_{in} & = & \bar{z}^{cp}_{in} + \bar{z}^{pp}_{in} & = d_{cp}m + d_{pp}(N-m-1) \\ \bar{z}^p_{out} & = & \bar{z}^{pc}_{out} + \bar{z}^{pp}_{out} & = d_{pc}m + d_{pp}(N-m-1). \end{array} \tag{2.11}$$

The average degrees, multiplied by the loan size w, give the size of the average interbank assets and liabilities for core and periphery banks.

The next step in the simulation set-up routine according to section 2.4 was the use of the external assets to fill any positive gaps between interbank assets and interbank liabilities. The average size of this gap may be different for core and periphery banks, and consequently core and periphery banks may receive different amounts of external assets in this step. This has two implications for the balance sheet proportions. First, if due to the parameterization of the network structure a large amount of the system-wide external assets is distributed to close the gap, only a small proportion of the external assets is distributed evenly over the banks. Consequently, the resulting distribution of external assets between core and periphery banks may be very skewed. This can contribute to the difference in the average total assets between core and periphery banks. Because bank net worth is proportional to bank total assets, this also has direct implications for the resilience of banks.

Second, the simulation algorithm takes as a starting point a shock proportional to the size of the external assets of the bank. If core banks, due to the network structure, receive a larger proportion of external assets, the initial shock may be more severe. Even if *on average* the in- and out-degree of banks are equal due to $d_{cp} = d_{pc}$, some banks might have a higher in-degree than out-degree, and consequently even in this case some of the external assets will be distributed in this step. Despite working with average bank degrees, it is thus necessary to look at the degree distributions in order to determine the amount of external assets that is used, on average, to close the gap.

The actual degree distributions of core and periphery banks can be calculated as follows. The probabilities for any two links to exist are pairwise independent. The probability of a core bank to have exactly x outgoing links to periphery banks is thus Bernoulli distributed

$$P(z^{cp}_{out} = x) = B_{N-m;d_{cp}}(x) = \binom{x}{N-m} d^x_{cp}(1-d_{cp})^{N-m-x}. \tag{2.12}$$

Similar, the probability of a core bank to have exactly y outgoing links to other core banks is given as $P(z^{cc}_{out} = y) = B_{m-1;d_{cc}}(y)$. The probability of a core bank to have an out-degree of exactly z, $P(z^{c}_{out} = z)$, is then calculated as the sum over the product of the probabilities for all pairs of x and y that sum up to z. Equation 2.13 shows the resulting formulation of the in- and out-degree distributions of core and periphery banks.

$$\begin{array}{rcl} P(z^{c}_{in} = z) & = & \sum_{y=0}^{z} \left[B_{N-m;d_{pc}}(y) \cdot B_{m-1;d_{cc}}(z-y) \right] \\ P(z^{c}_{out} = z) & = & \sum_{y=0}^{z} \left[B_{N-m;d_{cp}}(y) \cdot B_{m-1;d_{cc}}(z-y) \right] \\ P(z^{p}_{in} = z) & = & \sum_{y=0}^{z} \left[B_{m;d_{cp}}(y) \cdot B_{N-m-1;d_{pp}}(z-y) \right] \\ P(z^{p}_{out} = z) & = & \sum_{y=0}^{z} \left[B_{m;d_{pc}}(y) \cdot B_{N-m-1;d_{pp}}(z-y) \right]. \end{array} \tag{2.13}$$

Since the in- and out-degrees of banks are discrete random variables, the gaps between in- and out-degree are also random variables. We denote them as

$$\begin{array}{rcl} \Delta^{z}_{c} & = & z^{c}_{in} - z^{c}_{out} \\ \Delta^{z}_{p} & = & z^{p}_{in} - z^{p}_{out}. \end{array} \tag{2.14}$$

If their expected values are larger than zero, the expected amount of external assets needed to close these gaps is also larger than zero. Banks have at least a degree of 0 and at most a degree of $N-1$. Thus, the support for Δ^{z}_{c} and Δ^{z}_{p} is given as $\{-N+1, ..., 1, 0, 1, ..., N-1\}$. The distribution over the gap sizes Δ^{z}_{c} and Δ^{z}_{p} is constructed as follows. The probability for the difference δ between in- and out-degree is the sum over the joint probabilities that the in-degree is $\delta + i$ and the out-degree is exactly i. The sum is taken over all admissible values of i, $i \in \{0, ..., N-\delta-1\}$ so that the in-degree runs from 0 to the maximum possible degree $N-1$:

$$\begin{array}{rcl} p^{c}_{\Delta}(\delta) & = & P(\Delta^{z}_{c} = \delta) \quad = \quad \sum_{i=0}^{N-\delta-1} \left[P(z^{c}_{in} = \delta + i) P(z^{c}_{out} = i) \right] \\ p^{p}_{\Delta}(\delta) & = & P(\Delta^{z}_{p} = \delta) \quad = \quad \sum_{i=0}^{N-\delta-1} \left[P(z^{p}_{in} = \delta + i) P(z^{p}_{out} = i) \right] \end{array} \tag{2.15}$$

The gap between interbank assets and liabilities is obtained by multiplying the degree difference with the link weight,

$$\begin{array}{rcl} \Delta_{c} & = & w \cdot \Delta^{z}_{c} \\ \Delta_{p} & = & w \cdot \Delta^{z}_{p}. \end{array} \tag{2.16}$$

We are now interested in the expected values of these gaps, provided that they are positive. These can be calculated multiplying the probability $p^0_{\Delta^z_{c/p}}$ that the gap is positive in the first place with the expected value over the positive gap size:

$$\begin{array}{rcl} \tilde{e}_i^{c,gap} = E[max(0,\Delta_c)] & = & w \cdot p^0_{\Delta^z_c} \cdot \sum_{i=0}^{N-1} \left[i \cdot p^c_\Delta(i) \right] \\ \tilde{e}_i^{p,gap} = E[max(0,\Delta_p)] & = & w \cdot p^0_{\Delta^z_p} \cdot \sum_{i=0}^{N-1} \left[i \cdot p^p_\Delta(i) \right] \end{array} \tag{2.17}$$

where

$$\begin{array}{rcccl} p^0_{\Delta^z_c} & = & P(\Delta^z_c > 0) & = & \sum_{\delta=1}^{N-1} p^c_\Delta(\delta) \\ p^0_{\Delta^z_p} & = & P(\Delta^z_p > 0) & = & \sum_{\delta=1}^{N-1} p^p_\Delta(\delta). \end{array} \tag{2.18}$$

Equations 2.17 give us the expected amount of external assets that each core and periphery bank requires to fill the gap. In general, these values are nonzero even if on average, in- and out-degree are equal for all banks. We call the effect of an uneven distribution of external assets between core and periphery banks due to this filling up the "balance sheet effect" for short. Three important insights arise from this calculation. First, the gap is linearly increasing in $p^0_{\Delta^z_{c/p}}$, i.e. in the probability that the gap is larger than zero in the first place. For example, if $d_{pc} > d_{cp}$, the expected in-degree of core banks is larger than the expected out-degree. This increases the probability that core banks on average have more interbank liabilities than interbank assets, and thus $p^c_{\Delta_0}$ is larger than compared to the case where $d_{pc} < d_{cp}$.

Second, the gap is also linearly increasing in the link weight w. If interbank assets are larger as a result of increasing θ, for the same network specification, the gaps will on average be wider. In both cases, a larger proportion of external assets is used for filling up the gaps, leaving a smaller proportion of external assets to be distributed evenly across all banks. Finally, with a typical parametrization of $m << N$, $d_{cc} \approx 1$ and $d_{pp} \approx 0$, not only do core banks have on average a higher degree than periphery banks. But the core bank distributions are also wider than their periphery counterparts. This larger variance also increases the gap disproportionally for core banks, $\Delta_c > \Delta_p$. As a consequence, core banks will on average receive more external assets than periphery banks.

From the default parameter values given in table 2.1, $d_{cp} = d_{pc} = 0.5$. If we ignored the balance sheet effect, this would imply that neither core nor periphery banks have an expected

gap, $\tilde{e}_i^c = \tilde{e}_i^p = 0$. Thus, the external assets are distributed evenly across core and periphery banks, $e_i^c = e_i^p = E/N$. However if we account for the fact that realized bank degrees may give rise to banks that have a positive gap, $\tilde{e}_i^{c,gap} > 0$ and $\tilde{e}_i^{p,gap} > 0$ are determined by equation 2.17. The remaining external assets are then given as $\tilde{E}^{gap} = E - m \cdot \tilde{e}_i^{c,gap} - (N-m) \cdot \tilde{e}_i^{p,gap}$, resulting in

$$\begin{aligned} e_i^{c,gap} &= \tilde{e}_i^{c,gap} + \tilde{E}^{gap}/N \\ e_i^{p,gap} &= \tilde{e}_i^{p,gap} + \tilde{E}^{gap}/N \end{aligned} \tag{2.19}$$

Figure 2.8 demonstrates the balance sheet effect for changing the share of interbank assets and thus also the link weights w. It shows for core and periphery banks the ratio of external assets per bank if we neglect the balance sheet effect, and if we take the expected gap into account, $e_i^{c,gap}/e_i^c$ and $e_i^{p,gap}/e_i^p$. If the balance sheet effect did not play a role, these ratios would be constant at 1. As expected, we see that the balance sheet effect assigns disproportionally more external assets to core banks. They receive more external assets for filling the gap even for small values of θ. As the share of interbank assets becomes larger, the total amount of external assets assigned to core banks increases up to 30% above the non-adjusted value of 4000 while it falls below this level for periphery banks. The balance sheet effect creates ripple effects throughout the simulation. As discussed, this effect will directly affect the initial shock size. Furthermore, since the balance sheet effect impacts the size of total assets, it also widens the gap between total core and periphery bank net worth. Concluding, we can state that the particular algorithm used to initialize the balance sheets induces systematic asymmetries in the distribution of external assets between core and periphery banks. Under default parameters, this leads to core banks being assigned a larger share of the interbank assets.

2.6.2 Calculation of defaults

Motivated by the results of the full-scale simulation, we demonstrate the mean field approach only for initially shocked core banks. The initial shock to one of the core banks is given as the product of shock proportion s and the bank's external assets ea_c,

$$S(1) = s \cdot e\bar{a}_c. \tag{2.20}$$

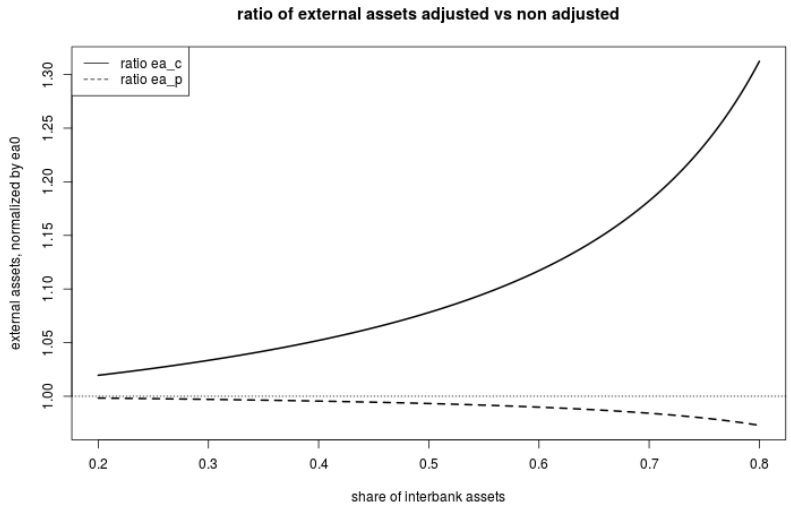

Fig. 2.8 Illustration of the balance sheet effect

The bank defaults if the shock exceeds its net worth, $S(1) > n\bar{w}_c$. In that case, each of its creditors receives a shock of size

$$S(2) = \frac{min(i\bar{bl}_c, S(1) - n\bar{w}_c)}{\bar{z}^c_{in}}. \tag{2.21}$$

The conditions for round 2 defaults are

$$\begin{array}{rcl} S(2) & > & n\bar{w}_c \\ S(2) & > & n\bar{w}_p \end{array} \tag{2.22}$$

On average, core banks have larger total assets and thus also a larger net worth than periphery banks, $n\bar{w}_c > n\bar{w}_p$. Thus, second round core bank defaults occur only if their counterparts in the periphery also fail. The newly default periphery banks emit to each of their creditors a shock of size

$$S_p(3) = \frac{max\left(0, min(i\bar{bl}_p, S(2) - n\bar{w}_p)\right)}{\bar{z}^p_{in}}, \tag{2.23}$$

and the newly default core banks emit to each of their creditors a shock of size

$$S_c(3) = \frac{max\left(0, min(i\bar{bl}_c, S(2) - n\bar{w}_c)\right)}{\bar{z}^c_{in}}. \tag{2.24}$$

The $max(.)$ indicates that the shock may be zero if the banks do not go default. In words, if the banks have a sufficient buffer of net worth, they do not transmit any shock. Should the shock exceed the net worth, they emit a shock that is at most as large as their interbank liabilities. Until now, the simulation is exact within the mean field approximation. This is due to the fact that each bank received at most one shock. From here on, banks may receive multiple shocks from different debtors. These aggregate shocks are linear combinations of the shocks emitted by default core and periphery banks. In round 3, they are given as

$$\begin{array}{rclcl} S_c^{in}(3) & = & S_{cc}^{in}(3)+S_{cp}^{in}(3) & = & n_{cc}^S(3)\cdot S_c(3)+n_{cp}^S(3)\cdot S_p(3) \\ S_p^{in}(3) & = & S_{pc}^{in}(3)+S_{pp}^{in}(3) & = & n_{pc}^S(3)\cdot S_c(3)+n_{pp}^S(3)\cdot S_p(3). \end{array} \tag{2.25}$$

The superscript ^{in} denotes incoming shocks as supposed to the outgoing shocks that we have explored so far. The factor $n_{cc}^S(3)$ denotes the number of shocks a core bank receives from other core banks in round 3. Similarly, $n_{cp}^S(3)$ denotes the number of shocks it receives from periphery banks in round 3, and so on. These factors of shocks follow a binomial distribution similar to those discussed in equation 2.13:

$$\begin{array}{rcl} P\left(n_{cc}^S(3)=x\right) & = & B_{z_{in}^{cc};d_{cc}}(x) \\ P\left(n_{cp}^S(3)=x\right) & = & B_{z_{out}^{cp};d_{cp}}(x) \\ P\left(n_{pc}^S(3)=x\right) & = & B_{z_{in}^{pc};d_{pc}}(x) \\ P\left(n_{pp}^S(3)=x\right) & = & B_{z_{out}^{pp};d_{pp}}(x) \end{array} \tag{2.26}$$

For our calculations, we take advantage of the fact that, in general, $S_c(3)$ and $S_p(3)$ are not multiples of each other. Thus, each aggregate shock $S_c^{in}(3)$ and $S_c^{in}(3)$ has only one possible decomposition in contributions from the core and from the periphery. Since the number of shocks that a bank receives from the core is independent from the number of shocks it receives from the periphery, the probabilities for the occurrence of shock combinations can be calculated as the product of the probabilities of its two components:

$$\begin{array}{l} P\left(S_c^{in}(3)=x\right)=P\left(S_{cc}^{in}(3)=x_c\wedge S_{cp}^{in}(3)=x_p\right)=B_{z_{in}^{cc};d_{cc}}(x_c)\cdot B_{z_{out}^{cp};d_{cp}}(x_p) \\ P\left(S_p^{in}(3)=x\right)=P\left(S_{pc}^{in}(3)=x_c\wedge S_{pp}^{in}(3)=x_p\right)=B_{z_{in}^{pc};d_{pc}}(x_c)\cdot B_{z_{out}^{pp};d_{pp}}(x_p) \end{array} \tag{2.27}$$

Core banks in round 3 go default if the incoming shock exceeds their net worth. This corresponds to the cumulative probability $P\left(S_c^{in}(3) > n\bar{w}_c\right)$ which can be calculated by enumerating the combinations of shocks in equation 2.25 that fulfill this condition. The expected number of newly default core banks in round 3, $\bar{n}_c^{def}(3)$, is then given by multiplying this probability with the number of nondefault core banks at the beginning of round 3, $(m-1-\bar{z}_{in}^{cc})$:

$$\bar{n}_c^{def}(3) = P\left(S_c^{in}(3) > n\bar{w}_c\right) \cdot (m-1-\bar{z}_{in}^{cc}) \tag{2.28}$$

At the end of the third round, banks have been subject to the distribution of aggregate shocks according to equations 2.25 and 2.27. Consequently, even if all core banks and periphery banks had initially been identical as assumed in this the mean field approach, in round 3 they evolve into a heterogeneous field of banks due to the different linear combinations of shocks they receive. Some banks fail while others, who received a different shock combination, are still healthy. Moreover, all we can say about the banks that have not yet failed is that the combination of shocks they received was not enough to deplete their net worth. However, these banks have most likely different levels of net worth left, again due to the different combinations of shocks they experienced. Thus in order to maintain an accurate picture of the state of the system, it would now be necessary to calculate the resulting distribution of remaining net worth among the nondefault banks, and the distribution of outgoing shocks from the newly default banks. This would, however, result in the individual tracking of each individual bank and thus a return to the full-scale simulation. We avoid this by just distinguishing between newly default banks and nondefault banks, and taking the average of each of these groups. We calculate the mean remaining net worth for nondefault core and periphery banks, and the mean size of outgoing shocks for the newly default core and periphery banks.[6] We can then compute the next round by working only with one size of shocks, and one size of remaining net worth, and avoid falling back into the full-scale simulation. As a result, at the end of round 3 we have the number of default and nondefault core and periphery banks, their average net worth, average remaining interbank liabilities

[6]To be even more precise: the weighted average of (i) the average outgoing shock size of newly default core banks and (ii) average outgoing shock size of the already default core banks. In this static setting, they can, in higher rounds, still transmit shocks although they are already default.

and average outgoing shock size. These inputs allow us to repeat the same algorithm for higher rounds.

2.6.3 Results

We now compare the mean field approximation with the full-scale simulations. Figure 2.9 shows the results for varying net worth, and 2.10 shows the results for varying the share of interbank assets. The mean-field approach results in a very good approximation of the full-scale simulation during the first three rounds. In round 2, the mean-field approximation exhibits step-wise transitions as opposed to the smooth change of the number of defaults in the full-scale simulation. This is due to the binary nature in mean field approach as shown in equation 2.22. Since we calculate block-wise averages, either all direct neighbors in a block fail, or none. Since the increase in round 3 core defaults for increasing net worth is directly related to the decrease in round 2 core defaults, this increase is step-wise as well. A similarly abrupt transition can be observed in round 2 periphery defaults in figure 2.10b.

For round 3 periphery defaults, figure 2.9b shows that the mean-field approach is capable of reproducing the smooth decline in the number of defaults that is observed in the full-scale simulation. This can be understood in the light of the previous derivations. In round 1 and 2, each bank receives at most one shock, and the number of defaults is governed by the average degrees. From round 3 on, this is replaced by the probabilistic approach culminating in equation 2.28 which allows for a more gradual transition in the number of defaults, also along parameters that do not impact the average degrees.

This comes at a cost, however, as the figures show. For rounds 4 and 5, the mean-field approximation cannot reproduce the behavior of the simulation accurately over the full parameter range. In figure 2.9b, round 4 periphery defaults registered only for very small values of η, and round 5 defaults are not produced at all by the mean field approach. For both varying η and varying θ, the mean field simulation of round 4 defaults breaks down as soon as the total number of defaults in each block is no longer maximal.

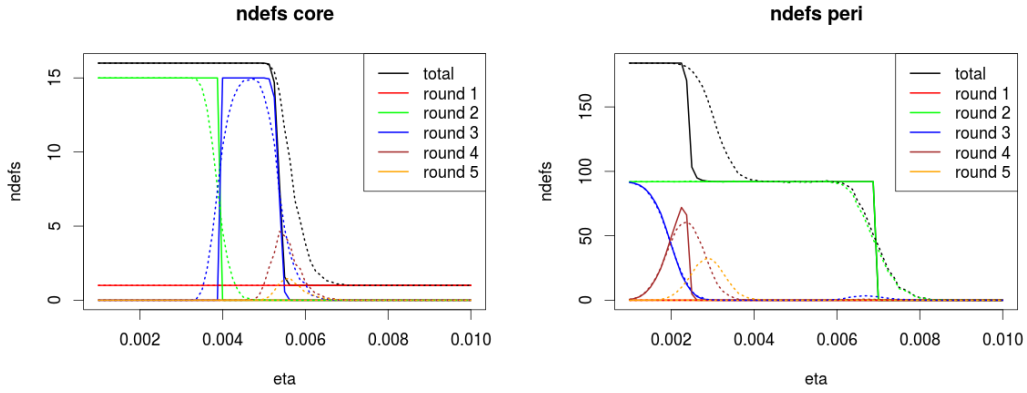

(a) defaults, core **(b)** defaults, periphery

Fig. 2.9 Comparison of mean field approximation (solid lines) and full-scale simulation (dotted lines) for varying net worth.

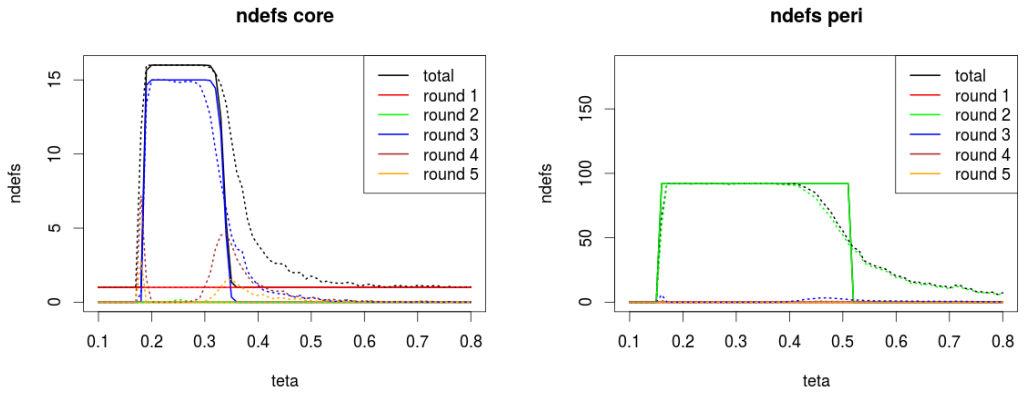

(a) defaults, core **(b)** defaults, periphery

Fig. 2.10 Comparison of mean field approximation (solid lines) and full-scale simulation (dotted lines) for varying share of interbank assets.

2.7 Conclusions

This paper extended the model of Nier et al. (2007) to core-periphery networks. The simulation results can be summarized as follows. Increasing bank's net worth has, unsurprisingly, a clear stabilizing effect. However, this stabilization happens at far lower levels of net worth than in the model by Nier et al. (2007). This is due to the fact that, in contrast to the original paper with 25 banks, our system is much more distributed with 200 banks. Consequently, the impact of a single bank decreases. The original shock equal to one bank's external assets would, if external assets were evenly distributed, be equal to E/N and thus decreasing in the number of banks in the system.

For very small amounts of interbank assets, the system tends to be stable. The number of defaults then jumps abruptly to a plateau for the share of interbank assets surpassing 0.15 before slowly decreasing again for the share of interbank assets exceeding 0.35 (core banks) and 0.45 (periphery banks).

The most interesting result comes from the periphery density. Even slightly increasing this parameter allows the periphery banks to act as a better buffer by resolving shocks among themselves instead of reflecting them nearly completely back into the core. This raises the question whether a pronounced core-periphery structure is optimal from a financial stability perspective.

In a second step, we examined whether the mean field approach May and Arinaminpathy (2010) applied to random networks can be applied to core-periphery networks as well. Before running the simulations, we examined the effect of the simulation initialization algorithm on bank balance sheets. We found that already the particular way the simulation is set up can increase the differences between core and periphery bank balance sheets significantly. Differences in balance sheet sizes between these two groups have thus two determining factors.

Calculating the shock propagation in the mean-field approximation, we found that defaults in the first three rounds are approximated very well. Round 2 defaults evolve step-wise, while round 3 defaults already allow the approximation to replicate the continuous development of the number of defaults. For higher-round defaults, banks become more and more heterogeneous since they experience different linear combinations of incoming shocks. In order to avoid falling back into the full-scale simulation, it becomes necessary to average over

banks at the end of each round. This averaging out leads to the mean-field approximation becoming less accurate, demonstrating the limits of this approach. For processes that last several rounds and nontrivial node transmission behavior, it quickly loses accuracy. This raises the question whether the mean-field approach can be modified or extended in order to arrive at a better approximation to the full-scale simulation.

Chapter 3

Bipartite Clustering in Bank-Firm Networks

3.1 Introduction

Credit is an integral part of modern economies. The provision of credit by banks to the real economy and its importance for economic dynamics have been come under increased scrutiny after the Global Financial Crisis. Duchin et al. (2010) provide evidence of the decline in real investment following constraints on financing. The authors demonstrate in particular the long-lasting effect of these constraints on real investment and growth. Campello et al. (2010) present survey-based empirical evidence of financial constraints severely limiting investment in technology, employment and capital. Furthermore, the authors show that firms who face constraints tend to draw on outstanding credit lines faster than firms who currently do not face financing constraints. In particular this last point emphasizes the interactions that may emerge between credit providers and firms. It shows that ignoring the structure of these interactions between firms and banks yields an incomplete picture. We can demonstrate this in a toy example.

Imagine an individual bank getting into distress and subsequently reducing its credit lines to its debtors. The consequences for real economic performance are likely to depend on the number of debtors, their economic importance, and their alternative, already existing credit lines. If these debtors are dependent on that single bank and do not have established connections to other banks, they may experience financial difficulties that in turn impact their economic performance. Alternatively, these debtors may all have an alternative bank to turn

to. However, for reasons such as sector-specific lending or others, they may all turn to the same bank which suddenly faces credit requests by a large number of firms, and it may not be in the position to satisfy them all. If our debtor firms all turn to different banks, the shock is more dispersed and may be buffered better by the whole banking system.

A similar argument can be made from the opposite viewpoint. The impact of a company defaulting on its credit depends on the structure of its neighborhood. The first point to consider is whether the impact of this default is concentrated on one bank, or whether it is spread on several banks. In both cases, the next question is the relative importance of that one debtor for its creditors. If it was one of a few important debtors, it may well have consequences for subsequent bank lending behavior. In the case of several creditors, we can make an argument similar to the one presented above. If all these banks adapt their credit policy in response to the default, and if they happen to lend to the same companies, the initial default may be reflected back onto those firms, suddenly making it more difficult for them to get credit from all of their creditors.

These rudimentary scenarios contain a lot of "ifs," and nearly all of these refer to the structure of the credit network between banks and firms. We did not know about the relative importance of the distressed institution for its credit counterparty, and also not about second order connections, that is further counterparties of that initial counterparty. Detailed knowledge of this linking structure is thus important for gaining insights into potential endogenous dynamics due to credit events.

Of course, this argument is not restricted to the possibility of an event as drastic as a default. Changes in revenue, profitability or other factors may all play a role in changing a bank's credit policy towards particular debtors. Similarly, these firm factors may also influence the firm's decisions on their borrowing strategy. Farinha and Santos (2002) confirm this in an empirical study on bank and firm lending in Portugal.

From a methodological viewpoint, this argument stands in broad analogy to the one brought forward by Acemoglu et al. (2012). Here, the authors explore the interaction effects between different sectors of the economy via input-output relations. They go then on to provide a model demonstrating that idiosyncratic shocks to individual sectors may give rise to aggregate fluctuations in output, depending on the network structure.

This paper contributes to the literature by providing an empirical analysis of the bank-firm credit network of the Spanish economy. This network contains two distinct classes of nodes –

banks and firms – , and credit connects nodes from the two sets, never nodes in the same set. It can thus be considered as a bipartite network. From an economic perspective, that means we have data only on real sector credit provision and no information on interbank credit. We subsume all network statistics that are a function of both bank and firm degrees and thus at least partially capture an aspect of this internal linking structure under "bipartite clustering." This is done in analogy to clustering in unipartite networks, a popular set of network-based statistics for the analysis of unimodal graphs.

The development of statistics for bipartite graphs is still subject to ongoing research. New statistics are still proposed in the literature to measure particular aspects of bipartite graphs, and there is so far no broad consensus on a set of standard measures for the description of bipartite networks. As a consequence, this paper has two intertwined goals. The first one is the analysis of the Spanish bank-firm networks. This entails the description of the empirical data with a variety of bipartite clustering statistics in section 3.2. In order to determine whether these statistics can be considered random or not, in section 3.3 we compare them to their counterparts that have been calculated from random networks. The results provide a basis for future research on the evolution of bank-firm credit network topologies.

As a secondary goal, we evaluate the performance of the measures that we employ. This is only possible since we employ various different measures. If one or several measures indicate the existence of trends in the empirical data or nonrandom features in comparison to the simulated networks while another measure does not indicate any differences, this may be seen as evidence against the suitability of that particular measure for the analysis of the networks at hand. While this analysis provides by no means a final answer to the quest for the best bipartite network statistics, it does provide a basis for further discussion.

In section 3.2 we provide a short discussion on methodology and present the empirical data. We analyze the bipartite networks directly and also present summary statistics for their projection networks. Section 3.3 then compares the results from the empirical analysis with results obtained from randomly generated counterparts of the empirical data. We conclude by discussing the potential implications for financial stability in section 3.4.

3.2 Bipartite clustering in the Spanish bank-firm network

3.2.1 Methodology and data

A bipartite network is defined by $G = \{T, B, E\}$ where T is a set of top nodes, B is a set of bottom nodes, and E is a set of links. These links can only be observed between nodes of different sets, not between two nodes of the same set. Many real-world systems exhibit this dichotomy and can thus be modeled as bipartite graphs. Popular examples of large bipartite graphs that have been analyzed in the academic literature are actor-movie networks as discussed in Watts and Strogatz (1998) and Newman et al. (2001), and scientist-publication networks as analyzed in Newman (2001a), Newman (2001b) and Newman (2001c). In the economic sphere, networks of corporate boards and directors have received attention by Battiston and Catanzaro (2004), Conyon and Muldoon (2004) and Robins and Alexander (2004), among others.

While there seems to exist an emerging minimal consensus for relevant statistics on unipartite networks (Newman 2003), the analysis of bipartite networks is still subject to ongoing research. In some cases, researchers overcome this problem by developing tools ad-hoc, for the network at hand. This often impedes the comparison of different networks analyzed by different researchers. Latapy et al. (2008) provide a survey over some of these statistics. Borgatti and Everett (1997) provide an extensive discussion of bipartite network statistics in the context of social network analysis. Among others, the authors present algorithms for cluster detection and centrality measures.

Given the lack of consensus, we employ several different measures of bipartite clustering in this study. This is beneficial for two reasons. As regards the insights into the particular networks at hands, different measures may pick up different aspects of the data. The picture that emerges is thus likely to be richer and more detailed than if we employed only a single measure. From the methodological perspective, this analysis also contributes to the ongoing debate about the suitability of each measure for capturing bipartite clustering.

One way to circumvent the challenges that come with the direct analysis of bipartite graphs is their transformation to unipartite graphs. These can then be analyzed with the established tools of unipartite network theory. This transformation usually is done via one-mode projections, where each bipartite graph gives rise to two projected unipartite graphs. In

one projection graph, the *top projection*, the set of top nodes is kept, and two top nodes are connected in the unipartite projection graph if they share at least one bottom neighbor in the bipartite graph. In the other projection graph, the *bottom projection*, the set of bottom nodes is kept, and two bottom nodes are connected in the unipartite projection graph if they share at least one top neighbor in the bipartite graph. An alternative way of describing the links in the projection graph is to say that two nodes are connected in the projection if the shortest path between them in the bipartite graph has a length of 2. If A is the $|T| \times |B|$ adjacency matrix of the bipartite network, the weighted adjacency matrix of the top projection, P^t, and of the bottom projection, P^b, are obtained as

$$\begin{aligned} P^t_{|T|\times|T|} &= A \cdot A^T \\ P^b_{|B|\times|B|} &= A^T \cdot A \end{aligned} \tag{3.1}$$

where the superscript ^{T} denotes the transpose. The weight of each link in the projections corresponds to the number of common bottom (top) neighbors. The adjacency matrices of the unweighted projections $P^{u,t}$ and $P^{u,b}$ can then be obtained as

$$\begin{aligned} p^{u,t}_{ij} &= min(p^t_{ij}, 1), \quad i,j = 1,..,|T| \\ p^{u,b}_{ij} &= min(p^b_{ij}, 1), \quad i,j = 1,..,|B|. \end{aligned} \tag{3.2}$$

Working with projections of bipartite networks, however, comes with its own challenges. First, there is a loss of information, in particular for unweighted projections. The reason is that the projection is not a bijective function.[1] That is, for a given projection there are multiple bipartite graphs that may have given rise to it. The problem of reconstructing bipartite graphs from projections and possible solutions are discussed by Guillaume and Latapy (2004). Du et al. (2008) explore the problem of information loss in the context of biclique detection. A more general discussion is given in Everett and Borgatti (2013). Here, the authors conclude that in many cases the simultaneous use of both projections is fully sufficient to recover the most important network characteristics, a position that is also maintained by Breiger (1974). For the special case of team identification or network partitioning, Guimerà et al. (2007) show that if weighted projections are used, the loss of information that arises from using only one projection is negligible.

[1] A one-to-one mapping between the two sets.

A second point to consider when working with projections is that the resulting networks are usually very dense. This is of no concern when dealing with benchmark networks in the social networks literature, which only have a few dozen nodes. When working with very large networks, however, this may significantly increase the computational costs of storing, analyzing and modifying the projections.

Finally, the projections may exhibit properties which are not due to particular characteristics in the bipartite graph but due to the application of the projection itself. The most prominent example is clustering. For unipartite random networks, global clustering as defined in equation 3.3 is usually close to zero. However, as Newman et al. (2001), Guillaume and Latapy (2004) and Guillaume and Latapy (2006) show, in unipartite networks arising from projection, global clustering is significantly different from zero.

The data in this study comes for the Bank of Spain Credit Register. It contains direct exposures of banks to firms. Banks are required to report exposures larger than 6'000 EUR. The data was made available in the form of anonymized adjacency matrices for the years 1999-2007. That is, for each year y we have a $|T^y| \times |B^y|$ adjacency matrix with entries $a_{ij}^y \in \{0,1\}$. We thus know only whether there is a loan from bank i to bank j, but not the amount. Furthermore, we do not have consistent bank or firm identification numbers, so we cannot track the individual banks and firms over time. In our case, the links are directed: credit relationships have a clearly defined borrower and a clearly defined lender. However, since all borrowers (firms) constitute the bottom set of nodes, and all lenders (banks) constitute the top set of nodes, the directed links all have the same direction. We can thus treat the network as undirected.

Table 3.1 gives an overview over the empirical data. The number of top nodes (banks), $n_t = |T|$ is declining continuously over the course of the sample. While in 1999 there where 227 banks in the sample, this number shrinks by more than 10% to 193 banks in 2007. The change in the number of bottom nodes (firms) is even more remarkable. It more than quadruples from nearly 50'000 firms in 1999 to more than 200'000 firms in 2007. This increase is accompanied by an increase in the number of bilateral credit connections. It rises from around 100'000 in 1999 to more than 300'000 in 2007. The resulting density of the network, defined as $D = \frac{z}{n_t n_b}$, stays almost constant and well below 1% over the whole sample period. The largest connected component, *LCC*, is defined as the largest connected

subgraph of the original network. Given the low network density, it is surprisingly large over the whole sample period. At each point in time, it contains nearly all nodes.

Given the only moderate increase in the number of banks, the increase in the number of links is reflected in a sizable shift in the degree distribution of banks. This is evident from the increase in the mean, median and maximum degree d^b. The degree distribution of banks is highly skewed, as indicated by the difference between mean degree and median degree. While the median degree increases from 40 to 133 over the sample period, the mean degree increases from 478 to 1771.

In contrast to banks, firms are far less connected. On average firms only have a degree d^f of around two. This average is slightly decreasing over the sample period. The maximum degree of 10 is three orders of magnitudes smaller than the maximum degree of banks. While the total number of links increases, the average number of links per firm actually decreases slightly over the sample. The increase in the number of links is accounted for by the strong increase in the number of firms. These results are in line with previous empirical work for the Japanese bank-firm network (De Masi and Gallegati 2012) and for the Italian bank-firm network (De Masi et al. 2011).

The shortest average path length S reported here is the average over all bank-bank pairs in the largest connected component. On average, it takes less than four steps (i.e. bank-firm-bank-firm-bank) from one bank to any other bank. This average distance becomes slightly shorter over the sample period.

Figure 3.1 sheds more light on the degree distributions of banks and firms. It shows the empirical cumulative degree distributions for banks and firms for each year in the sample. Figure 3.1a shows that bank degrees seem to follow a scale-free distribution over a wide range of the support. The distribution shifts slightly to the right over the course of the sample period, indicating the overall increase in connectivity. The distributions for 1999-2001 are nearly identical, and also the distributions for the years 2002-2004 and 2005-2007 each are very similar. For firms, this grouping is difficult to confirm since the support of the degree distribution is very small. The proportion of firms with a degree of five or less is steadily increasing over time.

	1999	2000	2001	2002	2003	2004	2005	2006	2007
n_t	227	216	218	214	213	209	189	195	193
n_b	54049	60007	61428	98288	108520	119506	183738	206453	202691
z	108610	117249	120698	177636	196045	212122	314574	349651	341899
D	0.009	0.009	0.009	0.008	0.008	0.008	0.009	0.009	0.009
LCC	54261	60219	61642	98496	108731	119711	183925	206640	202875
LCC_t	221	214	216	212	212	207	188	191	189
LCC_b	54040	60005	61426	98284	108519	119504	183737	206449	202686
S	3.80	3.82	3.79	3.72	3.70	3.70	3.66	3.64	3.63
$min(d^b)$	1	1	1	1	1	1	1	1	1
$med(d^b)$	40	41	43	61	65	80	117	124	133
$mean(d^b)$	478.46	542.82	553.66	830.07	920.40	1014.9	1664.4	1793.0	1771.5
$max(d^b)$	17711	19039	19497	27249	29673	31589	43486	48542	47075
$min(d^f)$	1	1	1	1	1	1	1	1	1
$med(d^f)$	2	1	1	1	1	1	1	1	1
$mean(d^f)$	2.01	1.95	1.96	1.81	1.81	1.77	1.71	1.69	1.69
$max(d^f)$	10	10	10	10	10	10	8	8	8
CC_4	0.34	0.36	0.36	0.38	0.38	0.39	0.44	0.46	0.47

Table 3.1 Summary statistics for the empirical bigraphs. For each year, the table shows the number of banks n_t; the number of firms n_b; the number of links z; the network density D; the size of the largest connected component for the total network (LCC) as well as for banks (LCC_t) and firms (LCC_b); the average shortest path length S; *min*imum, *mean*, *med*ian and *max*imum degree for banks (d^b) and firms (d^f); and the global clustering coefficient CC_4.

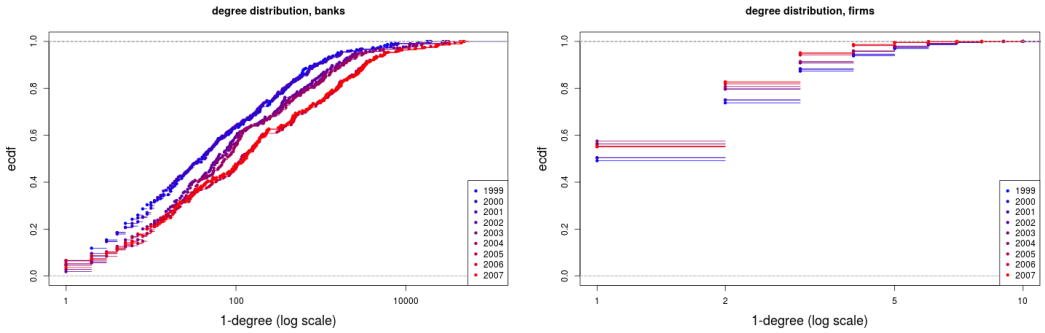

(a) ecdf banks. **(b)** ecdf firms.

Fig. 3.1 Empirical cumulative distribution function (ecdf) of (a) bank degrees and (b) firm degrees.

3.2.2 Bipartite clustering

The second set of statistics, comprising the main focus of this paper, have been designed specifically for bipartite networks. By definition, nodes in bipartite graphs form links only with nodes from the other set. In order to shed light on the structure of the connectivity between nodes of the same set, Latapy et al. (2008) recommend to include the analysis of the 2-degree, d_2. It is defined as the number of unique neighbors of a node's neighbors. In the context of our dataset, the 2-degree of a bank is the number of banks with whom it shares at least one direct credit exposure.

Latapy et al. (2008) point out that the 2-degree alone contains only limited information. A large 2-degree can either be driven by a large 1-degree of the original node, or by large non-overlapping neighborhoods of the node's neighbors. The two extreme cases can be described as follows. In the first case, the original node i is only connected to one node j of the other set, and that one node has degree $d_1(j) = d_2(i) + 1$ where $d_2(i)$ denotes the 2-degree of node i. In the second case, the original node i has $d_1(i) = d_2(i)$ neighbors. Each of these neighbors has a degree of two, and the intersection of any two neighborhoods consists only of node i. In other words, a large 2-degree of node i could be driven either by node i having many direct neighbors who in turn have a low degree, or by node i having few but highly connected neighbors. The authors thus recommend to examine the correlation of the degree and the 2-degree.

For banks, figure 3.2 presents the ratio of 1-degree and 2-degree ("degree ratio"). The first case described above would result to a degree ratio that approaches zero as the 1-degree becomes arbitrarily large. For the second case, this ratio approaches one. Given that firms have an average degree of around 2, we expect the results to be closer to the second case. Indeed, as figure the shows, the average degree ratio steadily increases with the 1-degree and approaches 1 for large 1-degrees. The ratio also becomes less dispersed as the 1-degree increases. Thus, while very large banks have almost as many 2-degree neighbors as 1-degree neighbors, the same cannot be said for medium and small banks. The creditors of large banks seem to be connected to other banks and, more importantly, not all to the same banks. Although the trend is not clear cut, the degree ratio shifts slightly upwards over time.

Figure 3.3 shows the relationship between 1-degree and 2-degree for firms. In this context, the 2-degree of a firm gives the number of other firms with whom it shares at least one common source of credit. Here, the y-axis shows the absolute 2-degree in logarithmic scale since it is orders of magnitudes larger than the 1-degree. Overall, 1-degree and 2-degree are positively correlated. For low-degree firms the 2-degree spans several magnitudes. High-degree firms, that is firms with a larger number of credit connections to different banks, seem to connect to at least one bank with a large number of creditors. Overall, the average 2-degree of firms seems to increase over time. This is not surprising given the temporal evolution of the bank degree distribution discussed before.

In unipartite networks, one popular set of statistics looks at the clustering of nodes. Most commonly, global clustering and local clustering are distinguished. Global clustering as introduced by Watts and Strogatz (1998) is a graph-level statistic. It is defined as the number of triangles, i.e. closed loops of length 3 in the graph G, divided by the number of paths of length 3.

$$C_3(G) = \frac{\Delta}{L_3} \tag{3.3}$$

where Δ is the number of triangles in the graph, and L_3 is the number of paths of length 3 in the graph. In contrast, local clustering is a node-specific statistic. It indicates the density of the subgraph spanned by the neighbors of node i. It is defined as the probability that two neighbors of a node are themselves connected directly:

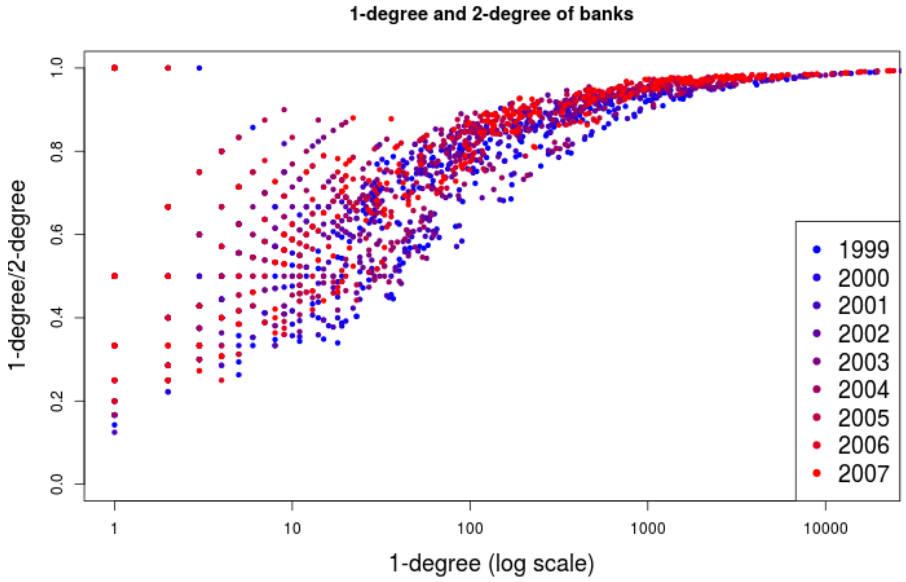

Fig. 3.2 1-degree and 2-degree for banks. The x-axis shows the 1-degree while the y-axis shows the 1-degree, divided by the 2-degree. Consequently, a value of 1 shows that 1-degree and 2-degree are equal.

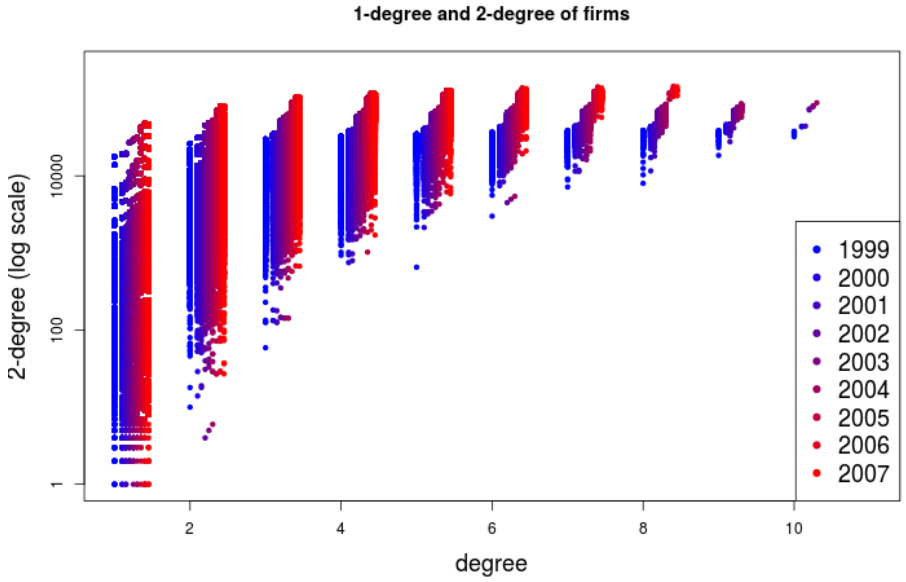

Fig. 3.3 1-degree and 2-degree for firms. The x-values have been shifted slightly to the right for each year of the sample in order to make the plot more readable.

$$C_3(i) = \frac{2t_i}{d_1(i)\,(d_1(i)-1)} \tag{3.4}$$

where t_i is the number of links connecting any two neighbors of node i. Both definitions of global and local clustering in unipartite networks rely on the existence of loops of length 3. Since by definition loops in bipartite networks must have an even length, the concepts of local and global clustering can not be transferred directly to bipartite networks. Researchers have thus come up with various adaptations of the global and local clustering concepts to bipartite networks.

Robins and Alexander (2004) as well as Latapy et al. (2008) extend the notion of global clustering to bipartite networks. The authors define a global bipartite clustering coefficient as four times the number of 4-cycles C_4 divided by the number L_3 of paths of length three,

$$CC_4 = \frac{4C_4}{L_3}. \tag{3.5}$$

The coefficient indicates the probability that among four randomly chosen nodes (two from each set) that are connected by three links, there is also a fourth link present which closes the loop. One interpretation of the coefficient in our context is to regard it as local credit portfolio overlap. It thus answers the following question: If bank i provides credit to firms s and t, and bank j provides credit to firm s, what is the probability that bank j also provides credit to firm t?[2] A coefficient close to 1 would imply that overall, bank portfolios exhibit a large overlap. A coefficient close to 0 would imply that bank portfolios hardly exhibit any overlap on average. The last row in table 3.1 shows the global bipartite clustering coefficient for the empirical networks. It starts off at 0.34 in 1999 and increases to almost 0.5 in 2007. Thus, on average there seems to be significant overlap in bank credit portfolios, and it increased over sample period. However, in particular given that the support of the bank degree distribution spans several orders of magnitude, this global perspective yields only limited information. It is thus necessary to also explore bipartite clustering coefficients on the local level, in analogy to unipartite networks.

Lind et al. (2005) introduce an adaptation of the local clustering coefficient to bipartite graphs. The authors define the bipartite clustering coefficient as

[2] By symmetry, the coefficient can also answer this question with reversed roles: Given that firm s receives credit form banks i and j, and firm t receives credit from bank i, what is the probability that form t also receives credit form bank j?

$$C_4(i) = \frac{\sum_{m=1}^{d(i)} \sum_{n=m+1}^{d(i)} q_i(m,n)}{\sum_{m=1}^{d(i)} \sum_{n=m+1}^{d(i)} [a_i(m,n) + q_i(m,n)]}. \tag{3.6}$$

where $q_i(m,n) = |N(m) \cap N(n)|$ is the number of common neighbors,[3] $\eta_i(m,n) = 1 + q_i(m,n)$, and $a_i(m,n) = (d(m) - \eta_i(m,n))(d(n) - \eta_i(m,n))$. The numerator gives the number of realized 4-cycles involving node i. This is equivalent to the size of the intersection of the neighborhoods of each pair of direct neighbors. The denominator indicates the number of possible 4-cycles. Note that it takes into account the actual degree of the neighbors m and n of node i. While the authors present their statistic as a straightforward extension of local clustering in unipartite graphs, there is a subtle but important conceptual difference between the local clustering definition in equation 3.4 and the local bipartite clustering coefficient as defined in equation 3.6 that deserves to be mentioned.

In the definition of local clustering in equation 3.4, the normalizing factor is given in the denominator as $0.5 \cdot d_1(i)(d_1(i) - 1)$. This is the theoretically maximal number of links between the $d_1(i)$ neighbors of node i, *regardless of their actual degree*. The degrees of node i's neighbors do not impact node i's clustering coefficient. In contrast, the definition in equation 3.6 explicitly accounts for the degrees of node i's neighbors.

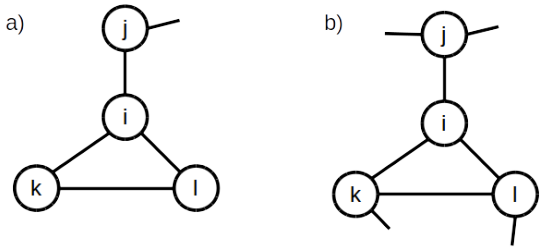

Fig. 3.4 Illustration of clustering coefficients that account for neighbor degrees.

Figure 3.4 illustrates this difference with an example. Assume we are interested in the clustering coefficient of node i. In both subfigures, there is only $t_i = 1$ link connecting its neighbors, the link between nodes k and l. In subfigure a), each neighbor of node i has a

[3] The original definition has an additional term that accounts for direct links between neighbors. Since our network is strictly bipartite, we can safely ignore that component.

degree of 2. Following the definition of local clustering in equation 3.4, we obtain for the local clustering coefficient $C_3(i) = \frac{2 \cdot 1}{3 \cdot 2} = 1/3$. If instead we ask, in analogy to the definition of bipartite clustering in equation 3.6, what the theoretical maximal number of links between neighbors of node i is, *given their degree*, we see that this maximum is one. Since each of the nodes j, k and l has a degree of 2, of which one is already used to connect to node i, only one more link can exist among these three nodes. Thus, a modified clustering coefficient for node i that accounts for the neighbor degrees would be $C_3'(i) = 1/1$.

In subfigure b), each neighbor of node i has a degree of 3. Now, the maximum number of links between neighbors of node i is equal to 3 since each of them could theoretically connect to each other. Just as before, only the link between nodes k and l is realized, and thus here the conditional clustering coefficient would be equal to its unconditional counterpart, $C_3(i) = C_3'(i) = 1/3$. With a larger number of neighbors and a heterogeneous distribution of degrees among them, the computation of the maximal number of links in node i's neighborhood becomes less trivial.[4] This small example shows that the transfer of local clustering as defined in equation 3.4 to bipartite clustering as defined in equation 3.6 does not necessarily allow to draw conclusions by analogy.

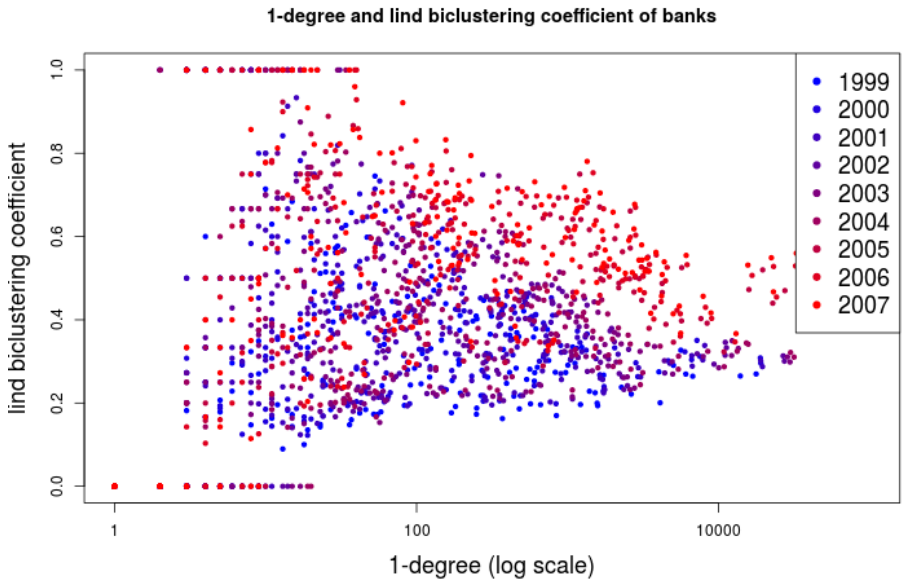

Fig. 3.5 Lind biclustering for banks

[4] To the author's knowledge, no closed-form solution or simple heuristic exists to compute it.

Figure 3.5 shows the bipartite clustering coefficient of banks plotted against the log node degree. There is no significant correlation between node degree and clustering coefficient. However, the dispersion is higher for low-degree nodes, with the coefficients spanning the full range between 0 and 1. With increasing node degree, this range shrinks to $[0.2; 0.5]$ for high degrees. Except for very low degree nodes, the clustering coefficients increase over time. From an economic perspective, the coefficient can be interpreted as follows. For a given bank i, it denotes how big the overlap is between the creditors of all its debtors. If the coefficient is equal to 1, all the bank's debtors share all the same creditors. If the coefficient is zero, the bank's debtors do not share any creditors apart from bank i. Thus, for most banks, there is at least some overlap between their debtors' creditors.

Latapy et al. (2008) and Borgatti and Everett (1997) provide an alternative definition of a bipartite clustering coefficient for pairs of nodes belonging to the same set. For two nodes i and j, it is defined in equation 3.7 as the number of common neighbors, normalized by the size of the union of the two neighborhoods.

$$CC(i,j) = \frac{|N(i) \cap N(j)|}{|N(i) \cup N(j)|} \tag{3.7}$$

If the overlap between the neighborhoods of node i and j is large, then also this clustering coefficient is closer to one. For disjoint neighborhoods, it is equal to 0. The coefficients are then reduced to individual node coefficients $CC(i)$ by averaging the pairwise coefficients over all node pairs (i,k) for which the neighborhood intersection is not empty,

$$CC(i) = \frac{\sum_{k \in N(N(i))} CC(i,k)}{|N(N(i))|}. \tag{3.8}$$

As Latapy et al. (2008) point out, definition 3.7 faces a potential drawback if the degree distribution in the node set is very dispersed. For two nodes i and j with $|N(i)| >> |N(j)|$, the resulting clustering coefficient will necessarily be very small. The reason is that the numerator in equation 3.7 has the smaller degree as an upper bound, $|N(i) \cap N(j)| \leq |N(j)|$, while the denominator has the larger degree as a lower bound, $|N(i) \cup N(j)| \geq |N(i)|$. In our data, the ratio between the largest and the smallest bank degree is on the order of 10^5, and thus this issue is relevant here.

In order to circumvent this problem, Latapy et al. (2008) propose to replace the denominator either with the smaller or the larger degree of the two nodes. This results in the min clustering coefficient

$$CC_{min}(i,j) = \frac{|N(i) \cap N(j)|}{min(|N(i)|, |N(j)|)} \tag{3.9}$$

and the max clustering coefficient

$$CC_{max}(i,j) = \frac{|N(i) \cap N(j)|}{max(|N(i)|, |N(j)|)} \tag{3.10}$$

which both are then reduced to coefficients for individual nodes in analogy to equation 3.8. We refer to the coefficient based on equation 3.7 as union clustering, to the one based on equation 3.9 as min clustering and the one based on equation 3.10 as max clustering.

Figure 3.6 shows the min and max clustering coefficients for banks, plotted against the node degree. The union clustering coefficient is not depicted here since it is almost identical to the max clustering coefficient. The max clustering coefficient in figure 3.6b is very close to zero for most banks. Only very few low-degree banks have a coefficient larger than zero.

The only way large-degree banks could have a max clustering effect significantly different from zero is for their debtors to be connected to other large-degree banks. Given that there are only few large degree banks in our data, this would imply a tightly knit club of a small number of banks with a large number of firms. However, the data do not support this hypothesis.

In contrast, figure 3.6a shows a u-shaped relationship between the min clustering coefficient and the degree. Min clustering decreases rapidly to zero for the degree increasing from one upwards. The coefficient then increases again for large degrees. Thus, low-degree banks exhibit significant portfolio overlap with the creditors of their debtors. To a lesser extent, also high-degree banks exhibit portfolio overlap. However, this overlap occurs most likely on the side of their debtors' low degree creditors since in equation 3.9 the denominator selects their degree instead of the high degree of node i.

The graphic shows that the min clustering coefficient for high-degree nodes decreased over the sample period. For the most connected nodes, a similar grouping arises as in the empirical degree distribution, with the data of the years 1999-2001,2002-2004 and 2005-2007 each being grouped close together.

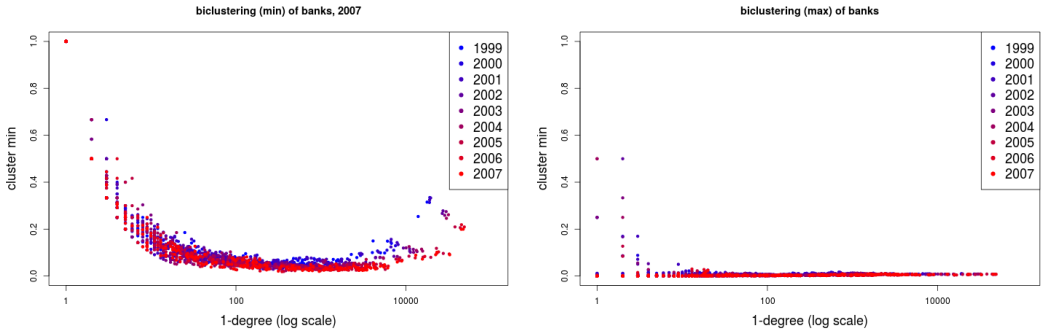

(a) min **(b)** max

Fig. 3.6 Local biclustering coefficients.

As a related statistic, Latapy et al. (2008) also introduce the redundancy coefficient. Its definition is given in equation 3.11. For a node i, the redundancy coefficient is defined as the fraction of the pairs of the direct neighbors of i that are also connected via a path of length 2 through a node other than i. It thus gives the fraction of pairs of neighbors of node i that would still be connected via a path of length 2 even if node i was removed.

$$rc(i) = \frac{|\{\{j,k\} \subseteq N(i), \exists i' \neq i, (i',j) \in E \, and \, (i',k) \in E\}|}{0.5|N(i)|(|N(i)|-1)} \tag{3.11}$$

With regard to projections, this coefficient also indicates whether the projections would change much if node i was removed from the bipartite graph. Thus, whereas the bipartite clustering coefficients indicates the local density, the redundancy coefficient asks whether the number of length-2 paths between two nodes is larger than one. In our context, the redundancy coefficient for banks gives the proportion of its debtors that would still be connected to a common creditor even if this particular bank was on longer part of the network. In a less extreme case, let us assume that one bank starts reducing its credit exposures. If the bank has a high redundancy coefficient, the bank's debtors share the same funding alternatives. Thus, these banks may be receive simultaneous requests for credit extensions from their existing debtors. In contrast, if the first bank had a low redundancy coefficient, these financing requests would be more dispersed in the banking system.

Figure 3.7 plots the bank redundancy coefficient against the bank degree. Overall, bank redundancy correlates negatively with the degree. Also the redundancy coefficients become

less dispersed for increasing node degree. For high degrees, the range spanned by the redundancy coefficients decreases from the interval $[0;1]$ to the narrow range $[0.1;0.3]$. In contrast to the min clustering coefficient before, there is no evidence of a temporal trend. In economic terms, only a small fraction of debtors of large banks shares common creditors beyond that particular bank. For smaller banks, a larger proportion of its debtors share multiple creditors.

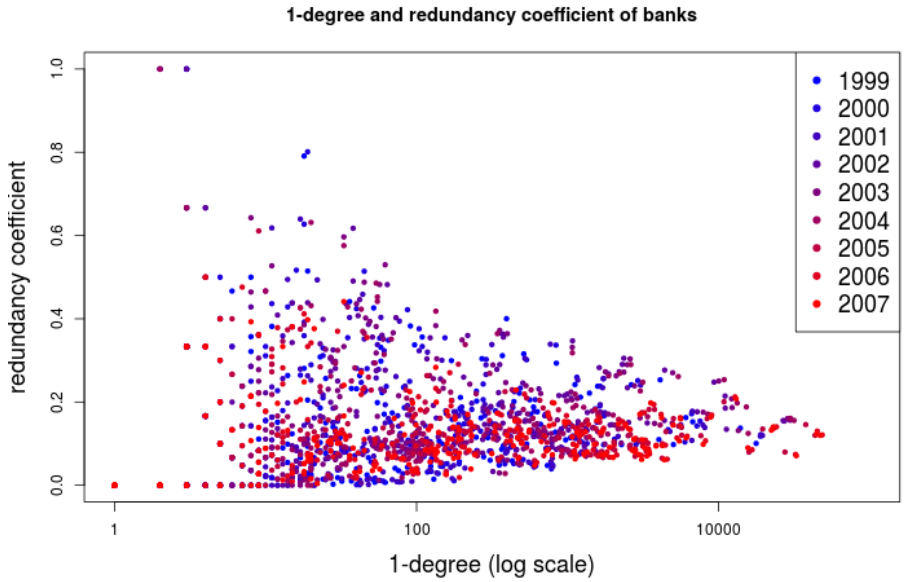

Fig. 3.7 1-degree and redundancy coefficient for banks.

3.2.3 Projections

As discussed in section 3.2.1, one way to circumvent the challenges associated with statistics on bipartite networks is to examine the one-mode projections. For computational reasons, we restrict ourselves at this point to the analysis of the top projections. Table 3.2 shows the summary statistics for the projections. The number of nodes n_t is of course identical to the number of banks in the bipartite networks. The number of links Z decreases over time, though not monotonously. The resulting density D of the networks is low and almost constant, ranging between 7% and 9% over the sample period. The minimum bank degree $min(d)$ in the projection is zero. This is the case for banks that have only have one counterparty. The

median degree $med(d)$ is almost constant over the sample period. The mean degree $mean(d)$ also shows little variation and is consistently larger than the median degree, indicating that the distribution is right-skewed. The maximum degree $max(d)$ decreases slightly over time, analogous to the decrease in firm degrees in the bipartite network. Taken together, the degree distribution as shown in Figure 3.8 appears to be fairly stable over time. Global clustering C_3 as defined in equation 3.3 hovers around 0.45. This is very large compared to random networks, in line with the discussion in section 3.2.1. The table also reports the assortativity A of the network. It is defined as the Pearson's correlation coefficient between a node's degree and the average degree of its neighbors, averaged over all nodes in the network. All graphs in our sample exhibit strong disassortative mixing, that is, the assortativity is smaller than 0. Moreover, it is nearly constant over time.

Figure 3.9 shows the local clustering coefficients. Both figures 3.8 and 3.9 illustrate the loss of information due to the use of projections. In contrast to some of the bipartite clustering statistics employed earlier, we cannot identify any trends over the sample period from the statistics of the projection networks.

	n_t	Z	D	$min(d)$	$med(d)$	$mean(d)$	$max(d)$	C_3	A
1999	227	3920	0.08	0	21.00	34.54	190	0.45	-0.43
2000	216	3501	0.08	0	19.50	32.42	183	0.44	-0.44
2001	218	3434	0.07	0	19.00	31.50	189	0.43	-0.45
2002	214	3663	0.08	0	21.50	34.23	188	0.44	-0.45
2003	213	3761	0.08	0	22.00	35.31	192	0.44	-0.46
2004	209	3578	0.08	0	22.00	34.24	187	0.43	-0.45
2005	189	3280	0.09	0	22.00	34.71	166	0.47	-0.45
2006	195	3372	0.09	0	22.00	34.58	171	0.45	-0.45
2007	193	3315	0.09	0	22.00	34.35	174	0.45	-0.46

Table 3.2 Summary statistics for the empirical top projections: number of nodes n_t; number of links Z; network density D; *min*imum, *med*ian, *mean* and *max*imum *d*egree; global clustering C_3; and assortativity A.

3.3 Comparison to random bipartite networks

The previous chapter introduced a number of statistics for bipartite graphs and described the empirical bank-firm networks of the Spanish economy. In this chapter we go one step further

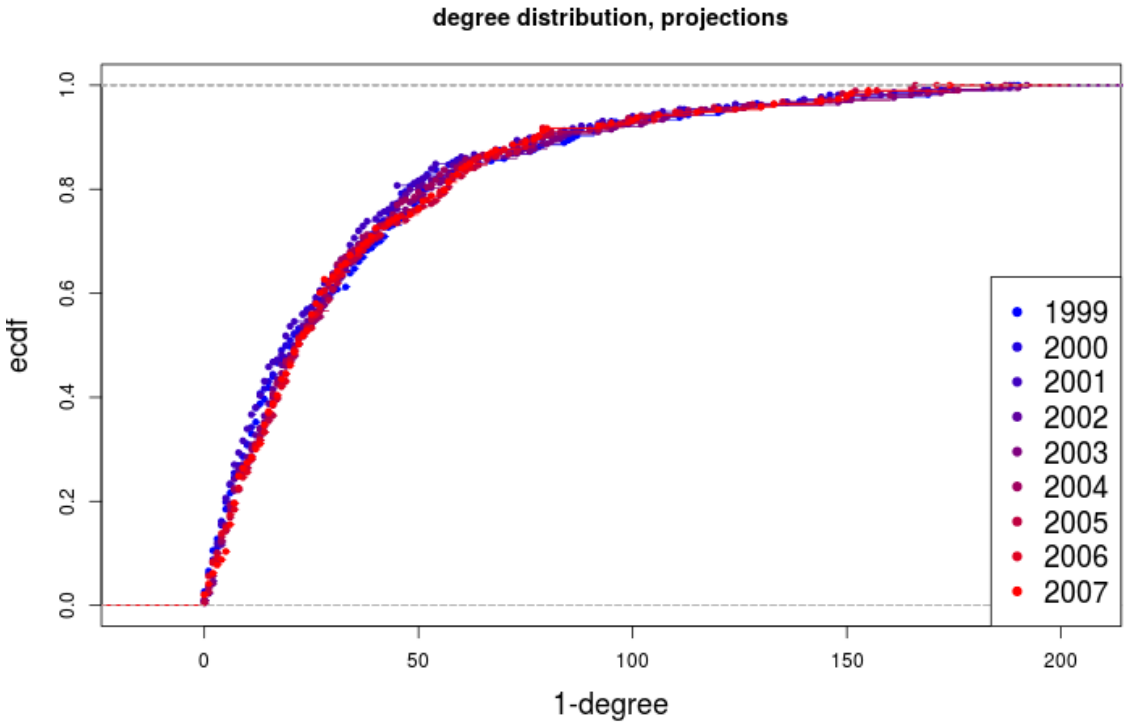

Fig. 3.8 Cumulative bank degree distribution, projections.

and compare the bipartite structure of the empirical networks to random bipartite networks. More precisely, we do not know to what extent the bipartite clustering coefficients that we observe are a consequence of the particular degree sequence of our bipartite networks, and to what extent they contain additional information. We want to distinguish those bipartite clustering values that arise naturally as a consequence of the degree sequence from those that arise specifically in our empirical data. For this purpose, we generate random networks with the same number of nodes as the empirical ones. We then calculate the bipartite clustering coefficients on these new networks and compare them to the empirical ones.

The question as to what extent local node properties such as the node degree distribution determine global network properties such as clustering is subject to ongoing research. Squartini et al. (2011a) and Squartini et al. (2011b) analyze the world trade web with respect to this problem. They find that if the network is unweighted, the degree sequence is fully informative. In other words, the assortative behavior and the clustering that are found in the network are typical for the given degree distribution. In contrast, for the weighted networks,

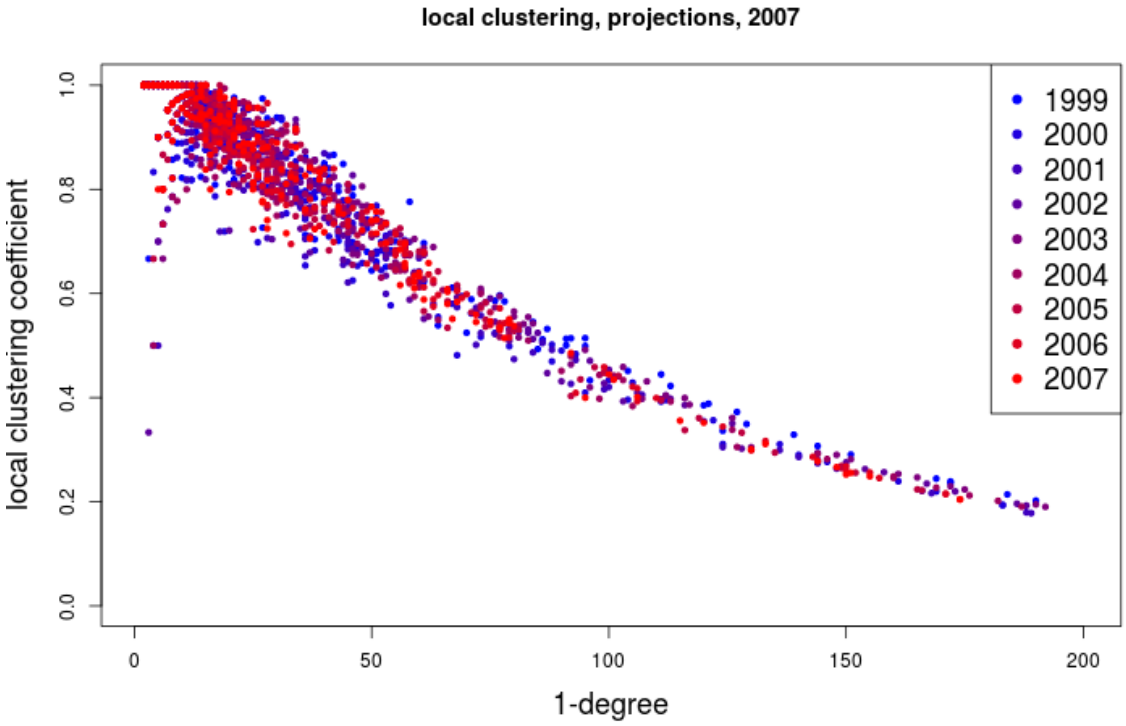

Fig. 3.9 Local clustering of banks, projections.

the values of these global properties differ significantly from their random counterparts and yield thus additional information.

The first question regarding the generation of random benchmark networks is whether we want to keep the node degrees in a statistical sense by preserving the mean node degree, or whether we insist on keeping the actual degree sequence. The former approach leads to random graph models while the latter are termed configuration models. Since the random graph approach only preserves the mean degree, it is best suited for networks where the degree distribution spans a narrow range and is fairly symmetrical. Given the large support of the bank degree distribution and its skewness, the random graph approach is thus most likely to produce vastly different graphs in our case. We thus use a configuration model, keeping the actual degrees of banks and firms from the empirical data but linking them randomly. This can be done in several ways. One approach that is often used is the *Local Rewiring Algorithm* (LRA) as described by Squartini et al. (2011a), among others. The algorithm consists of the repetition of a single step, often called *link swap*. First, we randomly select two links l_1 and

l_2 from the network. Let link l_1 connect the nodes a and b, and link l_2 connect the nodes c and d. It is important that the nodes a, b, c, and d are four distinct nodes, that is the links l_1 and l_2 must not share nodes. Then, we delete the links l_1 and l_2 in the network and replace them with the new links l_1' connecting nodes a and d and link l_2' connecting nodes b and c. One can model this procedure as a Markov Process where each admissible network is one state of the world. For a detailed discussion of the LRA and possible extensions, see Maslov and Sneppen (2002), Maslov et al. (2004), Serrano et al. (2007) and Opsahl et al. (2008).

The LRA shares a shortcoming with other network generating algorithms, and that is the fact that it may produce biased results. In other words, not all networks that are specified by fixing the degree sequence are equally likely to be generated. A detailed description of how the bias arises and potential remedies are described by Artzy-Randrup and Stone (2005). The authors suggest an extension of the LRA that they term "Switching and Holding" strategy. It manipulates the Markov transition probabilities in the above approach, i.e. the probability for the link pair to be swapped, in a way as to guarantee a uniform distribution over the graphs. Coolen et al. (2009) and Roberts and Coolen (2012) discuss this problem in a general framework for the analysis of constrained graph dynamics. The former develop the general solution for undirected graphs while the latter extend it to directed graphs. While these approaches are theoretically feasible, they are too computationally expensive for our purposes. Furthermore, the extension of these algorithms to bipartite networks has not yet been explored in practice.

As a consequence, we rely on a simpler, so-called *degree-stub* approach to generating random networks. Instead of starting with a complete network and then pairwise rewiring the links, we remove initially all the links from a network. The remaining skeleton contains only the nodes and for each node its target degree. We then pick randomly one top and one bottom node. If both have not yet reached their target degree, we link them together. If one of the nodes or both have already reached their target degree, or if there is already a link connecting these two nodes, we discard the pair and draw a new one. This procedure is repeated until all nodes have reached their target degree. For unipartite networks Squartini et al. (2013) and Squartini et al. (2015) point out that also this approach may be biased. However, since the question has not yet been answered for the case of bipartite networks, we give it the benefit of the doubt.

With the approach described above, we generate 100 random networks for each empirical network. Table 3.3 shows the summary statistics for the simulated bigraphs. Each cell shows the mean value over all 100 simulations, with the standard deviation given in parentheses. Just like their empirical counterparts, the largest connected components in the simulated networks cover nearly the entire network. The shortest average path lengths are, on average, significantly lower than those in the empirical networks. The simulated networks also have higher global biclustering coefficients. As an additional statistic, we look at the Jaccard Index to measure network similarity. It is defined on pairs of networks as

$$J = \frac{Z_{11}}{Z_{11} + Z_{10} + Z_{01}} \tag{3.12}$$

where Z_{11} is the number of links that are present in both networks, and Z_{01} and Z_{10} are the number of links that are present only in one of the networks but not in the other.

J_{emp} represents the average Jaccard index between each simulated network and its empirical counterpart. We can see that on average less than 10% of the links present in the empirical networks are also generated randomly in the empirical ones. J_{sim} represents the average Jaccard index over all 4550 unique pairings of simulated networks for each year. The similarity among them is of a similar magnitude as the similarity between simulated and empirical networks.[5]

We now look at the statistics we discussed in the previous section, computed for the simulated networks. Here we only report the results for the networks based upon the empirical network of 1999. The results for the other years are comparable, and the corresponding graphics can be found in the appendix.

Figure 3.10 shows the 1-degree and the degree ratio for banks, both for the empirical network (red) and the simulated ones (grey). Of course the 1-degree is the same for simulated and empirical networks. Thus, any difference between simulated and empirical networks in this figure arises from differences in the linking structure between firms and banks. For both empirical and simulated data, the degree ratio is positively correlated with the 1-degree. However, the figure shows that the simulated networks exhibit lower degree ratios for almost

[5] One has to interpret this statistic with caution. Since the nodes in our networks are only identified by their degree, it might be possible to arrive at a higher Jaccard index by switching nodes with the same degree in one network in order to increase network similarity. That is, if nodes k and l (both belonging to the same set) have the same degree, we could assign the links for node k to node l and vice versa.

	$\|LCC\|$	$\|LCC_t\|$	$\|LCC_b\|$	S	CC_4	J_{sim}	J_{emp}
1999	54272(0.0)	224(0.0)	54048(0.0)	3.24(0.011)	0.44(0.0012)	0.07(0.0005)	0.08(0.0006)
2000	60221(0.6)	215(0.5)	60006(0.1)	3.24(0.011)	0.47(0.0012)	0.09(0.0005)	0.09(0.0005)
2001	61644(0.3)	217(0.2)	61427(0.1)	3.24(0.016)	0.46(0.0010)	0.09(0.0005)	0.09(0.0005)
2002	98500(0.0)	213(0.0)	98287(0.0)	3.06(0.006)	0.52(0.0013)	0.07(0.0004)	0.07(0.0004)
2003	108731(0.0)	212(0.0)	108519(0.0)	3.02(0.007)	0.52(0.0013)	0.07(0.0004)	0.07(0.0003)
2004	119713(0.4)	208(0.2)	119505(0.1)	2.99(0.009)	0.53(0.0012)	0.07(0.0004)	0.07(0.0004)
2005	183925(0.4)	188(0.2)	183737(0.1)	3.05(0.015)	0.59(0.0010)	0.06(0.0003)	0.06(0.0003)
2006	206646(0.5)	194(0.3)	206452(0.2)	3.09(0.017)	0.61(0.0010)	0.06(0.0003)	0.06(0.0002)
2007	202882(0.4)	191(0.2)	202690(0.1)	3.08(0.016)	0.62(0.0009)	0.06(0.0003)	0.06(0.0003)

Table 3.3 Summary statistics for the simulated bigraphs. For each year, the table shows the size of the largest connected component for the total network (LCC) as well as for banks (LCC_t) and firms (LCC_b); the average shortest path length S; and the global clustering coefficient CC_4; and the Jaccard indices for the simulated networks (J_{sim}) and for the empirical networks (J_{emp}). Standard deviations are given in parentheses.

all banks. This is equivalent to stating that the simulated networks produce higher 2-degrees. Since the sum of bank degrees is the same in the simulated and the empirical networks, the only admissible interpretation is that in the simulated networks there is less overlap in the neighborhoods of firms that have at least one common creditor. Furthermore, the degree ratio is far less dispersed for the simulated networks.

Figure 3.11 shows the 2-degree for the firms. For small 1-degrees, the simulated and empirical data match well. As the 1-degree increases, the 2-degrees of the simulated networks span a larger ranges compared to their empirical counterparts. The 2-degrees of the empirical networks tend to be located close to the upper limit of these ranges. Taken together, the firms in the simulated networks exhibit lower 2-degrees on average.

Figure 3.12 shows the biclustering coefficients. The coefficients of the random networks differ significantly from their empirical counterparts. While 1-degree and biclustering coefficient are negatively correlated for the empirical data, the simulated data show a positive correlation. For both networks the dispersion of the clustering coefficient decreases with increasing 1-degree. However, overall the empirical data are far less dispersed than their empirical counterparts. This is similar to the results obtained for the 2-degree of banks in figure 3.10.

Figure 3.13 shows the min clustering coefficients. Overall the empirical data lie well within the narrow band spanned by the simulated networks. The figure shows the same

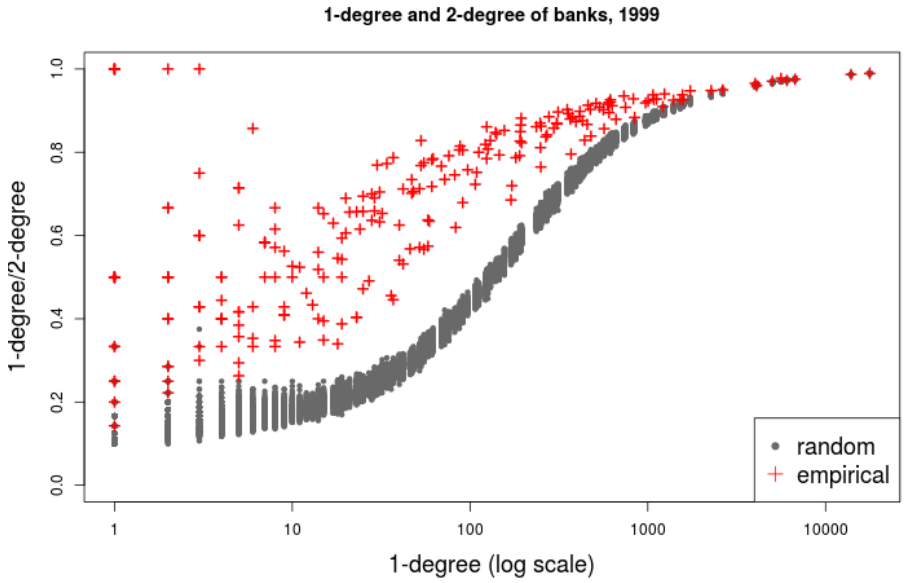

Fig. 3.10 Random networks: 1-degree and 2-degree, banks.

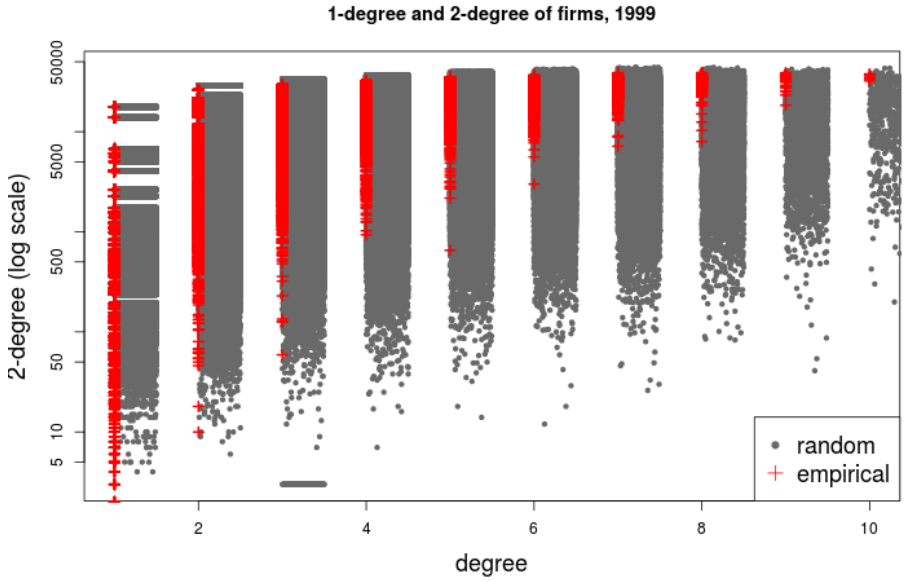

Fig. 3.11 Random networks: 1-degree and 2-degree, firms.

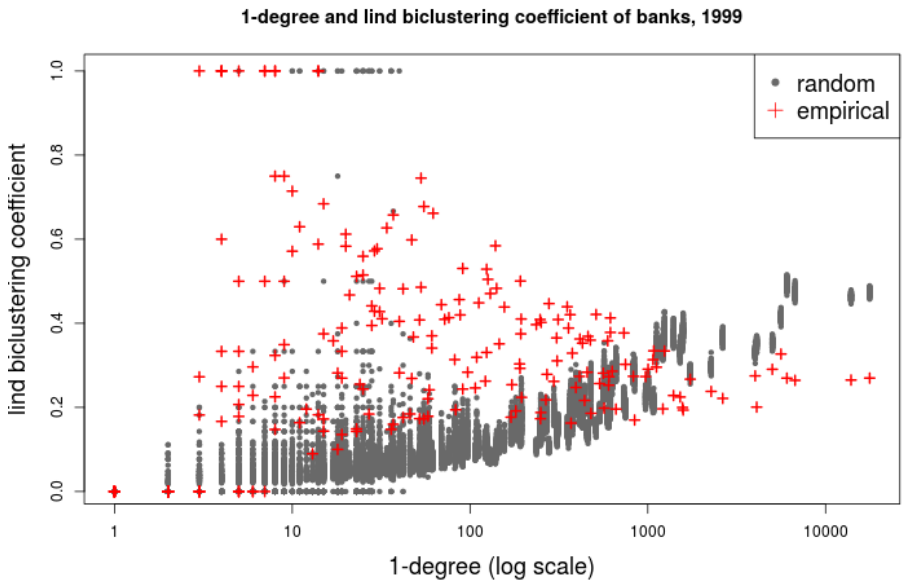

Fig. 3.12 Random networks: Lind biclustering, banks.

u-shaped relationship for the coefficients of the empirical and simulated networks. The only noteworthy difference is that for the two nodes with the highest degree, the empirical coefficients are slightly larger than their simulated counterparts.

Figure 3.14 shows the max clustering coefficient as defined in equation 3.10. While the coefficient does not deviate visibly from zero for the empirical graph, the coefficients of the simulated networks span the interval $[0.0; 1.0]$ for low degrees before they gradually decline to zero for degrees larger than 50. The empirical coefficients are well within the range of the simulated networks. They tend to stay at the lower bound of the range spanned by their simulated pendants.

Figure 3.15 shows the redundancy coefficients. Here, the difference between simulations and the empirical data is quite visible. For the simulated networks, except for a few low-degree nodes, no coefficient deviates from zero. This stands in stark contrast to the coefficients derived from the empirical network. They are scattered in a significantly broader range that becomes slightly narrower with increasing 1-degree.

Table 3.4 shows the aggregate network statistics for the bank projections. Each cell shows the average value across all 100 simulations, with the standard deviation given in parentheses. On average, the projections of the simulated networks have more than double the number of

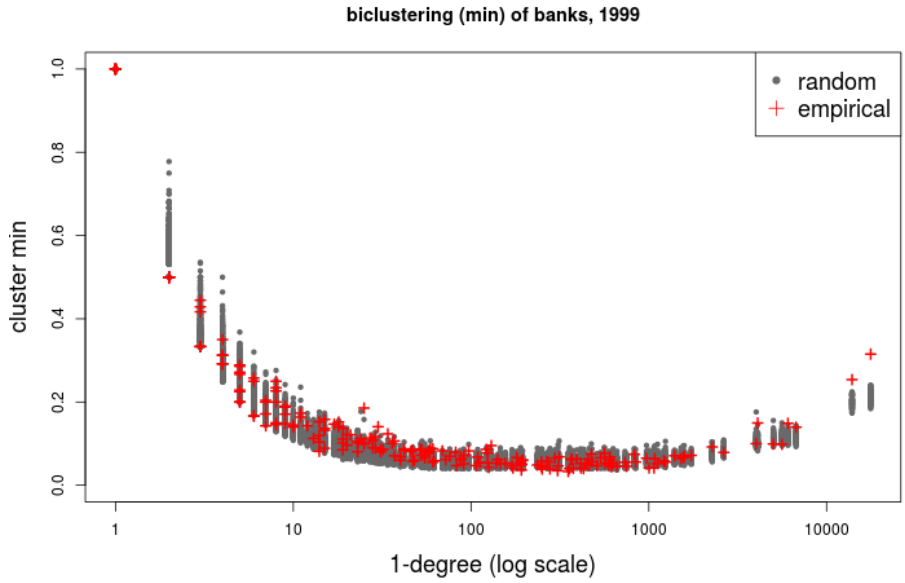

Fig. 3.13 Random networks: min clustering, banks.

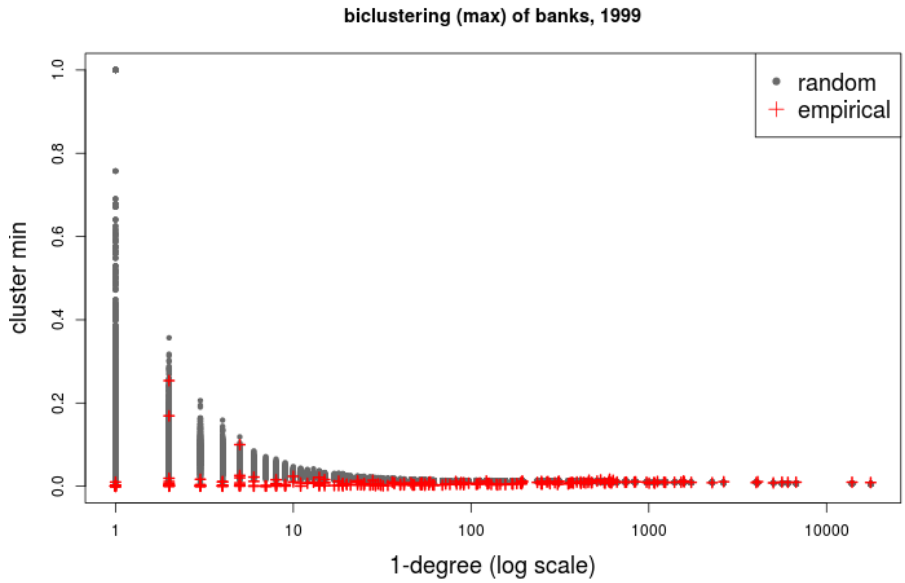

Fig. 3.14 Random networks: max clustering, banks.

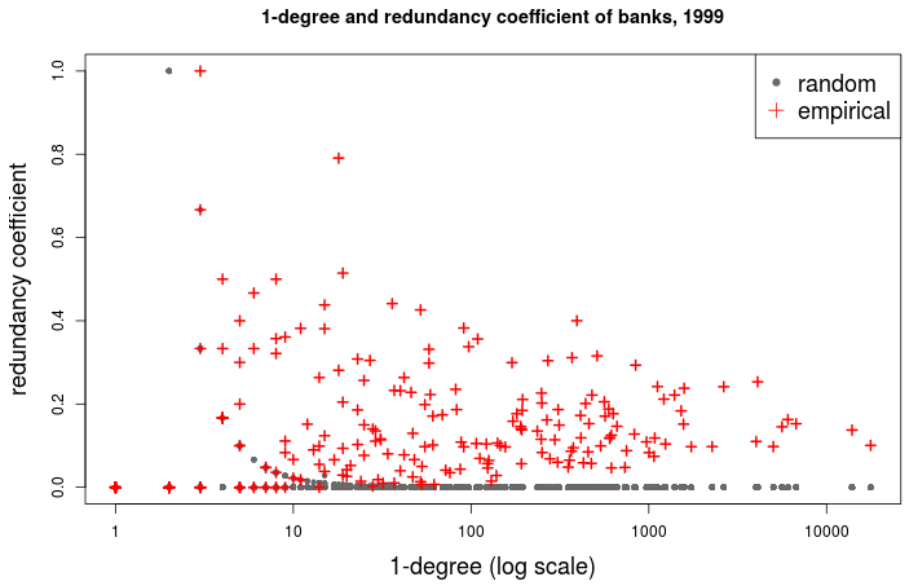

Fig. 3.15 Random networks: redundancy, banks.

links than the empirical projections. Of course, this implies the same relation in the network densities since the number of nodes is equal in empirical and simulated projections. Global clustering is also significantly higher in the simulated networks. Its average exceeds 0.7 over the whole sample period, compared to around 0.45 for the empirical projections. In contrast to the empirical projections, the simulated projections exhibit slightly positive assortativity. Taken together, while the projections do not indicate trends over the sample period, the empirical projections differ significantly from their simulated counterparts. This difference is further confirmed in the degree distributions of the simulated and empirical projections in figure 3.16. In the empirical projections, 80% of banks have a degree of less than 60. In contrast, in the simulated projections 40% of the banks have a degree of more than 130. Figure 3.17 shows the local clustering coefficients. They stay on one level around 0.7 for small 1-degrees. Only for 1-degrees larger than 100 do they correlate negatively with the degree. In contrast, the empirical data do not exhibit this plateau for small degrees.

	Z	D	C_3	A
1999	9910(53)	0.19(0.001)	0.72(0.003)	0.06(0.019)
2000	9018(50)	0.19(0.001)	0.71(0.003)	0.04(0.019)
2001	9224(52)	0.19(0.001)	0.71(0.003)	0.04(0.020)
2002	10665(52)	0.23(0.001)	0.74(0.003)	0.07(0.017)
2003	10956(48)	0.24(0.001)	0.75(0.003)	0.07(0.016)
2004	10918(54)	0.25(0.001)	0.76(0.002)	0.07(0.017)
2005	8599(42)	0.24(0.001)	0.79(0.003)	0.10(0.020)
2006	8868(48)	0.23(0.001)	0.79(0.003)	0.10(0.016)
2007	8678(45)	0.23(0.001)	0.78(0.003)	0.09(0.017)

Table 3.4 Summary statistics for the simulated top projections. For each year, the table shows the number of links Z; the network density D; the global clustering coefficient C_3; and the assortativity A. Standard deviations are given in parentheses.

3.4 Conclusions

This paper had two intertwined goals. The first goal was to describe the linking structure of the Spanish bank-firm credit network, and to test whether it can be considered random. The second goal was to examine different statistics on bipartite graphs as to whether they can detect differences between empirical and random networks. As for the first goal, we have provided strong evidence for nonrandom linking behavior in the Spanish bank-firm credit network. The second goal needs to be answered in a more detailed manner. The statistics employed in this study performed differently, both in detecting trends over time, and in distinguishing random and empirical networks.

Our first candidate statistic was the 2-degree. For both banks and firms, this statistic exhibits subtle trends over time. However, the statistic yields different results for banks and firms regarding the distinction of simulated and empirical networks. For banks, the degree ratio of the simulated networks moves in a narrow band. The data points of the empirical networks are clearly outside that band. For firms, the 2-degrees in the simulated networks exhibit a broader range than the ones in the empirical networks. The data points of the empirical networks are located at the upper limit of that range.

Next, we examined the biclustering coefficient. For the empirical networks, this coefficient does not exhibit a significant correlation with the 1-degree. However, the dispersion of

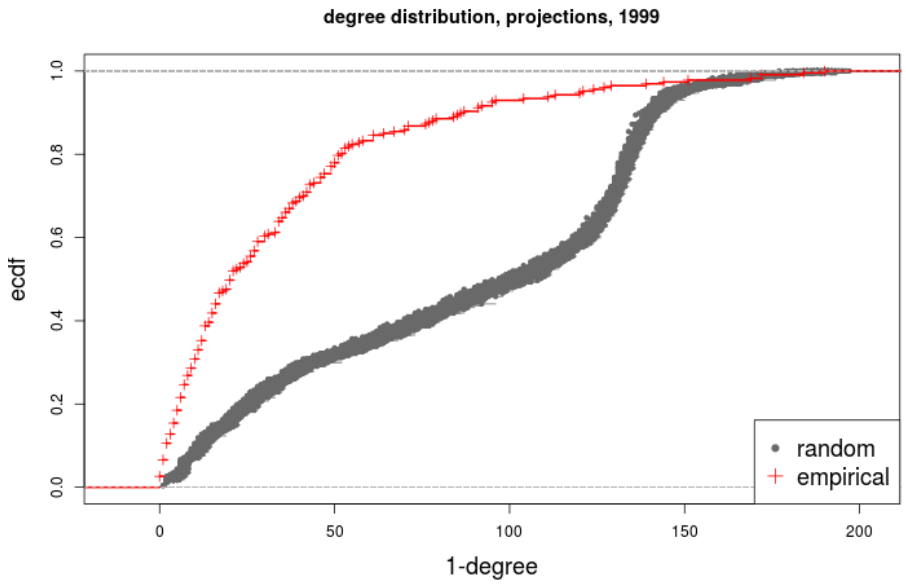

Fig. 3.16 Random networks: degree distribution of projections, banks.

the statistic decreases for increasing 1-degree. Also, there is a slight temporal trend visible. The biclustering coefficients in the simulated networks differ visibly from their empirical counterparts. They do not mirror the dispersion of the empirical coefficients but move in a narrow band, except for a few outliers. Moreover, the coefficients of the simulated networks are positively correlated with the 1-degree.

Union, min and max clustering differed in their performance both regarding the detection of temporal trends and the distinction of simulated and empirical data. Given the wide support of the bank degree distribution, union and max clustering turned out not to be very useful for our purposes. Both coefficients are very close to zero for most nodes. Min clustering, however, exhibited a u-shaped relationship to the 1-degree. For the most connected nodes, we also found a grouping over the years similar to the one in the degree distribution. The min clustering coefficients of the empirical networks were well within the narrow range spanned by their simulated counterparts. It was thus unable to detect any differences between the empirical and the simulated networks.

The most pronounced distinction between the empirical and the simulated networks is given by the redundancy coefficient. It is dispersed over a broad range for the empirical networks. In the simulated networks, however, it remains very close to zero for most nodes.

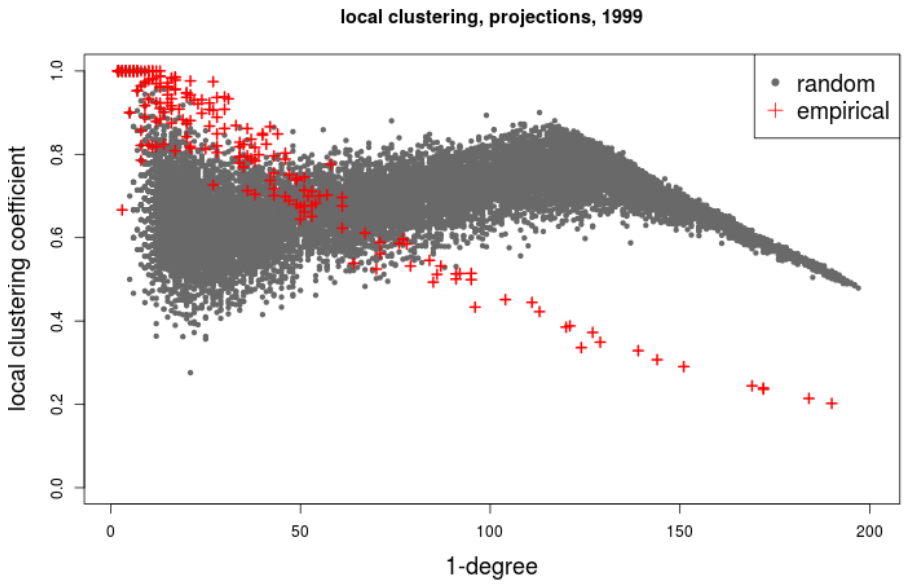

Fig. 3.17 Random networks: clustering in projections, banks.

The top projections of our data exhibit significant differences to their simulated pendants. The simulated networks are twice as dense as their empirical counterparts. They also have a significantly higher clustering coefficient. And while the empirical projections are strongly disassortative, the simulated networks are slightly assortative.

Moving beyond the statistics, what do these differences from random networks imply for financial and economic stability? On a global scale, the larger empirical 2-degree for small and medium-sized banks indicates that their debtors tend to share a large proportion of their financing alternatives. For large banks, the overlap between their debtor's creditors is less pronounced as compared to the random benchmark. Consequently, changes in the policy of a big bank, or even a default, is likely to spread out more among its debtor's other creditors. From a stability perspective, two consequences are possible. Either this spreading out dissipates the initial shock to an extent that is easily absorbed by the system. Or, in the case of a more severe shock, the distress spreads faster through the network since the affected number of banks is larger. Which of these two is more likely depends on parameters that are outside the scope of this paper, such as the size of loans and the behavior of banks and firms.

On the local level, the picture that emerges is slightly different. Both the biclustering coefficient and the redundancy coefficient indicate that for small banks, local clustering is

more pronounced than for large banks. The higher biclustering coefficient implies a larger proportion of pairwise credit portfolio overlaps for small and medium banks. Similarly, the higher redundancy coefficient for small and medium banks implies that in case of financial constraints imposed by one bank, other banks would be affected by reactions from multiple firms at the same time.

To sum up, the joint analysis of several bipartite clustering statistics has allowed us to clearly establish the nonrandom linking structure in the Spanish bank-firm network. While not all the measures we employed were able to detect these differences, they are nevertheless stable over the sample period. Three directions for further research emerge from the insights gained here. First, the exact behavior of these statistics and their relations to each other deserve further research efforts. Besides deepening our understanding of each of them, this will help to arrive at a commonly agreed upon set of measures for bipartite networks. Second, the question of why the empirical data deviate from their random pendants deserves attention. Richer datasets of bank-firm networks may explore possible avenues of explanation such as balance sheet variables, sectoral differences and geography. Finally, the implications of the bipartite particularities identified here for stability need to be explored along the lines of Lux (2016).

Chapter 4

Interactions of Macroprudential and Monetary Policy in Housing Markets

4.1 Introduction

Housing markets have played a pivotal role in many of the financial and banking crises in modern history. White et al. (2014) estimate that housing booms have preceded the majority of financial crises in recent years. With house purchases often being credit financed, they lend themselves to classic boom-bust cycles à la Kindleberger and O'Keefe (2001). This susceptibility for deep and prolonged crises is aggravated by housing supply being slow to adjust, and the indivisibility of housing (Hartmann 2015). In the Euro Area, at the end of 2016 outstanding housing credit stood at almost 150 % of GDP while outstanding housing credit constituted almost 15% of bank's total assets. Thus by size alone, the sector poses a potential risk to the financial system and the broader economy alike. On the household side, housing often constitutes the largest component of wealth.

This repeated occurrence of financial crises (Allen and Carletti 2013), in particular the Global Financial Crisis that started in 2007, has made it clear that monetary policy alone is inadequate to ensure financial stability. Not only is this not a primary goal of monetary policy (Taylor 2007), but even if it were, its effectiveness can be quite limited, as Lambertini et al. (2013) demonstrate. Thus, a further branch of regulation aimed at increasing the overall stability of the financial system, or macroprudential policy, has been continuously developed in the past years. The tool set available to macroprudential policy makers these days is broad. Among the options listed in ESRB (2014) are countercyclical as well as

systemic risk capital buffers, and caps on bank leverage ratios, loan-to-value (LTV) ratios and debt-service-to-income (DSTI) ratios. The novelty of these policy measures as compared to conventional monetary instruments, and the complex interactions between monetary and macroprudential policy, market participants and market dynamics make the impact assessment of macroprudential regulation an active area of research.

This paper contributes to the development of macroprudential policy by examining the joint effects of monetary policy and macroprudential policy on housing markets. In an agent-based model with agents following simple heuristics similar to those found in real-world housing markets, we explore the combined impact of interest rates on the one hand and maximum LTV and DSTI ratios on the other hand on the market outcome. Compared to generalizations drawn from empirical studies, our approach allows for potentially nonlinear feedback effects (Turrell 2016) and endogenous interactions between regulation, loan portfolios and housing markets. It thus responds to the need for an integrated analytical framework that has been pointed out by Galati and Moessner (2013) and others. Section 4.2 reviews the literature, section 4.3 presents and discusses our model design. Section 4.4 presents the results of our simulations, and section 4.5 concludes.

4.2 Literature

Although the Global Financial Crisis has boosted the discussion and development of macroprudential policy measures, there is no consensus in the literature regarding the ultimate roots of the housing bubble (Glaeser et al. 2012). A series of papers (Geanakoplos 2001; 2010a;b) makes the case for high bank leverage and low collateral requirements and against low interest rates as the primary causes. In a similar vein, Khandani et al. (2013) maintain that credit market conditions, not interest rates were the main driver of the pre-crisis housing boom. Duca et al (2011) as well as Haughwout (2011) agree on the importance of leverage for the crisis. However, the empirical analysis by Glaeser et al. (2012) raises doubts on leverage as the primary culprit of the housing boom in the early 2000s. The common denominator of this strand of literature is the agreement on the need for macroprudential regulation as a complement to monetary policy.

The origins of the concept of macroprudential regulation can be traced back all the way to the 1970s (Clement 2010). It is however not until the 2000s, especially after the onset of the

Global Financial Crisis in 2007 that the topic has received increased attention by academics and regulators alike (Hartmann 2015). Given the link between credit-fueled housing bubbles and financial crises, regulatory authorities around the world have begun to put increased focus on indirect housing market supervision through bank regulation. For a review of the debate surrounding the evolution of macroprudential regulation, see Clement (2010) and Galati and Moessner (2013). Nier et al. (2011) provide a discussion of the institutional designs of macroprudential policy. Akinci and Olmstead-Rumsey (2015) document the increase in the use of macroprudential policy measures following the onset of the Global Financial Crisis.

Discussions of the macroprudential policy tool box and their rationale can be found in Galati and Moessner (2013), Wachtel (2013) and Draghi (2014). Of these, Galati and Moessner (2013) highlight in particular the need to examine the potential interaction effects between monetary and macroprudential policy, though in their review the latter is mainly restricted to capital-based measures. Regarding the subset of borrower-based measures, Hartmann (2015) finds that LTVs, employed in 16 EU countries, are the most frequently used measure. This is confirmed by Darbar and Wu (2016) who, in a set of five case studies, find LTV ratios and DSTI ratios among the most popular macroprudential measures.

Assessing the effectiveness of macroprudential policy measures is still subject to ongoing research.[1] Since this type of policy is still at a comparatively early stage, the amount of empirical data is limited. Furthermore, cross-country heterogeneity severely limits the room for robust conclusions, as Hartmann (2015) points out. Alberola et al. (2011) analyze ten years of Spanish experience in macroprudential regulation. They come to the conclusion that dynamic risk provisions helped mitigate the build up of risk. The authors also hint at the unresolved challenge of integrating monetary policy and financial stability. Darbar and Wu (2016) provide country-specific descriptive analyses of macroprudential regulation for a set of five countries. The heterogeneity of the sample however prohibits generally applicable conclusions, highlighting one of the main challenges for the empirical impact assessment. Similarly, in a comprehensive analysis of the effects of macroprudential regulation in 49 countries, Lim et al. (2011) point to country heterogeneity as one of the main challenges. Cerutti et al. (2015) find macroprudential regulation to be more effective in less developed and more closed economies. Their analysis suggests that regulatory arbitrage may still be one

[1] Going even further, Galati and Moessner (2013) maintain that there is still no definite agreement on the very goals of macroprudential policy.

of the biggest hurdles for effective macroprudential regulation. Reinhardt and Sowerbutts (2015) present similar findings. The authors examine regulatory arbitrage as a reaction to macroprudential regulation. They find that while capital-based policy measures allow foreign branches to benefit from looser regulation in their respective home countries, policies aimed at the regulation of lending standards are more likely to provide a level playing field. Claessens et al. (2013) find that lending-based measures as well as measures aimed at curbing bank credit growth are more effective than countercyclical capital buffers in combating systemic risk. Overall, macroprudential policies are found to be more effective in reducing the boom than in mitigating realized systemic risk during the bust. This assessment is shared by Cerutti et al. (2015). Vandenbussche et al. (2015) analyze macroprudential measures in Central, Eastern and Southeastern Europe and find capital-based approaches to be the most effective.

On the theoretical side, Allen and Carletti (2013) demonstrate the effects of macroprudential policy in a rational agent model with a "normal" and a "boom and bust" regime. The authors find that low interest rates can trigger a housing bubble if sufficiently high LTV caps allow for a corresponding credit expansion. This demonstrates the need for a joint analysis of macroprudential and monetary policy. LTV caps themselves limit bubbles effectively, but the authors complement the empirical findings by pointing out that in regulatory practice the challenge to close loopholes such as foreign financing continues to exist. Agur and Demertzis (2015) provide a simple analytical model of the decision problem of banks facing monetary policy and macroprudential regulation. They show that even in the presence of macroprudential regulation, monetary policy still has an impact on financial stability. Benigno et al. (2011) study the interaction between monetary policy and macroprudential regulation in a model with nominal rigidity and financial frictions. The authors make a case for monetary policy to focus on inflation targets. Within their model, the gain in welfare from inflation-focused monetary policy always outweighs the costs in terms of financial stability.

Moving from the supply to the demand side, a number of authors have put forward models of housing markets aimed at replicating the stylized facts of boom-bust cycles. Barras (2005) provide a model of the London housing market. They note that rents and leases are slow to respond to market changes, due to long-running contracts. Given the low adjustment speed of supply that is inherent in housing markets, construction is always of speculative nature. For London, the authors document an average construction delay of two to three years and price

cycles with an average length of 12-15 years. Vacancies are negatively related to rent prices and positively related to the rate of completion while developments seems to extrapolate rent changes: high changes in real rent are followed by increased new construction. The authors then provide a model for the housing market in lagged linear differential equations based on a New-Keynesian growth model. Boom-bust cycles emerge endogenously as the result of fluctuations in construction, rent prices and vacancy rates.

Glaeser et al. (2008) provide a model where rational bubbles can exist only under the condition of a constant housing supply. However, if agents can exhibit irrational optimism, housing booms can also take place when housing supply is elastic. In this case, the benefit of shorter bubbles is outweighed by the costs of a larger build-up during the bubble, leading to an ultimate welfare loss from housing supply elasticity. The authors also point out that high transaction costs and the lack of short-selling opportunities may be partially responsible for sustained deviations from fundamentals.

In a setting of incomplete information, Glaeser and Nathanson (2015) provide a model with house buyers extrapolating recent transaction price trends into the future. These naive beliefs are sufficient to induce price swings that are in line with empirical facts. In particular, their model replicates house price momentum over one year, mean reversal over five years and excess long-term volatility.

The models discussed so far operate with representative agents. By construction then, they neglect the potential impact of household income and wealth distributions on housing market dynamics. However, several authors have argued that these features might be important to explain the recent housing bubble (Turrell 2016, Shiller 2012, Rajan 2011). Some, if not all (Baptista et al. 2016) of these shortcomings can be compensated for in agent-based models. By modeling not the aggregate market but the individual participants, household heterogeneity can easily be included into the model design. Agent-based models have also been used for years in the mortgage industry for the prediction of mortgage portfolio performance and prepayment prediction (Geanakoplos et al. 2012).

Gilbert et al. (2009) provide one of the first agent-based models of a housing market. In their spatial model, the authors focus on the interaction between buyers, sellers and realtors. Houses have a fixed location, and realtors cover specific geographical regions of the market. This is also reflected in the price setting, with prices of newly available houses being determined by the prices of recent transactions in the local neighborhood. The model

incorporates LTV caps and a broad analogy to what can be thought of as DSTIs. Households trade houses if the ratio of debt service to current income leaves a pre-specified band. The model demonstrates the emergence of richer and poorer areas as a result of the location-dependent price-setting. On the policy side, lower LTVs are shown to reduce the interest rate sensitivity of house prices.

Kouwenberg and Zwinkels (2015) adapt the methodology of numerical agent-based models as they have been pioneered in financial economics. In these models, agents are not modeled explicitly on the individual agent level. Instead, the proportions of a finite number of agent types in the population changes endogenously. In close analogy to structurally similar models of financial markets, the model produces endogenous house price fluctuations.

Erlingsson et al. (2014) examine the interaction of housing markets and business cycles in an agent-based model. The authors find a u-shaped relationship between credit conditions and output. While housing credit expansion may increase output in the short run, it makes the economy more susceptible to recessions. If credit conditions become too tight, however, output also suffers.

McMahon et al. (2011) run policy experiments in a spatial model of the housing market. The authors impose the actual interest rates set by the Federal reserve over the years 1993-2009 onto their model and show that this is sufficient to generate a housing bubble that bursts in 2007. However, the lack of explicit lending standards makes it impossible to compare this hypothesis to alternatives such as the often discussed low lending standards.

Pangallo et al. (2016) and Ge (2013) examine the interactions of income distributions and spatial segregation in housing markets. Ge (2013) find that ease of access to credit is positively correlated with higher prices but also with price volatility and the number of foreclosures. The presence of investors in the model, i.e. agents who buy to rent, increases spatial segregation.

Geanakoplos et al. (2012) build a detailed model of the housing market in the greater Washington D.C. area. The major innovation of their work is that it is built upon merged agent-level data on household income and wealth, housing features, transaction data and mortgage service data. In comparison to the previously discussed models, their framework allows for the detailed simulation of agent-level procedures of household search, loan approval and mortgage service. This illustrates the closer mapping between model and observed reality that can be implemented in computational agent-based models as opposed to more abstract

representations in the representative agent models discussed above. The authors succeed at replicating a variety of housing market statistics during the housing boom in the early 2000s. Using counterfactual simulations, the authors show that stricter lending standards in the form of lower LTVs would have been sufficient to prevent the housing bubble.

This approach is taken up by Baptista et al. (2016) who modify and extend the model by Geanakoplos et al. (2012) in their analysis of the UK housing market. Again in a model based on a vast array of agent-level empirical data, the authors find that the introduction of maximum loan-to-income ratios can significantly reduce housing booms.

4.3 Model Structure

Our model consists of n_h^0 houses, n_{hh}^0 households and n_b banks. Households have an initial income which is drawn from a gamma distribution, as proposed by Salem and Mount (1974), McDonald (1984) and Singh and Maddala (2008), plus a minimum income i^{min}. The gamma distribution is capped at the 99.5%-ile, and thus the support of household incomes is given by $[i^{min}, \Gamma^{-1}(.995)]$. Households also start with an initial wealth in the form of cash. It is set to a fixed multiple of their initial income, $c_i = \gamma \cdot i_i(0)$. Households are assumed to have an infinite lifespan. They may own a house, and they may take out a mortgage for purchasing a house. Households may move to another house within the model and they may exit from the model. We assume the houses to have an infinite lifespan, too, and unit size. Banks are the most passive actors in our model. They are only represented by the portfolio of loans they have granted, and the profit they earn on it. Banks have a maximum loan-to-value (LTV) ratio and a maximum debt-service-to-income (DSTI) ratio, both of which limit the size of loans they can offer to households. Both LTV and DSTI ratios are treated as exogenous in our model, representing regulatory constraints. The interest rate at which loans are offered is assumed to be exogenous, too, and the same for all banks. For the most part, we bundle all loans into one portfolio, equivalent to one bank. The model can easily be extended, however, to multiple banks.

The assumption of unit-sized households arises from the following considerations. First, with heterogeneous house sizes, matching buyers and sellers becomes more complicated and computationally intensive. Matching houses and households along two dimensions, budget and size, tends to make the housing market less efficient, resulting in fewer transactions for

a given number of houses and households. In order to obtain the same market liquidity as measured by transaction volume, a larger number of houses and households would be needed. Since the purpose of our model is not to examine market frictions and search and matching costs, we deem it acceptable to simplify the framework to unit size houses. Second, if house sizes and thus also house prices follow a nondegenerate distribution, the functioning of the housing market in the model depends on a proper match between the house price distribution and the distribution of household budgets. Changes in the regulatory environment can lead to sudden shifts in either of these two distributions. The resulting mismatch between the two distributions in the transition period can lead to a collapse of the model and thus limits the range of policy regime changes that can be examined with this model. For example, imagine that an increase in the loan-to-value ratio can shift the distribution of buyer's budgets suddenly upwards. If previously the budget distribution was roughly congruent with the price distribution, now we have high income households that cannot find a house in their price range, and small houses that are unattractive even for their previous low-income buyers. This necessitates further model features to adjust for the mismatch. While we can imagine that in the real world this collapse does not occur due to for example sufficiently adaptive agents, the limited scope of our model calls for simplification, and we have omitted this feature. Our model can thus be thought as representing a sufficiently homogeneous sector of the overall housing market.

The assumption of infinitely lived houses also arises from our intention to reduce the complexity of the model. If houses had a finite lifespan, this feature would have to be reflected in the valuation of houses. All else equal, houses with a residual lifespan of only a few periods would be expected to be less valuable than newly built houses that are expected to last many more periods. In earlier iterations of the model we accounted for this by representing the house price via a discounted cashflow model along the lines of Kajuth et al. (2013). While this can be made to work, it introduces an additional layer of complexity into the model without providing any additional explanatory power for our purpose. We thus simplified the model in later iterations and replaced the finite lifespan of houses with a simple stochastic mechanism. Each period, each house is destructed with a small but fixed probability $p_{destruct}$. While this provides a need for construction in order to maintain the housing stock, it relieves us from the necessity of lifespan-dependent valuations. In small-scale simulations, the model behavior did not change significantly due to this simplification.

Another simplification we implemented in the model regards the household budgeting. We keep the cash position of each household constant over time. In the real world, the repayment of mortgages increases the equity of households, which, in case of a transaction, becomes available as cash. The stock of cash is thus experiencing exponential growth, rendering the model nonstationary. We examined several options during model development in order to cope with this. First, we can accept it as a feature of real-world housing markets and restrict ourselves to studying the detrended model results where appropriate. Second, we can introduce model features that depreciate the value of housing to the extent that it compensates for the growth in equity induced by mortgage repayments, for example by means of maintenance costs. This would yield a potentially stationary but more complex model. Third, we can allow ourselves to relax the household budget calculation by assuming a constant cash position. This solution unites both advantages, and we arrive at a simpler model that still is potentially stationary. Since the cash position is only relevant at the time of a house purchase, one possible interpretation is that new buyers always come from outside the model, drawn from a stable income and cash distribution. Again, several options were tested in a small-scale version of the model, and this simplification did not induce any significant change in the results.

The simulation runs for t_{max} periods. Each period t, the following steps are executed. Households that have been homeless for more than t_{mh} periods are removed from the simulations. This simulates households that have grown frustrated with the long search for an affordable house and leave the market. In order to keep the overall number of households constant, leaving households are one by one replaced with new households. The aggregate income of the newcomers is equal to the aggregate income of the quitters in order to keep the total income in the model constant.[2]

Next, household incomes are updated. They follow a mean-reverting process that keeps the aggregate income constant. First, each household's income $i(t-1)$ is updated to $i^*(t)$ by a mean-reverting shock as shown in equation 4.1 with mean reversion parameter α. The innovations $\varepsilon_i(t)$ are i.i.d normally distributed, $\varepsilon_i(t) \sim N(\mu_i, \sigma_i)$.

[2]Again, this is a simplification. A more realistic alternative would be to have a constant influx of new households looking for a house, and having this influx reach an equilibrium with the number of households that quit. However, in this setting it is less obvious how to keep aggregate income constant.

$$i_i^*(t) = i_i(t-1) + \alpha \cdot (i_i(0) - i_i(t)) + i_i(t-1) \cdot \varepsilon_i(t) \tag{4.1}$$

Second, in order to keep the aggregate income constant, each household's income $i_i^*(t)$ is adjusted by the normalization factor $\nu = \frac{\sum_j i_j(t-1)}{\sum_j i_j^*(t)}$ as shown in equation 4.2. If the shocks increased the aggregate income, i.e. if the mean shock was larger than zero, ν will be smaller than one, thus decreasing each household income so that the sum of incomes is the same as last period. If the mean shock was smaller than zero, ν will be larger than one, and household incomes are increased, again to ensure that the sum of incomes stays the same as last period.

$$i_i(t) = i_i^*(t) \cdot \nu \tag{4.2}$$

With a fixed probability p_{move}, each household that currently owns a house is moving within the city, thus putting its house on the market.[3] Now, households check whether they are default. This can happen for two reasons. First, due to the income shocks they just received, household's residual income, i.e. income minus mortgage payment, may fall below a certain absolute minimum income $\underline{i}$. This reflects the minimum residual income that is needed to cover the per-period costs of living. If households cannot cover these costs, they default on their mortgage. Second, households may default if the market value of their house is lower than the outstanding mortgage, resulting in negative equity. In both cases, households are removed from the model, and their houses are put on the market. Also the construction projects that were initialized l_c periods ago are now finished and put on the market as well.

The price of houses that are newly available for sale is set at a constant markup $\overline{m}$ over last period's average transaction price $\overline{p}(t-1)$,

$$p_k^{ask}(t) = (1+\overline{m}) \cdot \overline{p}(t-1). \tag{4.3}$$

[3] In earlier iterations of the model and in analogy to Barras (2005), households would move only if their income change put their preferred debt-service-to-income (DSTI) ratio outside a prespecified band, such as $[.2; .4]$. That approach, however, required a very careful calibration of the parameters of the mean-reverting income processes in order to arrive at a somewhat stable number of movers and thus a stable housing market without adding any explanatory power.

Now, all households that are looking for a house - we denote them as active - calculate their budget. Household budgets $b_i(t)$ consist of the cash c_i and loan assurances from banks as equation 4.4 shows.

$$b_i(t) = c_i + l_i^{max}(t) \tag{4.4}$$

The maximum loan households can obtain is the smaller of the maximum loan under the LTV constraint and the maximum loan under the DSTI constraint,

$$l_i^{max}(t) = min\left(l_i^{LTV}(t), l_i^{DSTI}(t)\right). \tag{4.5}$$

The maximum loan under the LTV constraint is calculated as follows. From the budget equation 4.4 and the definition of the maximum LTV as the ratio of loan and price,

$$LTV := \frac{l_i(t)}{p_k^{ask}(t)}, \tag{4.6}$$

we can derive the following relation between the cash position $c_i(t)$ and the maximum loan for a given LTV:

$$l_i^{LTV}(t) = c_i \cdot \frac{LTV}{1 - LTV}. \tag{4.7}$$

The second restriction is the maximum debt service to income (DSTI) ratio of households. This can be thought of either as a restriction on the side of households, i.e. they prefer to pay at most $s = \alpha \cdot i_i(t)$, $\alpha \in [0,1]$ in monthly payments, where α is the affordability parameter. Alternatively, this can also be viewed as a regulatory constraint requiring banks to limit debt service to a maximum proportion of the debtor's income. For a loan with nominal amount l, duration T_m and per-period interest rate r, the size of the per-period payment for each period $t = 1...T$ can be calculated as

$$s = l \cdot \frac{(1+r)^{T_m}}{\sum_{\tau=0}^{T_m-1}(1+r)^{\tau}}. \tag{4.8}$$

From this, we can solve for the maximal nominal l given a payment s as

$$l = s \cdot \frac{\sum_{\tau=0}^{T_m-1}(1+r)^{\tau}}{(1+r)^{T_m}}. \tag{4.9}$$

Restricting the DSTI ratio to α amounts to setting $s = \alpha \cdot i_i(t)$, and we obtain a second upper bound for the loan as

$$l_i^{DSTI}(t) = \alpha \cdot i_i(t) \cdot \frac{\sum_{\tau=0}^{T_m-1}(1+r)^\tau}{(1+r)^{T_m}} \tag{4.10}$$

Combining the two, the maximum loan available to household i is given by equation 4.5, and the budget by equation 4.4.

With houses for sale and potential buyers fully specified, the market works as follows. For each house that is for sale, we first determine the set of suitable buyers. For a given house k, a household most fulfill three conditions to be considered suitable. First, it must be active, i.e. currently looking for a house to buy. Second, its budget $b_i(t)$ must be larger than the asking price of the house, $b_i(t) \geq p_k(t)$. Third, the asking price of the house must be equal to or greater than a fixed fraction of the household's budget, $p_k(t) \geq f_i \cdot b_i(t)$. This reflects the preference of households to employ as much of their budget as possible. If there is more than one household that fulfill all three conditions, the buyer is chosen at random, and the house is transacted to its new owner. The new owner takes out the maximal admissible loan and pays for the rest with cash. This maximal admissible, or final, loan is calculated as

$$l_i^{final}(t) = min\,(l_i^{max}(t), p_k(t) \cdot LTV) \tag{4.11}$$

The first term in the brackets is known from equation 4.5 and reflects the binding constraint. The second term reflects the fact that if the LTV is binding, the maximal admissible loan may be less than the theoretically maximal loan in equation 4.7. The reason is that the maximal loan in equation 4.7 was calculated indirectly, from the cash position. This implicitly assumes that the household buys a house at a price equal to its total budget. If the actual price is smaller than the household budget, i.e. if the denominator in the Loan-To-Value is smaller, the same loan would result in a higher realized LTV.

Let us clarify this last point with a small numerical example for better understanding. Imagine that the LTV is at 50% and binding. For a household with a cash position of 1.0, this results in a theoretically maximal loan of 1.0 and a budget of 2.0. If this household acquires a house at the price of 1.8, it cannot take the full loan promise made by the bank. The reason is that at a price of 1.8, a loan of 1.0 would result in a realized LTV of $1.0/1.8 = 55.6\%$.

This violates the maximum LTV constraint of 50%. Instead, at a transaction price of 1.8 and an LTV of 50%, the household can take out a loan only of 0.9.

Bank loans are kept in a single portfolio. This allows us to track credit volume as well as return on the credit portfolio over time. We refrain from modeling banks in more detail at this point due to bank level heterogeneity (Buch and Goldberg 2016).

The average price of all successful transactions $\overline{p}(t)$ is recorded as reference price for next period's new offers. The prices of unsold houses are decreased by a fixed fraction d_r,

$$p_k^{ask}(t+1) = (1-d_r) \cdot p_k^{ask}(t). \tag{4.12}$$

Houses are destructed if their ask price falls below a certain fraction f_{pmin} of this average transaction price,

$$p_k^{ask}(t+1) < f_{pmin} \cdot \overline{p}(t). \tag{4.13}$$

In a last step, we update construction. The process of constructing new houses is assumed to take l_c periods until the houses are completed and can be put on the market. In line with previous literature (Krainer 2002), we assume that the level of new construction activity $C(t)$ is linear in the expected price level at the time the construction is finished:

$$C(t) = \alpha_0 + \alpha_1 E_t[\overline{p}(t+l_c)]. \tag{4.14}$$

Expectations are formed by simple extrapolation from current price level and the average price change over the past l_p periods:

$$E_t[\overline{p}(t+l_c)] = \overline{p}(t) + \frac{l_c}{l_p} \sum_{\tau=1}^{l_p} \cdot (\overline{p}(t-\tau+1) - \overline{p}(t-\tau)) \tag{4.15}$$

Thus, at time $t+l_c$, $C(t)$ new houses will be put on the market. Table 4.1 provides the default values for all parameters of our model.

parameter	description	value
n_h^0	initial number of houses	2000
n_{hh}^0	initial number of households	3000
$\underline{i}$	lower bound income distribution	500
s_Γ	shape parameter income distribution	1.3
r_Γ	rate parameter income distribution	0.001
α_i	mean reversion household income	0.2
μ_i	mean shock household income	0.0
σ_i	standard deviation household income	.15
p_{move}	probability for household to move	0.02
$p_{destruct}$	probability for houses to be destructed	0.005
$\overline{m}$	mark-up for house sale	0.02
d_r	mark-down for unsold houses	0.01
l_c	construction lag	12
l_p	lookback period for price expectation	12
f_{pmin}	fraction minimum house price	0.8
r	interest rate on mortgages	0.03/12
T_m	mortgage duration	$15 \cdot 12$
LTV_0	loan-to-value ratio	0.7
α_0	debt-service-to-income ratio	0.3

Table 4.1 Model baseline parameters.

4.4 Results

4.4.1 Illustration of model dynamics

In this section we illustrate the temporal evolution of the major model variables and the reaction of the model to changes of the policy parameters. When examining policy changes, our model runs over four phases. The first one is used to allow the model to settle into a statistical equilibrium. Here, we use a burn-in period of 2000 simulation steps. The second phase of another 1000 time steps is used to collect the pre-change statistics. Policy changes are then executed over a transition period of 100 periods during which the chosen policy parameter changes linearly from its old to its new value. Afterwards, the model runs for another 1000 periods which allows us to collect the post-change statistics.

Figure 4.1 shows an example of the temporal evolution of our simulated housing market. In this case, the maximal LTV changes at $t = 3000$ from $LTV_{lo} = 0.5$ to $LTV_{hi} = 0.9$ during the transition period, indicated by the vertical dotted lines in the graphs. The first 1000 periods in the graphs show that the model has settled into a statistical equilibrium. All variables fluctuate within narrow ranges. The policy change over the periods 3000-3100 impacts nearly all variables of interest in the model. Figure 4.1a shows the average transaction price and the range of transaction prices. We see that in line with expectations the transaction price level increases as a reaction to the policy change. In the post-change period, the average transaction price is 9.2% higher than in the pre-change period. The increase in the average price level is accompanied by an increase in volatility, with the standard deviation increasing from 1.5% to 2.5%. The shaded area shows the range spanned by minimal and maximal transaction price in each period. It stays roughly the same at 6% of the average transaction price. The figure shows also the quasi-periodic nature of transaction prices, which seems to be more pronounced at higher LTV levels. Figure 4.1b shows evolution of the housing stock. The construction sector reacts to the increase in transaction prices by increasing the supply of housing. In comparison to the price level, the housing stock takes a much longer time to settle into a new equilibrium.

Since defaults in the model are very rare, Figure 4.1c shows the aggregate number of defaults in a moving 100 period window. While the model offers the possibility of both strategic defaults and defaults due to adverse income shocks, only the latter materialize in

this simulation. With an increase in the LTV, this number begins to rise as well. Figure 4.1d shows the impact of the policy change on the binding credit constraints of house buyers. We would expect that if the LTV constraint is loosened, less households experience it as the binding constraint in their application for a loan. This intuition is confirmed by the simulation: With the increase in the maximum LTV ratio, the proportion of new loans for which the LTV is the binding constraint - we call it "LTV ratio" for short - decreases from 73% to 33%. Figure 4.1e shows the impact on the size of the loan portfolio of banks. First, we see that the portfolio increases by almost 50%. This is a combined effect of higher mortgages on already existing houses and a larger overall number of houses and thus mortgages due to increased construction. Figure 4.1f demonstrates the effect on per-period bank profits. For the most part, profits remain at the level of interest rates. The downward spikes that occur in irregular intervals are defaults of individual households. Their seemingly pronounced impact on bank profits in this graphic has two reasons. First, the impact of an individual loan on the profit of the portfolio decreases with the number of loans in the sample. Since the number of agents and thus loans in this simulation is limited and thus portfolio concentration is relatively high, each household has significant impact on the performance of the portfolio. Second, the graph depicts the per-period profit. With periods roughly modeled as months, aggregating them into quarterly or annual numbers would smooth out the spikes considerably. In analogy to figure 4.1c, figure 4.1f shows the increase in the number of defaults as an increase in the number of negative spikes. Still, the effect on average profit is negligible. Compared to the pre-change period, the slightly increased number of defaults reduces the profit only by 1%.

4.4.2 Exploration of policy parameter space

In order to get an idea of the overall behavior of the model under different policy settings, we simulated the model for a three-dimensional grid spanned by the policy parameters LTV, DSTI and interest rate. Table 4.2 shows the policy parameter ranges that we explored. Overall, this approach resulted in nearly 2000 simulations. Here we present the most interesting findings.

Each of the following heat maps shows the average value of one model variable. We keep one policy parameter fixed, and the remaining two parameters vary along the axes of the heat

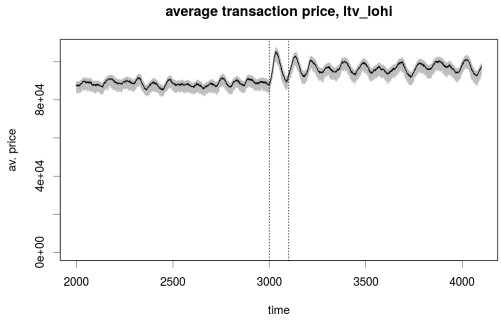

(a) transaction price.

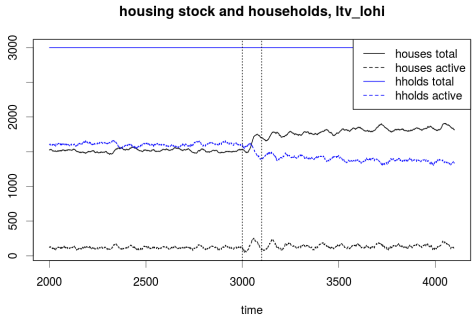

(b) number of houses and households.

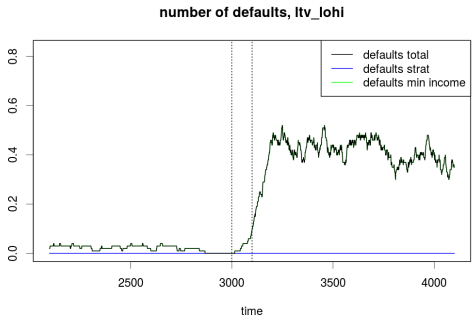

(c) number of defaults.

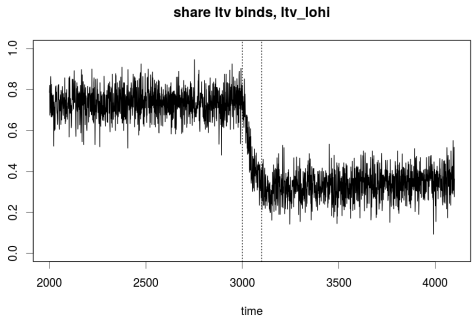

(d) share ltv binds.

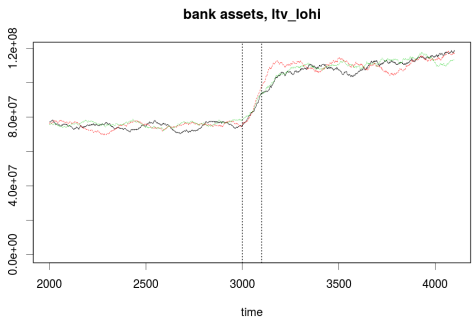

(e) bank assets.

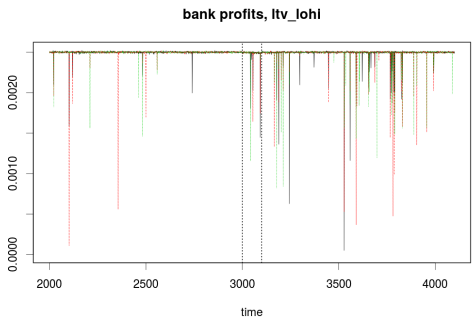

(f) bank profits.

Fig. 4.1 Reaction of the model to an increase in the LTV.

parameter	min	max	steps
maximum LTV	0.5	0.9	11
maximum DSTI	0.2	0.6	11
interest rate	0.01/12	0.08/12	15

Table 4.2 Policy parameter ranges.

map. Similar to before, all statistics were computed from 1000 periods after a burn-in period of length 2000.

Figure 4.2a shows the average transaction price along DSTI and interest rate for an LTV of 0.9. The heat map shows that the interest rate has hardly any influence on the average transaction price level. Similarly, in figure 4.2b, we can see that the share of new loans for which the LTV is the binding constraint depends only moderately on the interest rate. The reason for this is that with the given parameters, the DSTI loan constraint in equation 4.10 is far more sensitive to changes in the DSTI than to changes in the interest rate. However, the interest rate does have an impact on the number of transactions as well as on the number of defaults, as figures 4.3a and 4.3b show.

The number of defaults increases in both DSTI and interest rates. As before, all defaults are due to household income falling below the minimum household income needed for survival. Higher DSTIs allow households to have a smaller buffer of income above the residual income, thus increasing the probability that a series of negative income shocks drives them into insolvency. Higher interest rates ceteris paribus also increase the monthly payment, thus having a similar effect on the default probability. The average number of transactions also reacts to both interest rate and DSTIs. Both higher DSTIs and lower interest rates potentially increase the maximum loans that households can obtain. While this may mean for some high-income households that their budget increases to a point where they are no longer classified as suitable buyers, the larger number of low-income households that can now afford a house leads to an overall increase in potential buyers. Consequently, the number of transactions increases.

On the bank side, figure 4.4 shows the pronounced difference between a low and a high LTV environment. Figure 4.4a shows that for an LTV of 0.5, the DSTI plays hardly any role for the volume of the loan portfolio. The reason is that the low LTV acts as the binding constraint for the majority of new loans, effectively rendering the DSTI unimportant. The

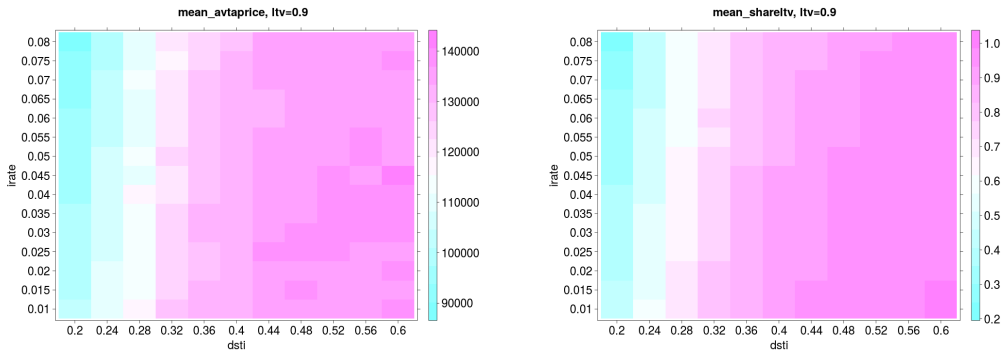

(a) average transaction price **(b)** share of new loans bound by LTV

Fig. 4.2 Average prices and binding credit constraints, LTV=0.9

17% increase in total loans along the interest rate dimension only reflects larger payments on loans that have otherwise the same nominal size. With a high LTV of 90%, the picture changes completely, as figure 4.4b shows. Now, going from a low DSTI of 0.2 to a high DSTI of 0.6 triples the amount of total loans, thus having a far bigger effect than the interest rate effect discussed above. Not surprisingly, this difference is not visible in bank profits in figure 4.5 which depend almost exclusively on the interest rate.

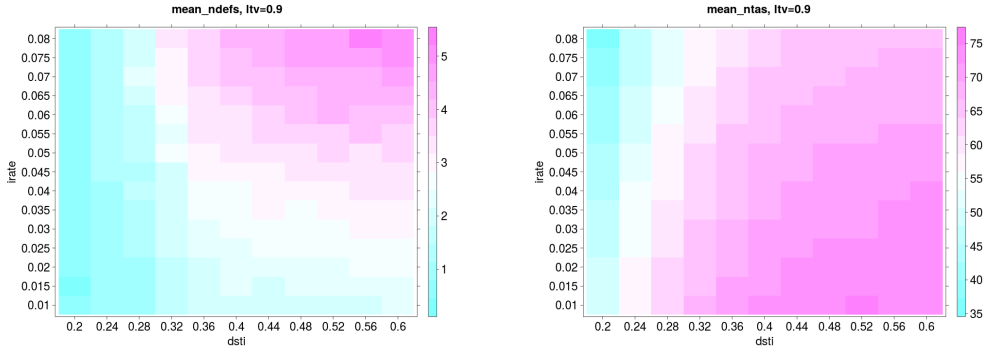

(a) number of defaults **(b)** number of transactions

Fig. 4.3 Defaults and market liquidity, LTV=0.9

Keeping the maximum DSTI ratio fixed, figure 4.6 shows that the LTV has a far stronger impact on the price level than interest rates, regardless of the level of the DSTI ratio. However, for a both high and low DSTIs, price sensitivity towards LTVs increases with the level of

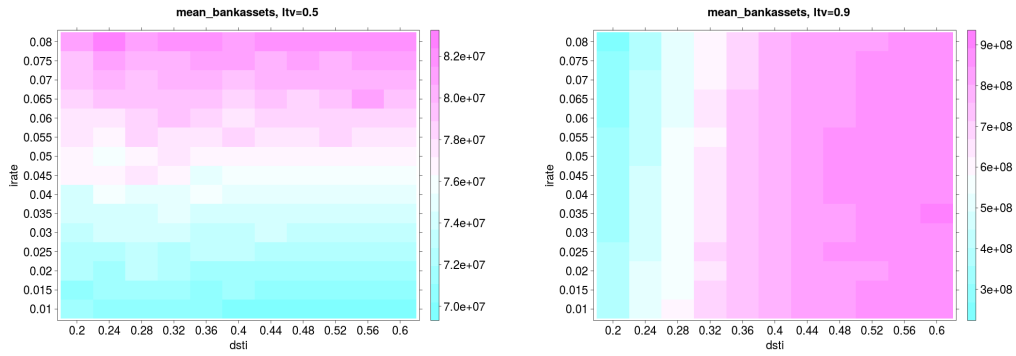

(a) LTV = 0.5 **(b)** LTV = 0.9

Fig. 4.4 Loans, total volume

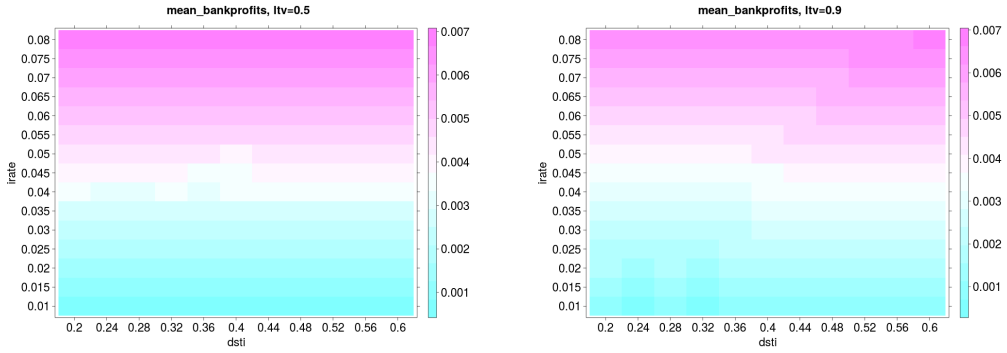

(a) LTV = 0.5 **(b)** LTV = 0.9

Fig. 4.5 Return on loan portfolio

LTVs. In the low DSTI environment in figure 4.6a the interest rate still has a clearly negative effect on the price level. For high DSTIs, there is no systematic relation between interest rates and price levels. The number of defaults exhibits a similar behavior relative to LTVs, only increasing significantly for LTVs larger than 0.7 in a low DSTI setting and for LTVs exceeding 0.8 in a high DSTI setting.

Figure 4.8 shows the share of new loans constrained by LTV. For low DSTIs, the shift towards DSTI binding occurs already for moderately high LTVS. The share of loans bound by LTVs decreases all the way down to around 20% for high LTVs. In contrast, in a high DSTI setting, only very few households experience the DSTI binding, even for very high

LTVs. The total amount of loans outstanding is highly sensitive to the LTV for both high and low DSTI settings, reflecting binding character of the LTV constraint. Still, in the high DSTI setting the total loans span a broader range than in the low DSTI setting.

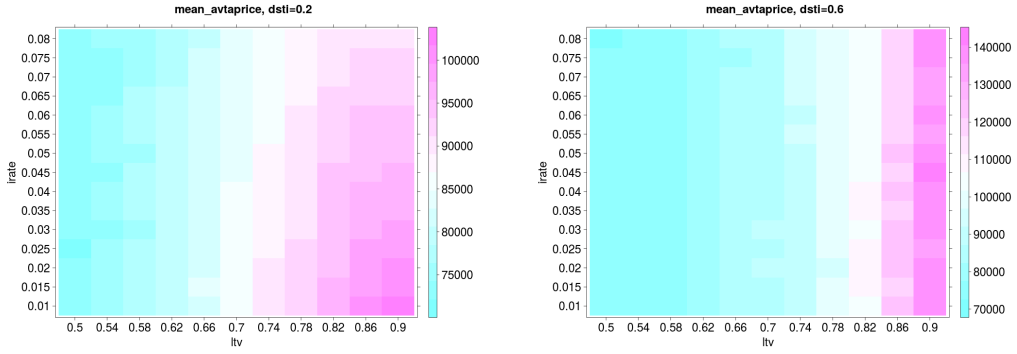

(a) DSTI = 0.2 **(b)** DSTI = 0.6

Fig. 4.6 Average transaction price

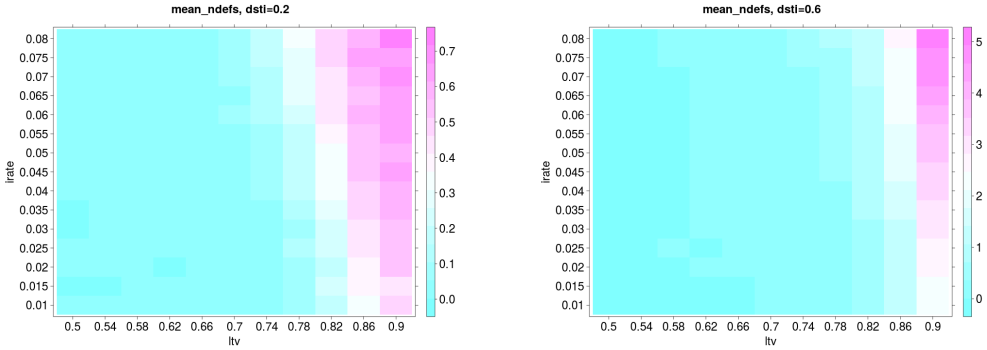

(a) DSTI = 0.2 **(b)** DSTI = 0.6

Fig. 4.7 Number of defaults

Figure 4.10 shows the average transaction prices for fixed interest rates. At low rates, the price level is insensitive to DSTI and LTV levels unless both parameters are chosen to be at the upper end of their respective range. For high interest rates, however, the DSTI becomes the primary determinant of the average price level. Counter-intuitively, however, the price level decreases by ca. 17% for an increase in the DSTI from 0.2 to 0.6. This can be considered an artifact of this particular model. Low DSTIs imply more restrictive

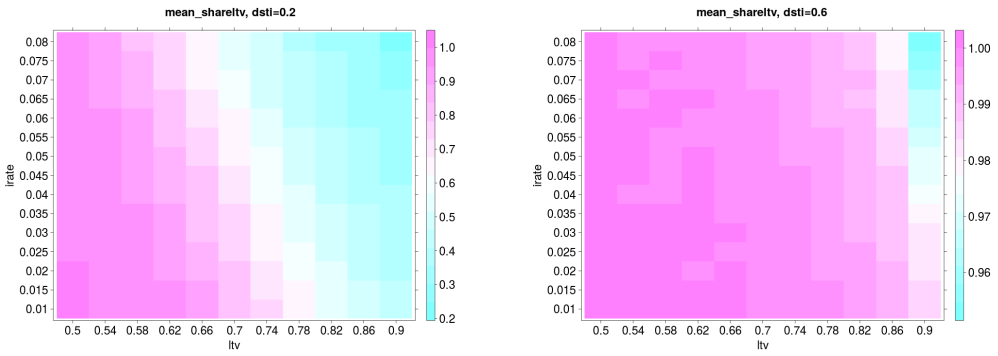

(a) DSTI = 0.2 **(b)** DSTI = 0.6

Fig. 4.8 Share of loans bound by LTV

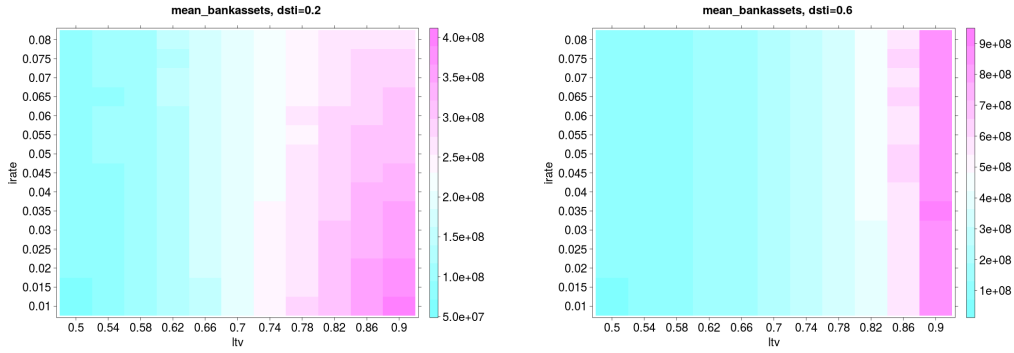

(a) DSTI = 0.2 **(b)** DSTI = 0.6

Fig. 4.9 Loans, total volume

budget constraints. This translates into fewer buyers that might drive the price up. Since construction is proportional to extrapolated *changes* in house prices, construction decreases as a consequence. On a first look, this should increase the house price level due to a decrease in supply. There is, however, a second effect. The volatility of average transaction prices decreases with a higher DSTI. Due to the lower volatility of the house prices at high DSTIs, the band of house prices covers a smaller part of the support of the budget distribution. Thus, lower price volatility means that the market is suited for fewer buyers. During our experiments, the average time houses were on the market roughly doubled from 5 to 10

periods. According to equation 4.12, this depressed house prices. Figure 4.11 shows that the loan portfolio develops similarly to the average transaction prices.

Figure 4.12 shows that in a low-interest environment, defaults only arise in the case of very high LTVs. For high interest rates, the number of defaults is overall much lower, and it is mainly dependent on the DSTI. Throughout the simulation, all defaults were due to household incomes breaching the lower bound, and no strategic defaults could be observed.

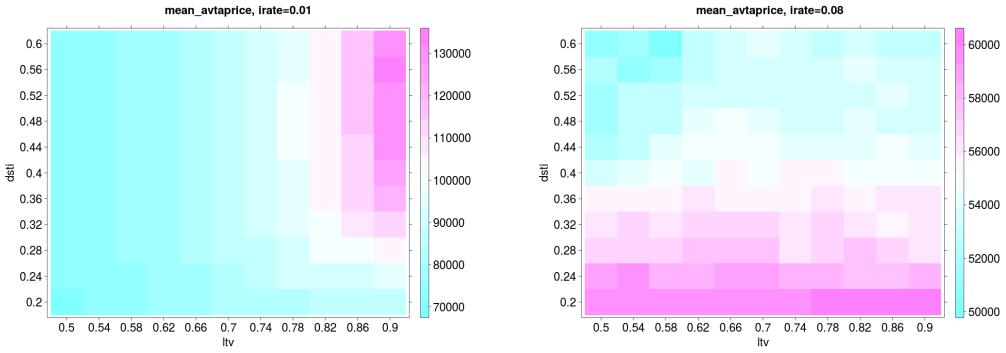

(a) r = 0.01 **(b)** r = 0.08

Fig. 4.10 Average transaction price

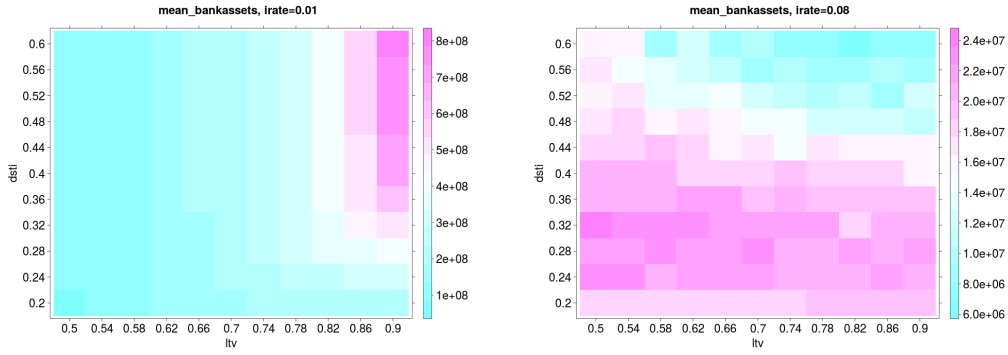

(a) r = 0.01 **(b)** r = 0.08

Fig. 4.11 Size of loan portfolio.

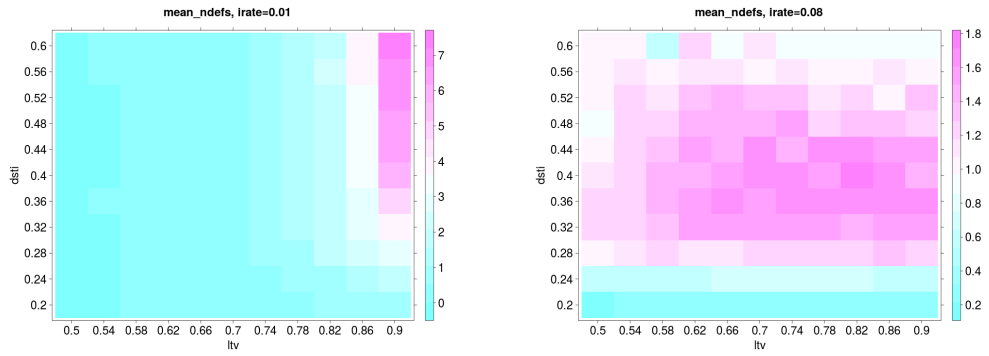

(a) r = 0.01 **(b)** r = 0.08

Fig. 4.12 Number of defaults

4.5 Conclusions

In this paper we provided a simple agent-based model of the housing market. Our agents, in particular house buyers and the construction sector, make use of simple heuristics as they can be found in the literature. Our model exhibits a wide range of dynamics. In particular, we demonstrated the challenge to examine the effectiveness of individual macroprudential measures in isolation. In all our simulations, the impact of one individual policy parameter was highly dependent on the other policy parameters. This paper complements empirical research on the effectiveness of macroprudential measures and the interaction of macroprudential and monetary policy.

In most simulations, the impact of the level of the interest rate on model outcomes was smaller than the impact of the macroprudential policy parameters. Especially with regard to average transaction price levels and to the number of defaults, the macroprudential policy parameters turned out to be the main influence. This supports the fundamental argument for macroprudential policy discussed in section 4.2. At the same time, our model has successfully demonstrated that the effectiveness of individual policy parameters is difficult to evaluate in isolation. In particular, the effect of a low DSTI ratio versus a high DSTI ratio depended strongly on the maximum LTV ratio. In a high LTV setting, a low DSTI becomes the main budget constraint, whereas in a low LTV setting the DSTI ratio at times has hardly any impact at all. Of course, the same holds for the impact of the LTV.

The model can be extended in various directions. First, an increase the number of agents may move the model closer to reality. At the time of this writing, the first agent-based models emerge in the literature that model full-scale economies. For example, Axtell (2016) provides a model of the US economy with 120 million agents. Moving towards full scale removes one potential drawback of agent-based models, and that is n-dependence. This is the observation that even if the behavioral rules of agents are not changed, the model outcome may depend on the number of agents. For examples and discussions of this problem, see Alfarano and Milaković (2009) and Alfarano et al. (2005).

Second, our model abstracted from a number of features that can be found in real-world housing markets. As an example, a few models in the literature have developed intricate algorithms of mortgage negotiation, market clearing and default resolution that could be integrated. As we discussed in section 4.3, each new feature adds complexity to the model and makes it harder to track causality. Thus, each extension demands a discussion of its benefits in order to properly weigh detail against tractability. Third, banks have so far been represented only as passive actors in the form of a loan portfolio. Implicit in this representation were the assumptions that (a) banks do not restrict credit supply and (b) banks set their credit requirements automatically to the maximum allowed by the regulator. Both aspects deserve further attention in an extended model with endogenous bank behavior. Combining the last two points, it is noteworthy that in real-world banks, accounting rules may allow for a significant lag between household insolvency and the recognition of default on the bank side. This may add yet another explanatory factor for housing market dynamics.

Chapter 5

Concluding remarks

The research presented here contributes to the economic literature in at first seemingly unrelated areas. The common denominator is the disaggregate, bottom-up perspective on economic and financial systems. In the first contribution in chapter 2, we extended an existing model of static interbank networks to more realistic core-periphery structures. We found that while some overall tendencies of system stability translate from the benchmark random network case to the core-periphery setting, some new insights can be gained. In particular, within the logic of the model, the low periphery density severely limits the capability of the system to absorb shocks. Moreover, we analyzed the accuracy of a meanfield approach relative to the full simulation results. While this provided good approximations to the full-scale simulation in early rounds, its performance in later rounds deteriorated. We found that this shortcoming is rooted in the initial bank heterogeneity. It should further be noted that the shock transmission behavior in this model was highly stylized. Thus, further research into actual bank behavior especially in situations of distress is needed. Once reliable empirical insights have been obtained, it would be interesting to come back to the theoretical setting in order to examine the effect of this increased complexity on the agent level.

The second paper contributes to the empirical knowledge base of the structure of real-world economic systems. We provided a statistical analysis of the topology of the bipartite network of credit exposures between Spanish banks and firms. Our results showed that the linking structure found in the empirical data exhibits significant differences to those found in their simulated pendants. As a secondary goal, the use of multiple measures of bipartite clustering enabled us to compare their relative performance. These showed interesting

variations. While some measures successfully detected the difference between the empirical networks and their randomly linked counterparts, other measures were better suited to extract the subtle temporal trend that was present in the empirical data. Together with the short methodological discussion on the transfer of the clustering concept from unipartite to bipartite networks, it is clear that future research is needed in both directions. On the economic side, the reason for the nonrandom structure deserves further attention. It will be interesting to isolate the reasons for this nonrandomness in a richer dataset. Then we will be able to provide this particular behavior with an economic interpretation as opposed to the primarily network-theoretic interpretation we were able to give in this paper. Moreover, the impact of these particular topologies on economic dynamics and stability deserves further attention. On the network theoretic side, our research contributed to the debate on bipartite network statistics. The mixed results clearly demonstrate the need for further investigation.

Our last paper provided a simple agent-based model of the housing market. It served to demonstrate the interactions between monetary and macroprudential policy and their joint impact on the dynamics of the housing market. We found that the effectiveness of individual macroprudential measures varies significantly based on the policy environment where they are set. At the time of writing, despite the confidence that can be found in most publications by regulators and policy makers, the gap between knowledge based on theory and models on the one hand and the regulatory practice on the other hand is still rather large. The former often suffer from a lack of microlevel data and have thus to fall back on intuition and uninformed assumptions, especially regarding the behavior of financial institutions The latter is still often guided by rules of thumbs, case-by-case considerations and political and institutional constraints. Our paper is one of many puzzle pieces that contribute to the intense discussion and ultimately to the convergence of these two strands.

For a final remark, I would like to zoom out from the particular research in the preceding chapters. It is refreshing to see that the number of economists who ask critical questions regarding the status quo of economic methodology is rising. To the author, the bottom-up formulation has appeared as a promising perspective on economic and financial systems for years. Beyond all the technical arguments that we have reviewed in the beginning and that shine through at a few places throughout this thesis, it is quite simply the most natural mapping from a world that we observe daily as consisting of many different agents who interact locally, into models that aim to make sense and to explain the causes and

consequences of these interactions. From that viewpoint, this thesis has been a valuable exercise in operationalizing this approach. Reflecting on the biggest challenges this strand of research faces, the author was able to observe two promising trends during his work. First, the knowledge base regarding the internal structure of the economic and financial system is constantly growing. This will provide invaluable orientation for the design and evaluation of agent-based models in the future. Second, there is growing awareness that the diverse literature of computational agent-based models needs to be consolidated. One of the biggest drawbacks of the agent-based approach is the lack of a canonical model. Arriving at least at a partial a consensus and maybe even at a set of benchmark models will greatly improve the stance of this type of thinking in the economic discipline.

References

Acemoglu, D., Carvalho, V. M., Ozdaglar, A., and Tahbaz-Salehi, A. (2012). The network origins of aggregate fluctuations. *Econometrica*, 80(5):1977–2016.

Agur, I. and Demertzis, M. (2015). Will macroprudential policy counteract monetary policy's effects on financial stability? Technical report, International Monetary Fund.

Akinci, O. and Olmstead-Rumsey, J. (2015). How effective are macroprudential policies? An empirical investigation.

Alberola, E., Trucharte, C., and Vega, J. L. (2011). Central banks and macroprudential policy: Some reflections from the Spanish experience. Technical report, Bank of Spain.

Alfarano, S., Lux, T., and Wagner, F. (2005). Estimation of agent-based models: the case of an asymmetric herding model. *Computational Economics*, 26(1):19–49.

Alfarano, S. and Milaković, M. (2009). Network structure and n-dependence in agent-based herding models. *Journal of Economic Dynamics and Control*, 33(1):78–92.

Allen, F. and Babus, A. (2008). Networks in finance.

Allen, F. and Carletti, E. (2013). Systemic risk from real estate and macro-prudential regulation. *International Journal of Banking, Accounting and Finance*, 5(1-2):28–48.

Allen, F. and Gale, D. (2000). Financial contagion. *Journal of political economy*, 108(1):1–33.

Allen, L. J., Brauer, F., Van den Driessche, P., and Wu, J. (2008). *Mathematical epidemiology*. Springer.

Anderson, C. J., Wasserman, S., and Faust, K. (1992). Building stochastic blockmodels. *Social networks*, 14(1):137–161.

Artzy-Randrup, Y. and Stone, L. (2005). Generating uniformly distributed random networks. *Physical Review E*, 72(5):056708.

Axelrod, R. (1981). The evolution of cooperation. *Science*, (4489):1390–1396.

Axtell, R. L. (2016). 120 million agents self-organize into 6 million firms: a model of the US private sector. In *Proceedings of the 2016 International Conference on Autonomous Agents & Multiagent Systems*, pages 806–816. International Foundation for Autonomous Agents and Multiagent Systems.

Baianu, I. C. (1986). Computer models and automata theory in biology and medicine. *Mathematical Modelling*, 7(9-12):1513–1577.

Ballerini, M., Cabibbo, N., Candelier, R., Cavagna, A., Cisbani, E., Giardina, I., Lecomte, V., Orlandi, A., Parisi, G., Procaccini, A., et al. (2008). Interaction ruling animal collective behavior depends on topological rather than metric distance: Evidence from a field study. *Proceedings of the national academy of sciences*, 105(4):1232–1237.

Baptista, R., Farmer, J. D., Hinterschweiger, M., Low, K., Tang, D., and Uluc, A. (2016). Macroprudential policy in an agent-based model of the UK housing market.

Barras, R. (2005). A building cycle model for an imperfect world. *Journal of Property Research*, 22(2-3):63–96.

Battiston, S. and Catanzaro, M. (2004). Statistical properties of corporate board and director networks. *The European Physical Journal B-Condensed Matter and Complex Systems*, 38(2):345–352.

Bech, M. L. and Atalay, E. (2010). The topology of the federal funds market. *Physica A: Statistical Mechanics and its Applications*, 389(22):5223–5246.

Benigno, G., Chen, H., Otrok, C., Rebucci, A., and Young, E. (2011). Monetary and macro-prudential policies: An integrated analysis. *Unpublished manuscript*.

Borgatti, S. P. and Everett, M. G. (1997). Network analysis of 2-mode data. *Social networks*, 19(3):243–269.

Borgatti, S. P. and Everett, M. G. (2000). Models of core/periphery structures. *Social networks*, 21(4):375–395.

Boss, M., Elsinger, H., Summer, M., and Thurner 4, S. (2004). Network topology of the interbank market. *Quantitative Finance*, 4(6):677–684.

Brée, D. S., Challet, D., and Peirano, P. P. (2013). Prediction accuracy and sloppiness of log-periodic functions. *Quantitative Finance*, 13(2):275–280.

Breiger, R. L. (1974). The duality of persons and groups. *Social forces*, 53(2):181–190.

Buch, C. M. and Goldberg, L. (2016). Cross-border prudential policy spillovers: how much? how important? evidence from the International Banking Research Network. Technical report, National Bureau of Economic Research.

Caldwell, B. (1993). Economic methodology: rationale, foundations, prospects. *Rationality, Institutions and Economic Methodology, London and New York: Routledge*, pages 45–60.

Campello, M., Graham, J. R., and Harvey, C. R. (2010). The real effects of financial constraints: Evidence from a financial crisis. *Journal of Financial Economics*, 97(3):470–487.

Cerutti, E., Claessens, S., and Laeven, L. (2015). The use and effectiveness of macroprudential policies: new evidence. *Journal of Financial Stability*.

Chang, G. and Feigenbaum, J. (2006). A bayesian analysis of log-periodic precursors to financial crashes. *Quantitative Finance*, 6(1):15–36.

Cifuentes, R., Ferrucci, G., and Shin, H. S. (2005). Liquidity risk and contagion. *Journal of the European Economic Association*, 3(2-3):556–566.

Claessens, S., Ghosh, S. R., and Mihet, R. (2013). Macro-prudential policies to mitigate financial system vulnerabilities. *Journal of International Money and Finance*, 39:153–185.

Clement, P. (2010). The term 'macroprudential': origins and evolution. *BIS Quarterly Review*, pages 59–67.

Cocco, J. F., Gomes, F. J., and Martins, N. C. (2009). Lending relationships in the interbank market. *Journal of Financial Intermediation*, 18(1):24–48.

Coddington, P. D. (1996). Tests of random number generators using ising model simulations. *International Journal of Modern Physics C*, 7(03):295–303.

Conyon, M. J. and Muldoon, M. R. (2004). The small world network structure of boards of directors. *Available at SSRN 546963*.

Coolen, A., De Martino, A., and Annibale, A. (2009). Constrained markovian dynamics of random graphs. *Journal of Statistical Physics*, 136(6):1035–1067.

Craig, B. and Von Peter, G. (2014). Interbank tiering and money center banks. *Journal of Financial Intermediation*, 23(3):322–347.

Darbar, S. M. and Wu, X. (2016). Experiences with macroprudential policy—five case studies. *Journal of International Commerce, Economics and Policy*, 7(03):1650014.

De Masi, G., Fujiwara, Y., Gallegati, M., Greenwald, B., and Stiglitz, J. E. (2011). An analysis of the Japanese credit network. *Evolutionary and Institutional Economics Review*, 7(2):209–232.

De Masi, G. and Gallegati, M. (2012). Bank–firms topology in Italy. *Empirical Economics*, 43(2):851–866.

Draghi, M. (2014). Flagship report on macro-prudential policy in the banking sector. *European Systemic Risk Board*.

Du, N., Wang, B., Wu, B., and Wang, Y. (2008). Overlapping community detection in bipartite networks. In *Proceedings of the 2008 IEEE/WIC/ACM International Conference on Web Intelligence and Intelligent Agent Technology-Volume 01*, pages 176–179.

Duchin, R., Ozbas, O., and Sensoy, B. A. (2010). Costly external finance, corporate investment, and the subprime mortgage credit crisis. *Journal of Financial Economics*, 97(3):418–435.

Erlingsson, E. J., Teglio, A., Cincotti, S., Stefansson, H., Sturlusson, J. T., Raberto, M., et al. (2014). Housing market bubbles and business cycles in an agent-based credit economy. *Economics: The Open-Access, Open-Assessment E-Journal*, 8(2014-8):1–42.

ESRB (2014). The esrb handbook on operationalising macro-prudential policy in the banking sector. Technical report, European Systemic Risk Board.

Everett, M. G. and Borgatti, S. P. (2013). The dual-projection approach for two-mode networks. *Social Networks*, 35(2):204–210.

Farinha, L. A. and Santos, J. A. (2002). Switching from single to multiple bank lending relationships: Determinants and implications. *Journal of Financial Intermediation*, 11(2):124–151.

Fienberg, S. E. and Wasserman, S. (1981). Categorical data analysis of single sociometric relations. *Sociological methodology*, 12:156–192.

Freixas, X., Parigi, B. M., and Rochet, J.-C. (2000). Systemic risk, interbank relations, and liquidity provision by the central bank. *Journal of money, credit and banking*, pages 611–638.

Fricke, D. and Lux, T. (2015). Core–periphery structure in the overnight money market: evidence from the e-mid trading platform. *Computational Economics*, 45(3):359–395.

Galati, G. and Moessner, R. (2013). Macroprudential policy–a literature review. *Journal of Economic Surveys*, 27(5):846–878.

Ge, J. (2013). Who creates housing bubbles? an agent-based study. In *International Workshop on Multi-Agent Systems and Agent-Based Simulation*, pages 143–150. Springer.

Geanakoplos, J. (2001). Liquidity, default and crashes: Endogenous contracts in general equilibrium.

Geanakoplos, J. (2010a). The leverage cycle. *NBER macroeconomics annual*, 24(1):1–66.

Geanakoplos, J. (2010b). Solving the present crisis and managing the leverage cycle.

Geanakoplos, J., Axtell, R., Farmer, D. J., Howitt, P., Conlee, B., Goldstein, J., Hendrey, M., Palmer, N. M., and Yang, C.-Y. (2012). Getting at systemic risk via an agent-based model of the housing market. *The American Economic Review*, 102(3):53–58.

Gilbert, N., Hawksworth, J. C., and Swinney, P. A. (2009). An agent-based model of the English housing market. In *AAAI Spring Symposium: Technosocial Predictive Analytics*, pages 30–35.

Glaeser, E. L., Gottlieb, J. D., and Gyourko, J. (2012). Can cheap credit explain the housing boom? In *Housing and the Financial Crisis*, pages 301–359. University of Chicago Press.

Glaeser, E. L., Gyourko, J., and Saiz, A. (2008). Housing supply and housing bubbles. *Journal of Urban Economics*, 64(2):198–217.

Glaeser, E. L. and Nathanson, C. G. (2015). An extrapolative model of house price dynamics. Technical report, National Bureau of Economic Research.

Guillaume, J.-L. and Latapy, M. (2004). Bipartite structure of all complex networks. *Information processing letters*, 90(5):215–221.

Guillaume, J.-L. and Latapy, M. (2006). Bipartite graphs as models of complex networks. *Physica A: Statistical Mechanics and its Applications*, 371(2):795–813.

Guimerà, R., Sales-Pardo, M., and Amaral, L. A. N. (2007). Module identification in bipartite and directed networks. *Physical Review E*, 76(3):036102.

Hartmann, P. (2015). Real estate markets and macroprudential policy in Europe. *Journal of Money, Credit and Banking*, 47(S1):69–80.

Hausman, D. M. (1989). Economic methodology in a nutshell. *The Journal of Economic Perspectives*, 3(2):115–127.

Hausman, D. M. (1994). *The philosophy of economics: an anthology*. Cambridge University Press.

Helbing, D., Farkas, I., and Vicsek, T. (2000). Simulating dynamical features of escape panic. *Nature*, 407(6803):487–490.

Hemelrijk, C. K. and Hildenbrandt, H. (2011). Some causes of the variable shape of flocks of birds. *PloS one*, 6(8):e22479.

Hofstadter, D. H. (1980). *Gödel, Escher, Bach: An Eternal Golden Braid;[a Metaphoric Fugue on Minds and Machines in the Spirit of Lewis Carroll].* Penguin Books.

Holland, P. W., Laskey, K. B., and Leinhardt, S. (1983). Stochastic blockmodels: First steps. *Social networks*, 5(2):109–137.

Hommes, C. H. (2006). Heterogeneous agent models in economics and finance. *Handbook of computational economics*, 2:1109–1186.

Jackson, M. O. et al. (2008). *Social and economic networks*, volume 3. Princeton university press Princeton.

Kajuth, F., Knetsch, T., and Pinkwart, N. (2013). Assessing house prices in Germany: Evidence from an estimated stock-flow model using regional data. *Bundesbank working paper*, (46).

Karimi, F. and Raddant, M. (2016). Cascades in real interbank markets. *Computational Economics*, 47(1):49–66.

Khandani, A. E., Lo, A. W., and Merton, R. C. (2013). Systemic risk and the refinancing ratchet effect. *Journal of Financial Economics*, 108(1):29–45.

Kindleberger, C. P. and O'Keefe, R. (2001). *Manias, panics, and crashes*. Springer.

Kirman, A. P. (1992). Whom or what does the representative individual represent? *The Journal of Economic Perspectives*, 6(2):117–136.

Kouwenberg, R. and Zwinkels, R. C. (2015). Endogenous price bubbles in a multi-agent system of the housing market. *PloS one*, 10(6):e0129070.

Krainer, J. (2002). House price dynamics and the business cycle.

Lambertini, L., Mendicino, C., and Punzi, M. T. (2013). Leaning against boom–bust cycles in credit and housing prices. *Journal of Economic Dynamics and Control*, 37(8):1500–1522.

Langfield, S., Liu, Z., and Ota, T. (2014). Mapping the UK interbank system. *Journal of Banking & Finance*, 45:288–303.

Latapy, M., Magnien, C., and Del Vecchio, N. (2008). Basic notions for the analysis of large two-mode networks. *Social networks*, 30(1):31–48.

Lim, C. H., Costa, A., Columba, F., Kongsamut, P., Otani, A., Saiyid, M., Wezel, T., and Wu, X. (2011). Macroprudential policy: what instruments and how to use them? lessons from country experiences. Technical report, International Monetary Fund.

Lind, P. G., González, M. C., and Herrmann, H. J. (2005). Cycles and clustering in bipartite networks. *Phys. Rev. E*, 72:056127.

Lorrain, F. and White, H. C. (1971). Structural equivalence of individuals in social networks. *The Journal of mathematical sociology*, 1(1):49–80.

Lu, L. and Wang, G. (2008). A study on multi-agent supply chain framework based on network economy. *Computers & Industrial Engineering*, 54(2):288–300.

Lux, T. (2016). A model of the topology of the bank-firm credit network and its role as a channel of contagion. *Journal of Economic Dynamics and Control*, 66:36–53.

Maslov, S. and Sneppen, K. (2002). Specificity and stability in topology of protein networks. *Science*, 296(5569):910–913.

Maslov, S., Sneppen, K., and Zaliznyak, A. (2004). Detection of topological patterns in complex networks: correlation profile of the internet. *Physica A: Statistical Mechanics and its Applications*, 333:529–540.

May, R. M. and Arinaminpathy, N. (2010). Systemic risk: the dynamics of model banking systems. *Journal of the Royal Society Interface*, 7(46):823–838.

McCloskey, D. N. (1998). *The rhetoric of economics*. Univ of Wisconsin Press.

McDonald, J. B. (1984). Some generalized functions for the size distribution of income. *Econometrica: journal of the Econometric Society*, pages 647–663.

McMahon, M., Berea, A., and Osman, H. (2011). An agent-based model of the housing market. *Computers, Environment and Urban Systems*.

Mirowski, P. (1991). The when, the how and the why of mathematical expression in the history of economics analysis. *The Journal of Economic Perspectives*, 5(1):145–157.

Mistrulli, P. E. (2011). Assessing financial contagion in the interbank market: Maximum entropy versus observed interbank lending patterns. *Journal of Banking & Finance*, 35(5):1114–1127.

Nagel, K. and Schreckenberg, M. (1992). A cellular automaton model for freeway traffic. *Journal de physique I*, 2(12):2221–2229.

Newman, M. E. (2001a). Scientific collaboration networks. I. network construction and fundamental results. *Physical review E*, 64(1):016131.

Newman, M. E. (2001b). Scientific collaboration networks. II. shortest paths, weighted networks, and centrality. *Physical review E*, 64(1):016132.

Newman, M. E. (2001c). The structure of scientific collaboration networks. *Proceedings of the National Academy of Sciences*, 98(2):404–409.

Newman, M. E. (2003). The structure and function of complex networks. *SIAM review*, 45(2):167–256.

Newman, M. E., Strogatz, S. H., and Watts, D. J. (2001). Random graphs with arbitrary degree distributions and their applications. *Physical review E*, 64(2):026118.

Nier, E., Osinski, J., Madrid, P., et al. (2011). Institutional models for macroprudential policy. Technical report, International Monetary Fund.

Nier, E., Yang, J., Yorulmazer, T., and Alentorn, A. (2007). Network models and financial stability. *Journal of Economic Dynamics and Control*, 31(6):2033–2060.

Opsahl, T., Colizza, V., Panzarasa, P., and Ramasco, J. J. (2008). Prominence and control: the weighted rich-club effect. *Physical review letters*, 101(16):168702.

Pangallo, M., Nadal, J. P., and Vignes, A. (2016). Price formation on a housing market and spatial income segregation. *arXiv preprint arXiv:1606.00424*.

Rajan, R. G. (2011). *Fault lines: How hidden fractures still threaten the world economy*. Princeton University Press.

Reinhardt, D. and Sowerbutts, R. (2015). Regulatory arbitrage in action: evidence from banking flows and macroprudential policy. Technical report, Bank of England.

Roberts, E. and Coolen, A. (2012). Unbiased degree-preserving randomization of directed binary networks. *Physical Review E*, 85(4):046103.

Robins, G. and Alexander, M. (2004). Small worlds among interlocking directors: Network structure and distance in bipartite graphs. *Computational & Mathematical Organization Theory*, 10(1):69–94.

Salem, A. and Mount, T. (1974). A convenient descriptive model of income distribution: the gamma density. *Econometrica: journal of the Econometric Society*, pages 1115–1127.

Serrano, M. Á., Boguná, M., and Vespignani, A. (2007). Patterns of dominant flows in the world trade web. *Journal of Economic Interaction and Coordination*, 2(2):111–124.

Sheldon, G., Maurer, M., et al. (1998). Interbank lending and systemic risk: an empirical analysis for Switzerland. *Revue Suisse d'econmie politique et de statistique*, 134:685–704.

Shiller, R. J. (2012). *The subprime solution: how today's global financial crisis happened, and what to do about it*. Princeton University Press.

Singh, S. and Maddala, G. S. (2008). A function for size distribution of incomes. In *Modeling income distributions and Lorenz curves*, pages 27–35. Springer.

Snijders, T. A. and Nowicki, K. (1997). Estimation and prediction for stochastic blockmodels for graphs with latent block structure. *Journal of classification*, 14(1):75–100.

Soramäki, K., Bech, M. L., Arnold, J., Glass, R. J., and Beyeler, W. E. (2007). The topology of interbank payment flows. *Physica A: Statistical Mechanics and its Applications*, 379(1):317–333.

Sornette, D., Johansen, A., and Bouchaud, J.-P. (1996). Stock market crashes, precursors and replicas. *Journal de Physique I*, 6(1):167–175.

Sornette, D., Johansen, A., et al. (2001). Significance of log-periodic precursors to financial crashes. *Quantitative Finance*, 1(4):452–471.

Squartini, T., Fagiolo, G., and Garlaschelli, D. (2011a). Randomizing world trade. i. a binary network analysis. *Physical Review E*, 84(4):046117.

Squartini, T., Fagiolo, G., and Garlaschelli, D. (2011b). Randomizing world trade. ii. a weighted network analysis. *Physical Review E*, 84(4):046118.

Squartini, T., Mastrandrea, R., and Garlaschelli, D. (2015). Unbiased sampling of network ensembles. *New Journal of Physics*, 17(2):023052.

Squartini, T., Picciolo, F., Ruzzenenti, F., and Garlaschelli, D. (2013). Reciprocity of weighted networks. *arXiv preprint arXiv:1208.4208*.

Taylor, J. B. (2007). Housing and monetary policy. Technical report, National Bureau of Economic Research.

Thurner, S., Hanel, R., Pichler, S., et al. (2003). Risk trading, network topology and banking regulation. *Quantitative Finance*, 3(4):306–319.

Turrell, A. (2016). Agent-based models: Understanding the economy from the bottom up. *Bank of England Quarterly Bulletin*, Q4.

Upper, C. (2007). Using counterfactual simulations to assess the danger of contagion in interbank markets.

Upper, C. and Worms, A. (2004). Estimating bilateral exposures in the german interbank market: Is there a danger of contagion? *European Economic Review*, 48(4):827–849.

van Lelyveld, I. et al. (2014). Finding the core: Network structure in interbank markets. *Journal of Banking & Finance*, 49:27–40.

Vandenbussche, J., Vogel, U., and Detragiache, E. (2015). Macroprudential policies and housing prices: a new database and empirical evidence for Central, Eastern, and Southeastern Europe. *Journal of Money, Credit and Banking*, 47(S1):343–377.

Wachtel, P. (2013). Is macro prudential regulation possible? *Budgetary Research Review*, 5(1):40–53.

Wasserman, S. and Faust, K. (1994). *Social network analysis: Methods and applications*, volume 8. Cambridge university press.

Watts, D. J. and Strogatz, S. H. (1998). Collective dynamics of 'small-world' networks. *nature*, 393(6684):440–442.

Weintraub, E. R. (2002). *How economics became a mathematical science*. Duke University Press.

White, E. N., Snowden, K., and Fishback, P. (2014). *Housing and Mortgage Markets in Historical Perspective*. University of Chicago Press.

White, H. C., Boorman, S. A., and Breiger, R. L. (1976). Social structure from multiple networks. I. Blockmodels of roles and positions. *American journal of sociology*, pages 730–780.

Appendix A

Simulation results for bipartite networks

A.1 Simulation results, year=2000

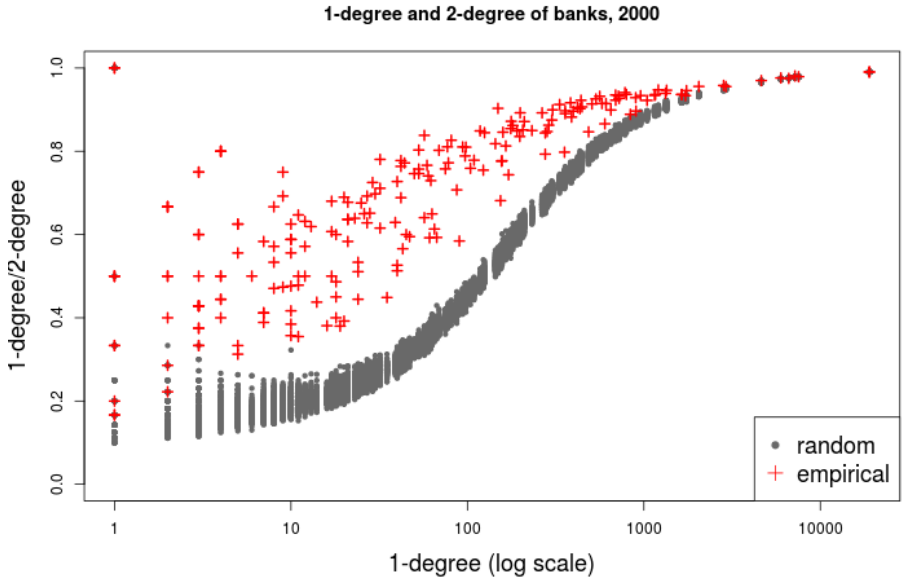

Fig. A.1 Random networks, year=2000: 1-degree and 2-degree, banks.

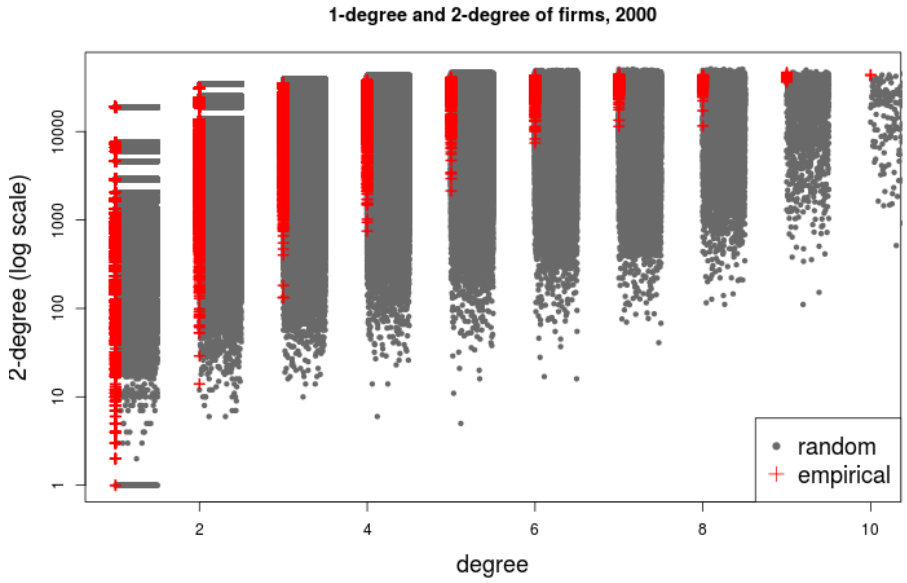

Fig. A.2 Random networks, year=2000: 1-degree and 2-degree, firms.

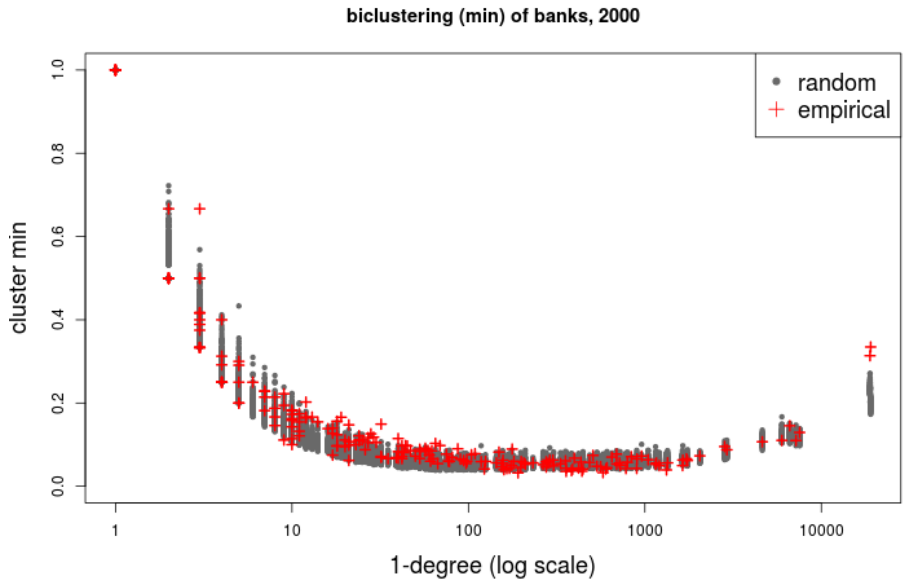

Fig. A.3 Random networks, year=2000: minclustering, banks.

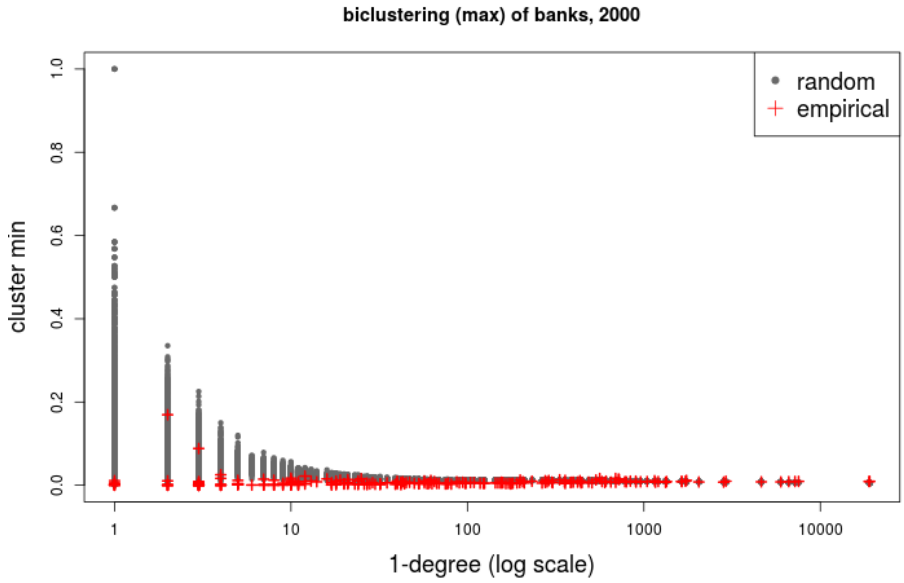

Fig. A.4 Random networks, year=2000: max clustering, banks.

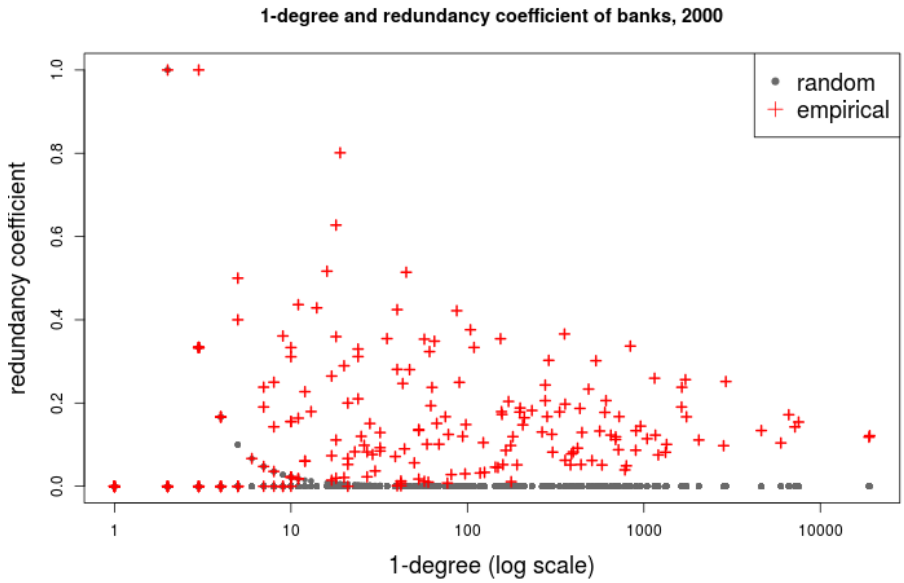

Fig. A.5 Random networks, year=2000: redundancy, banks.

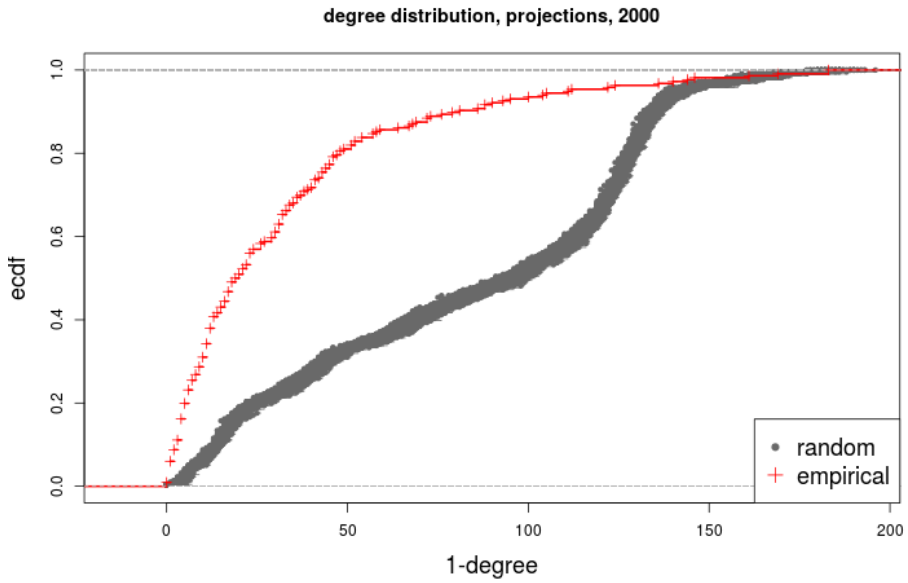

Fig. A.6 Random networks, year=2000: degree distribution of projections, banks.

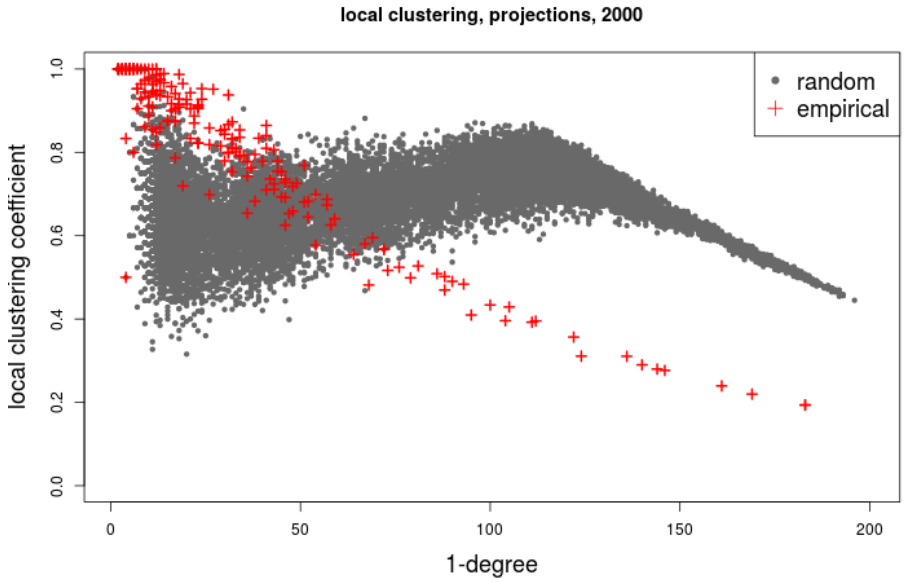

Fig. A.7 Random networks, year=2000: clustering in projections, banks.

A.2 Simulation results, year=2001

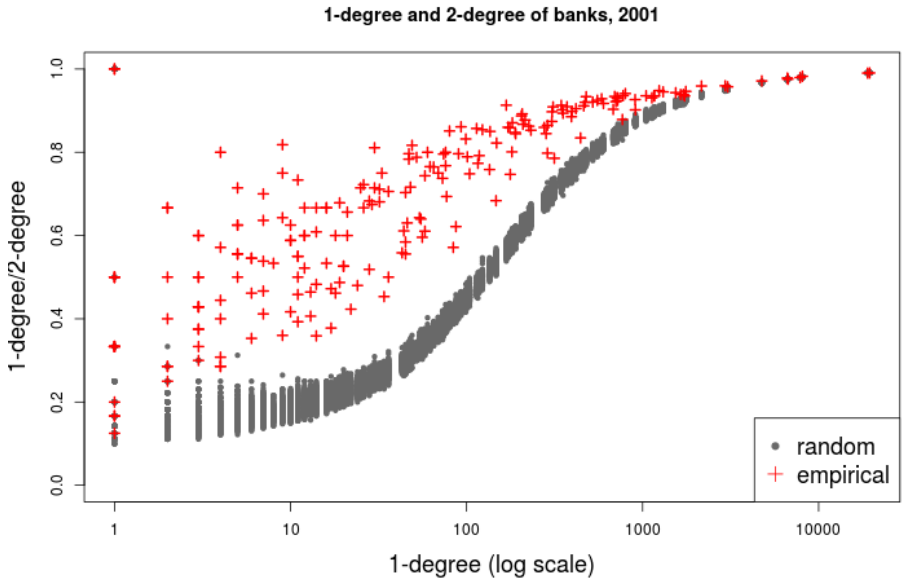

Fig. A.8 Random networks, year=2001: 1-degree and 2-degree, banks.

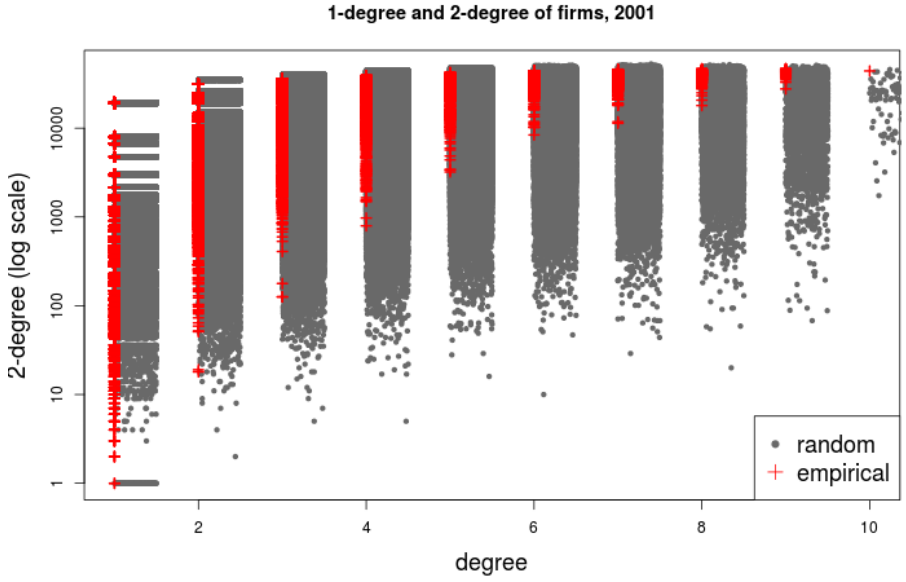

Fig. A.9 Random networks, year=2001: 1-degree and 2-degree, firms.

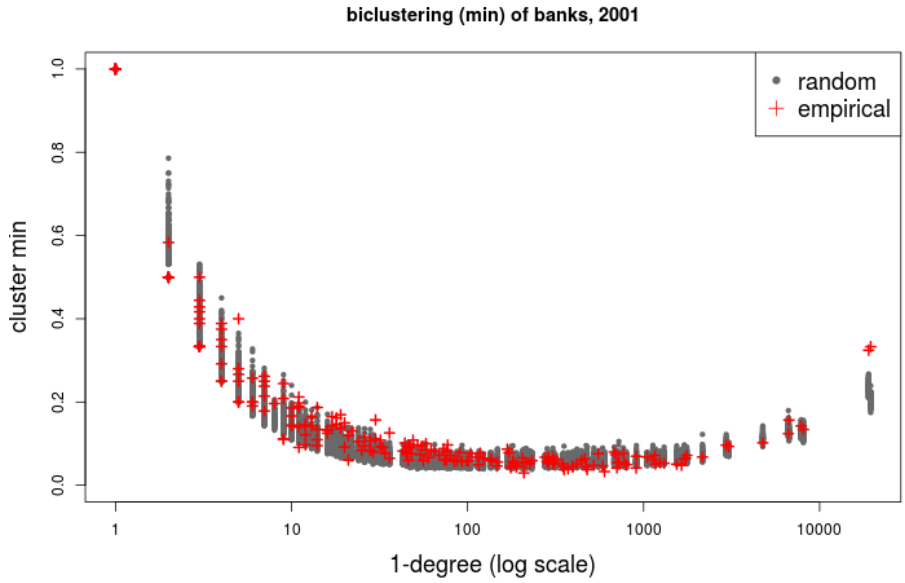

Fig. A.10 Random networks, year=2001: min clustering, banks.

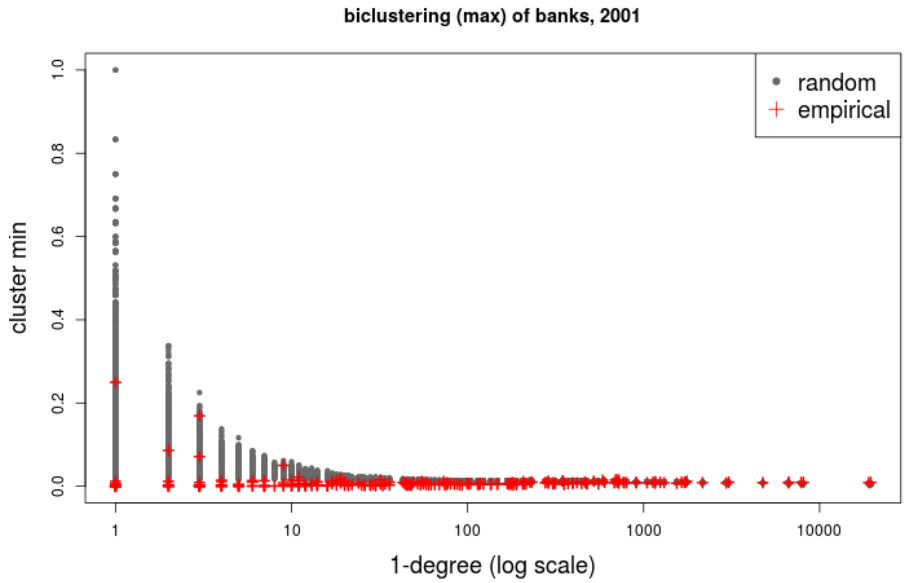

Fig. A.11 Random networks, year=2001: max clustering, banks.

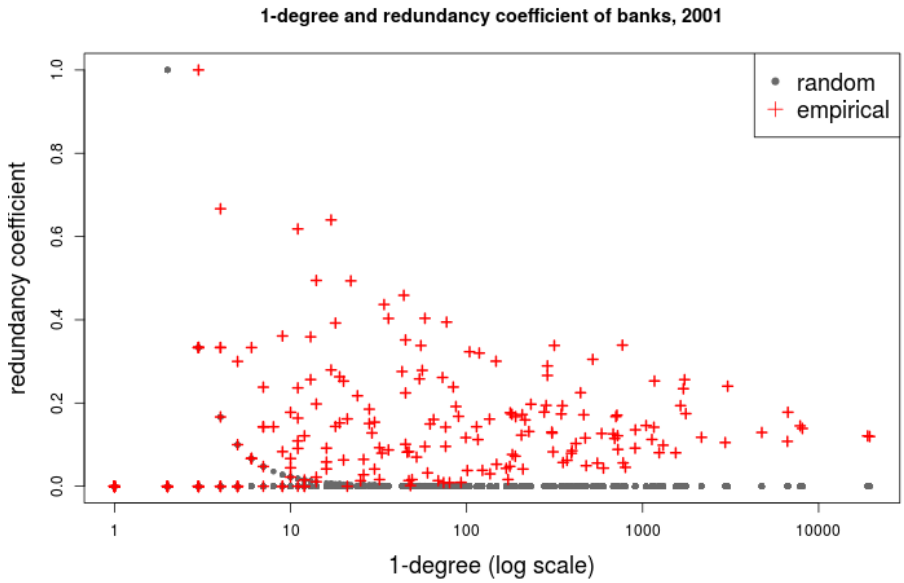

Fig. A.12 Random networks, year=2001: redundancy, banks.

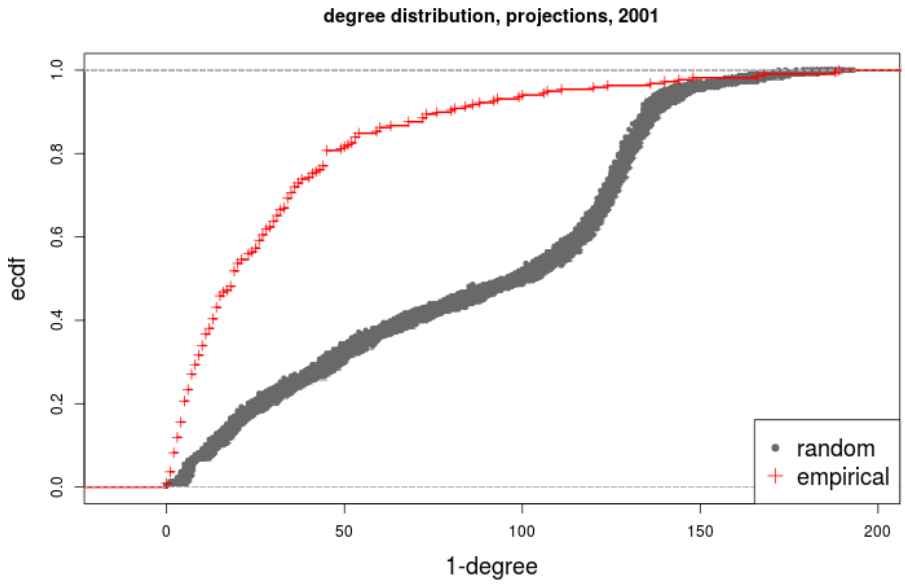

Fig. A.13 Random networks, year=2001: degree distribution of projections, banks.

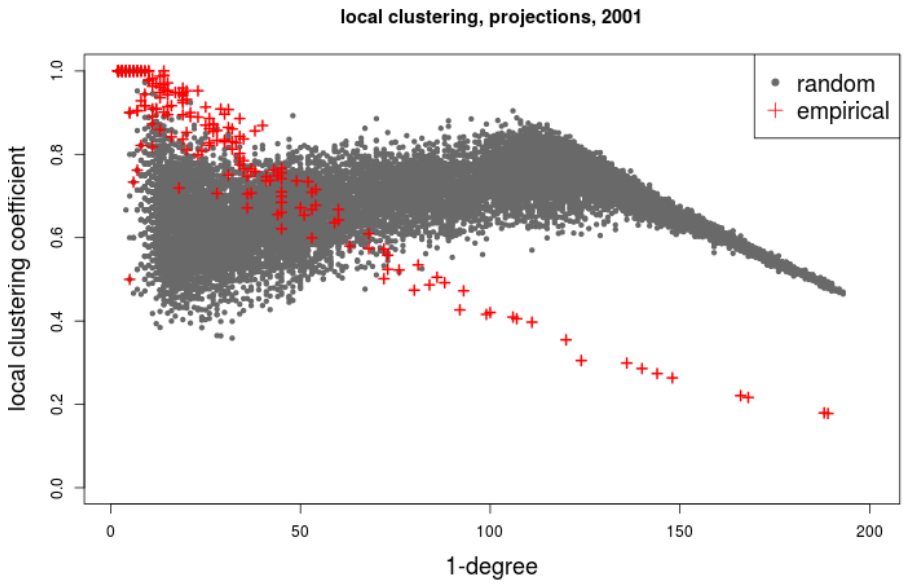

Fig. A.14 Random networks, year=2001: clustering in projections, banks.

A.3 Simulation results, year=2002

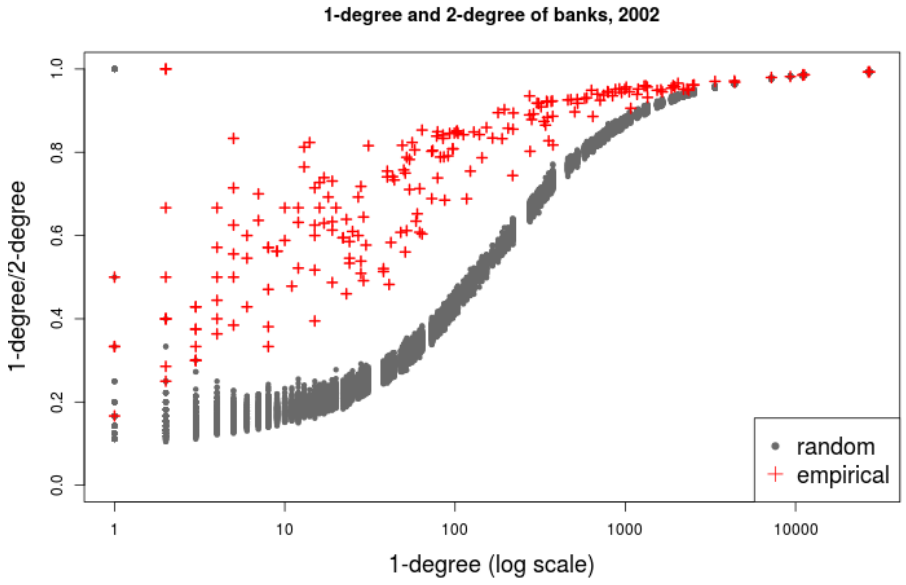

Fig. A.15 Random networks, year=2002: 1-degree and 2-degree, banks.

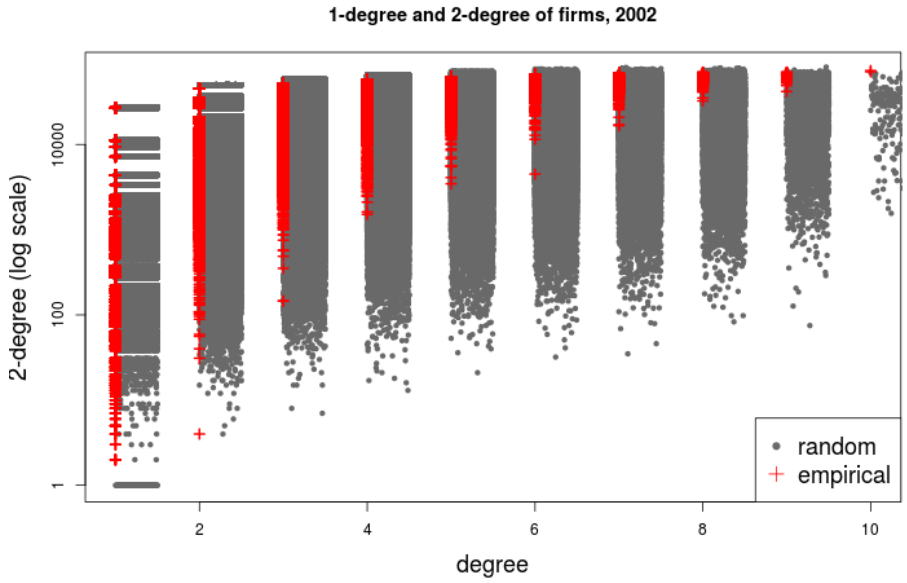

Fig. A.16 Random networks, year=2002: 1-degree and 2-degree, firms.

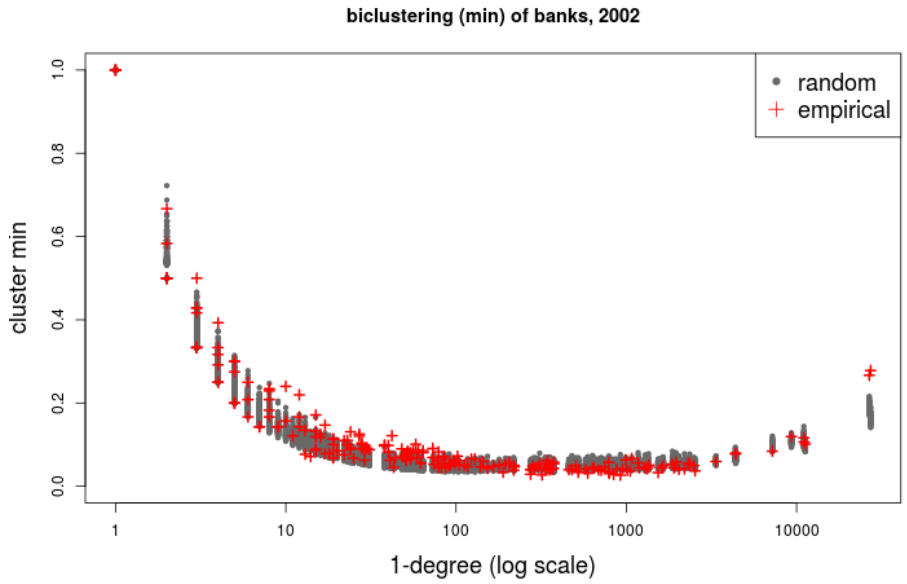

Fig. A.17 Random networks, year=2002: min clustering, banks.

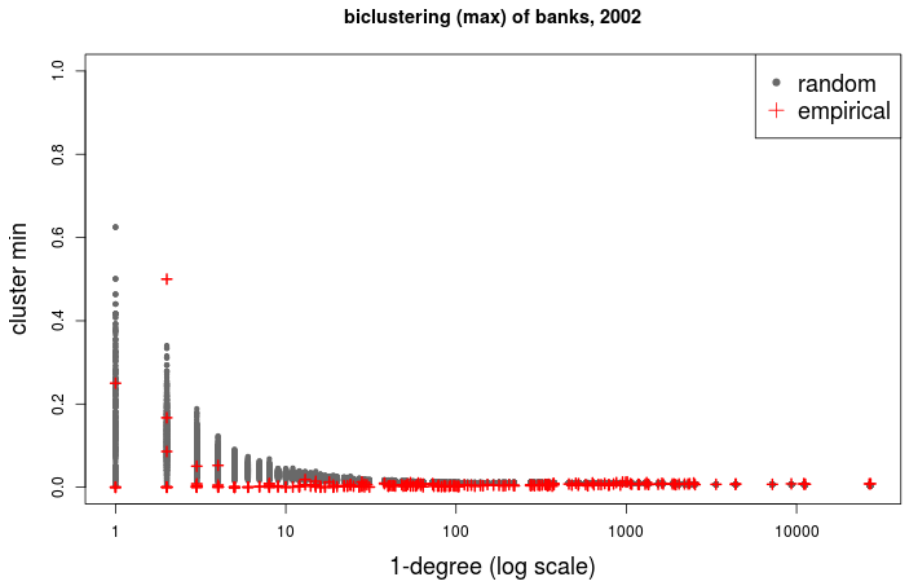

Fig. A.18 Random networks, year=2002: max clustering, banks.

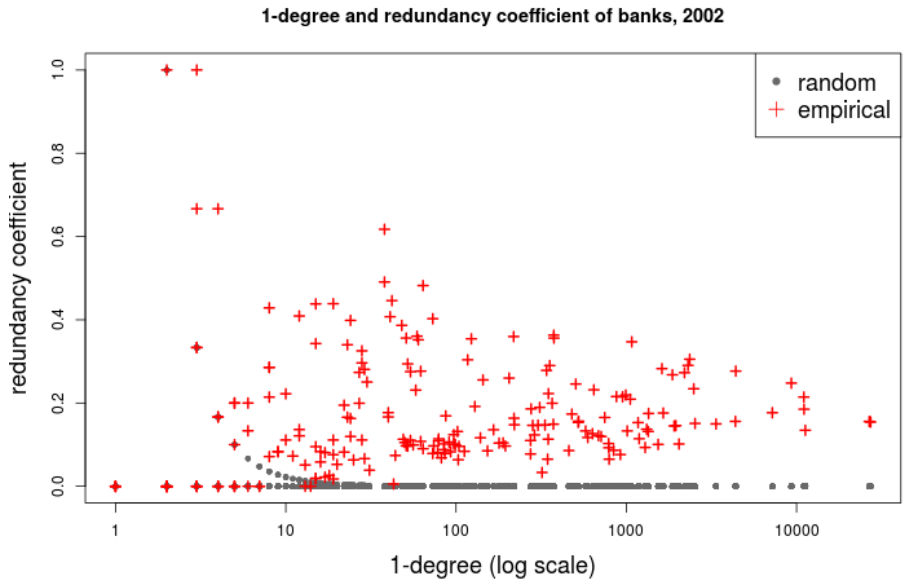

Fig. A.19 Random networks, year=2002: redundancy, banks.

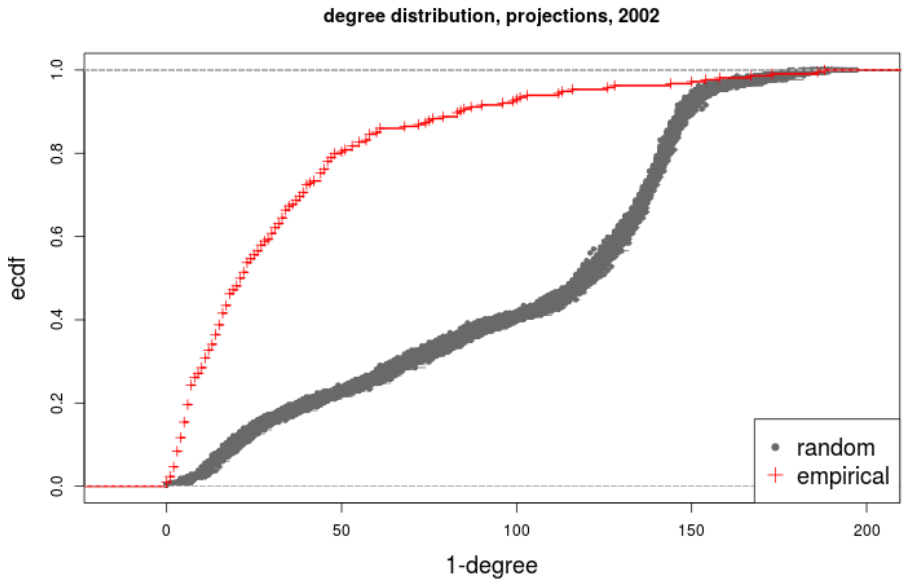

Fig. A.20 Random networks, year=2002: degree distribution of projections, banks.

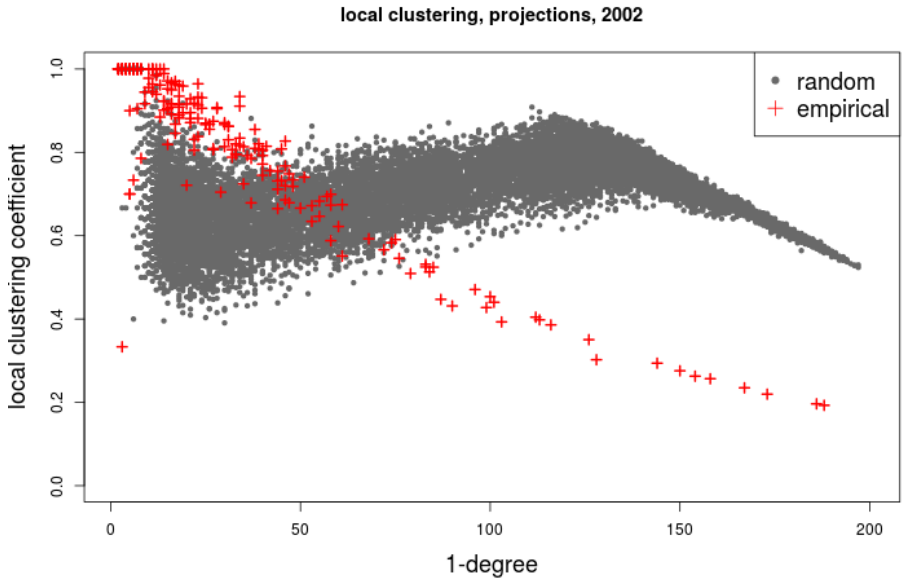

Fig. A.21 Random networks, year=2002: clustering in projections, banks.

A.4 Simulation results, year=2003

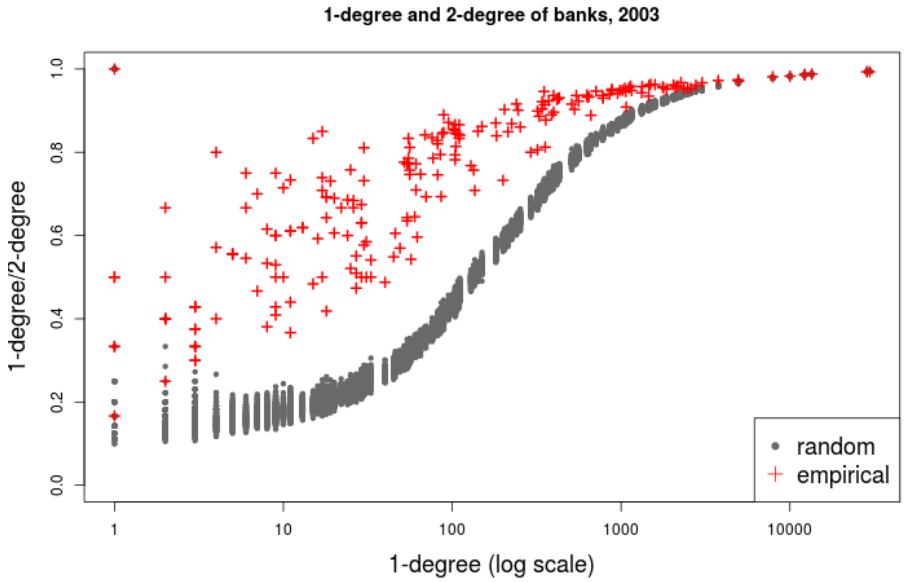

Fig. A.22 Random networks, year=2003: 1-degree and 2-degree, banks.

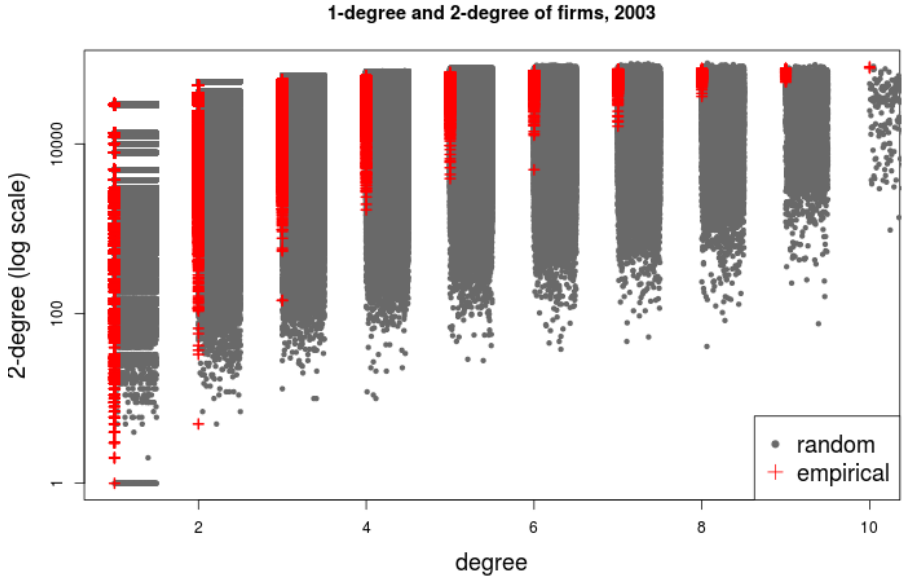

Fig. A.23 Random networks, year=2003: 1-degree and 2-degree, firms.

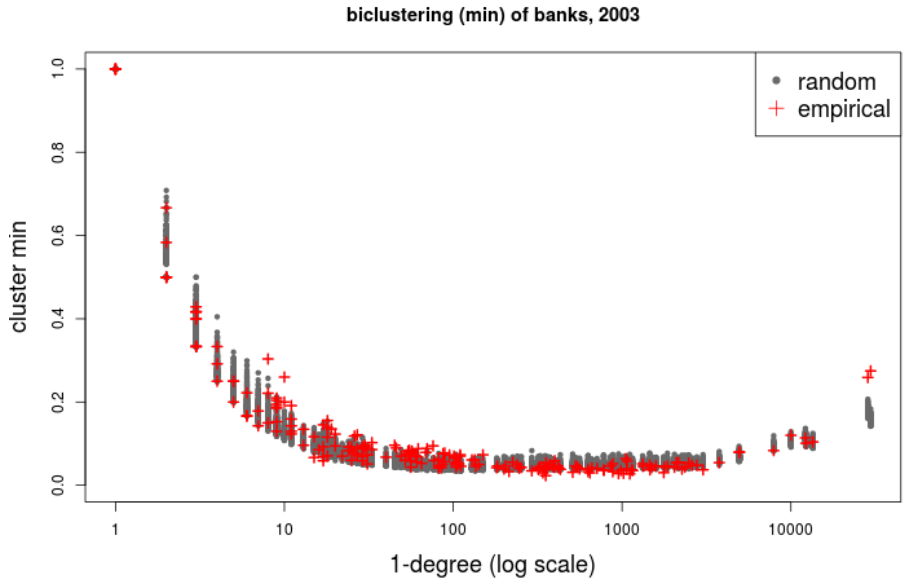

Fig. A.24 Random networks, year=2003: min clustering, banks.

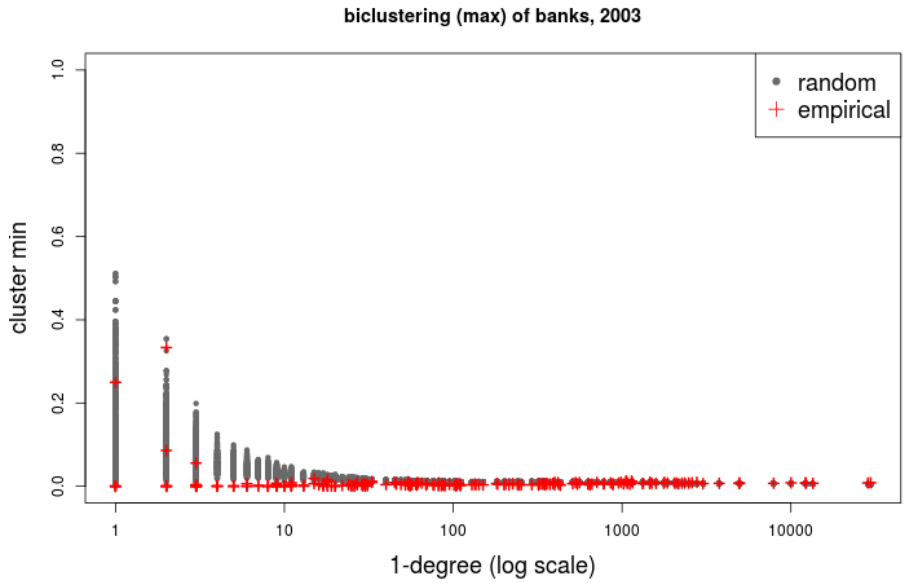

Fig. A.25 Random networks, year=2003: max clustering, banks.

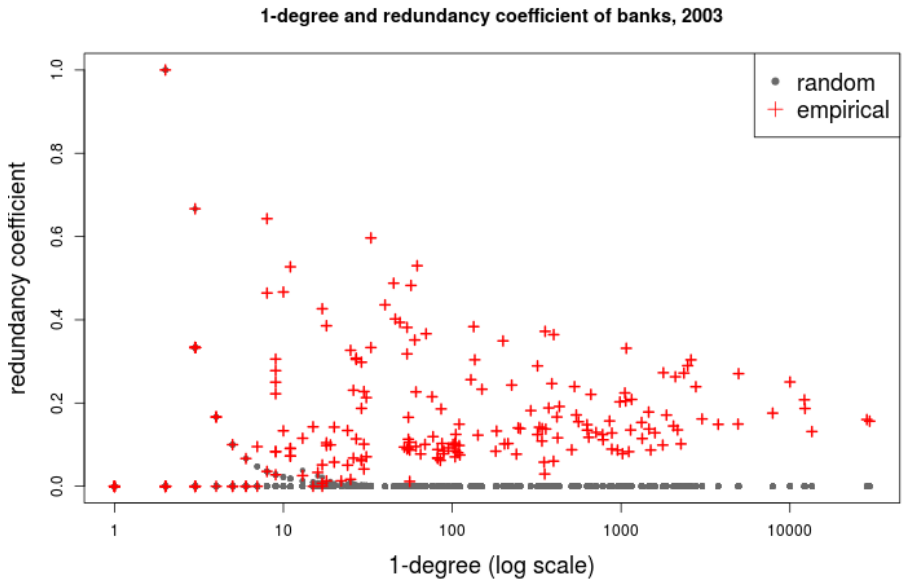

Fig. A.26 Random networks, year=2003: redundancy, banks.

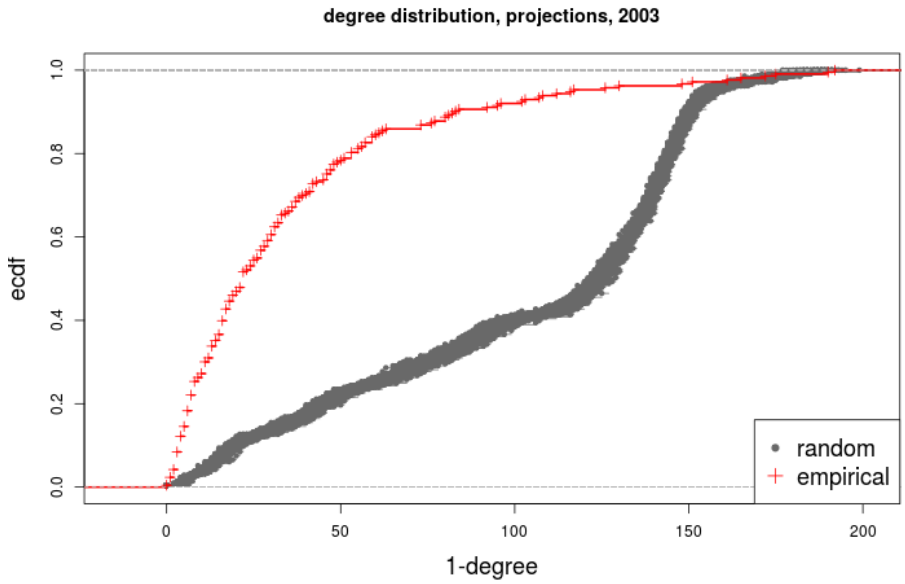

Fig. A.27 Random networks, year=2003: degree distribution of projections, banks.

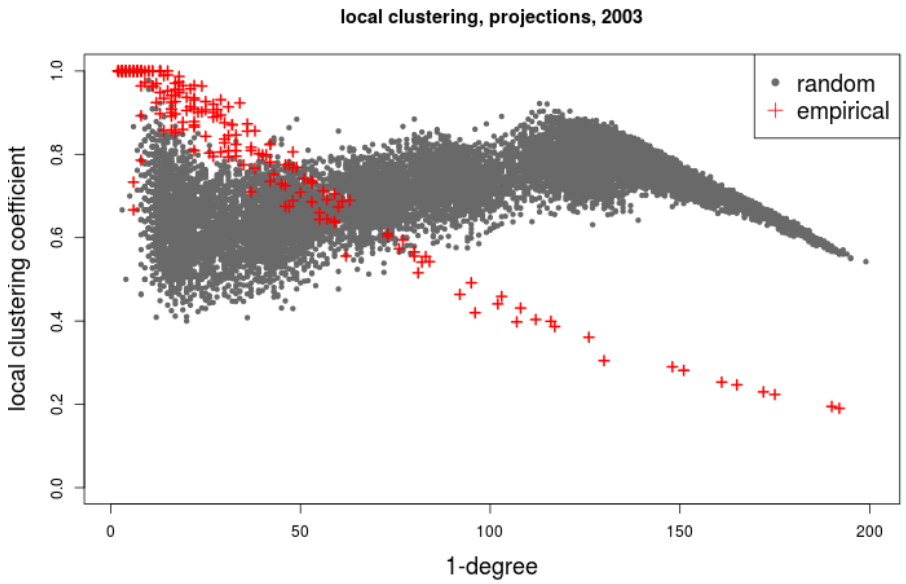

Fig. A.28 Random networks, year=2003: clustering in projections, banks.

A.5 Simulation results, year=2004

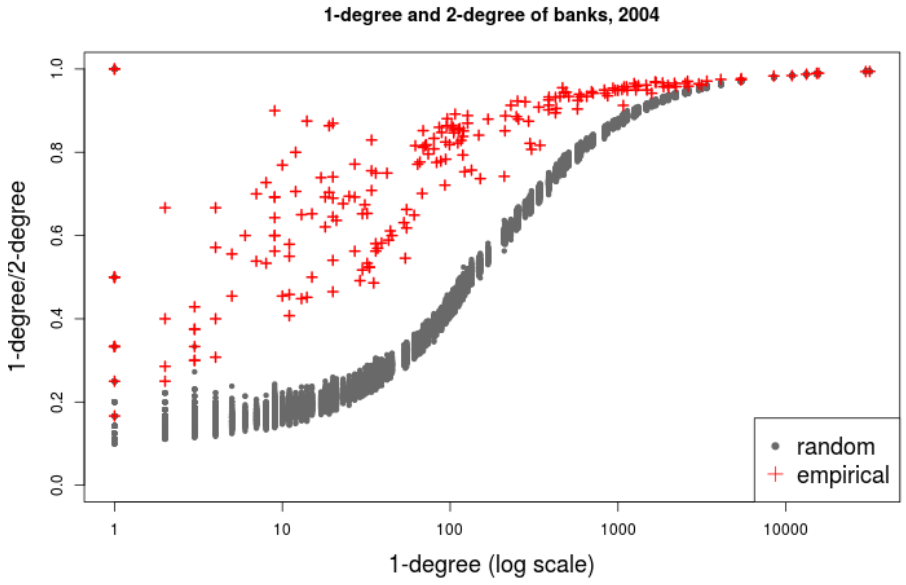

Fig. A.29 Random networks, year=2004: 1-degree and 2-degree, banks.

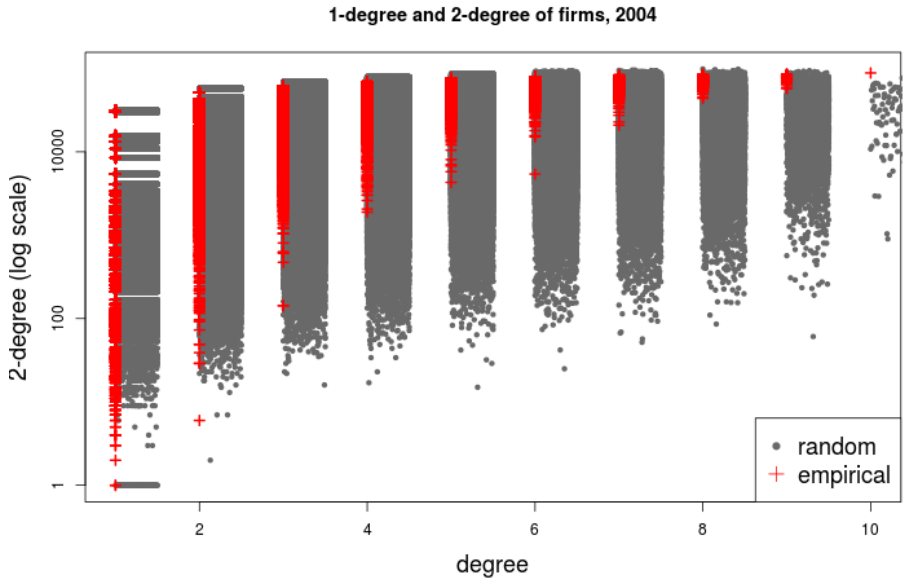

Fig. A.30 Random networks, year=2004: 1-degree and 2-degree, firms.

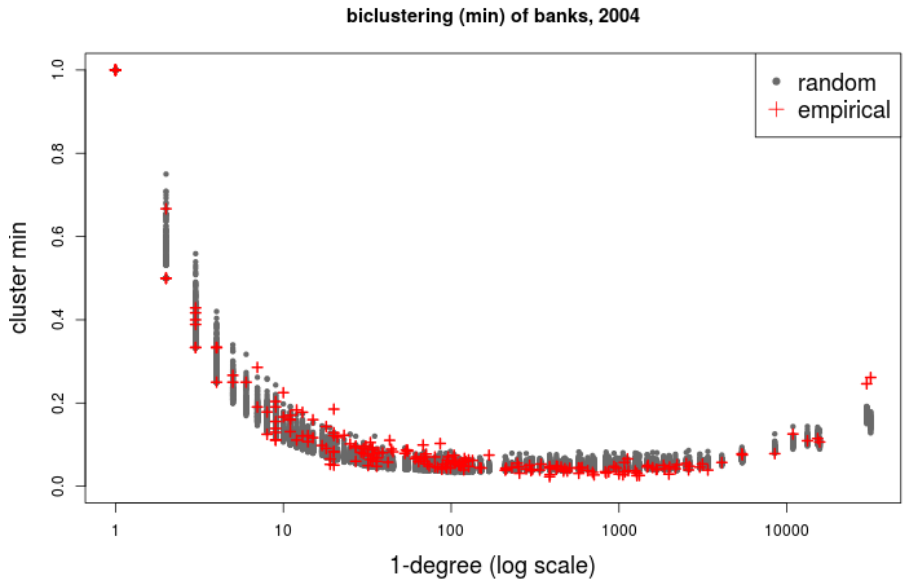

Fig. A.31 Random networks, year=2004: min clustering, banks.

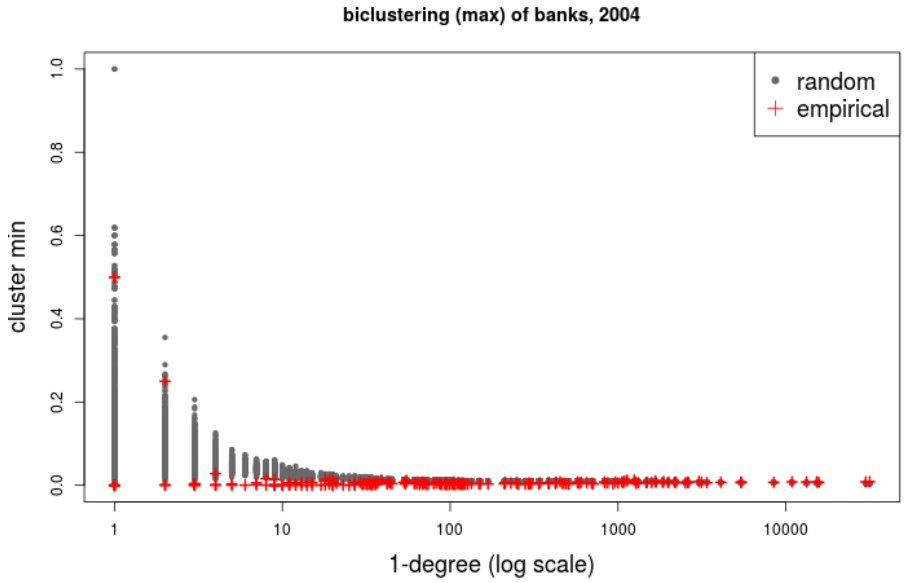

Fig. A.32 Random networks, year=2004: max clustering, banks.

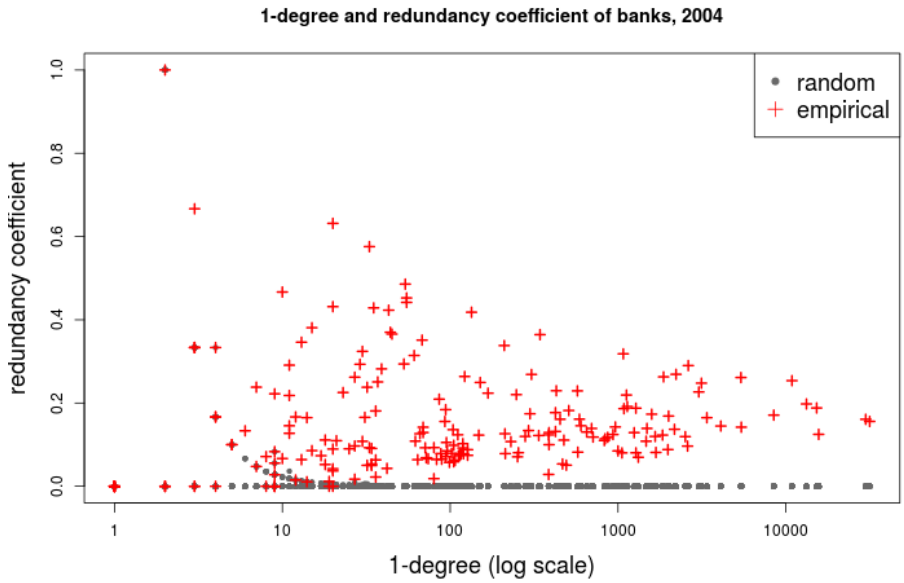

Fig. A.33 Random networks, year=2004: redundancy, banks.

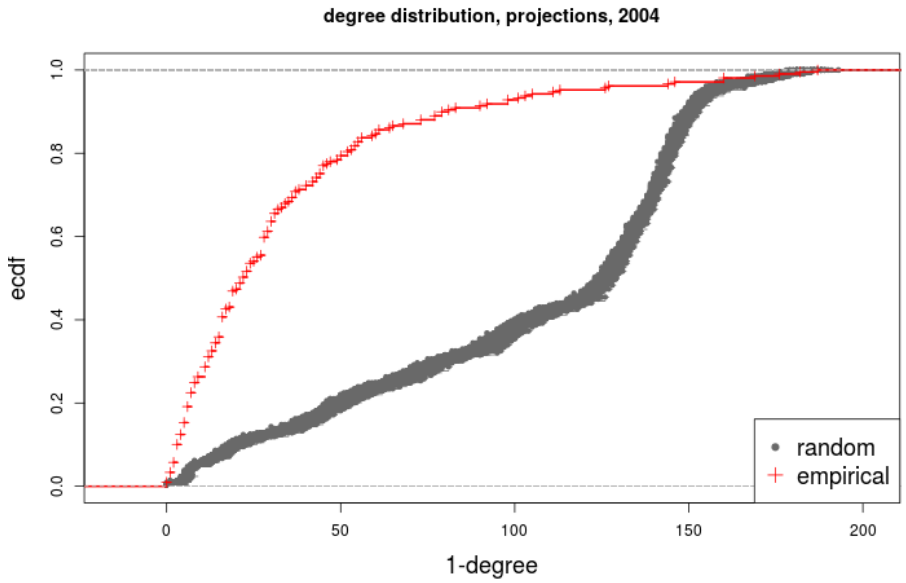

Fig. A.34 Random networks, year=2004: degree distribution of projections, banks.

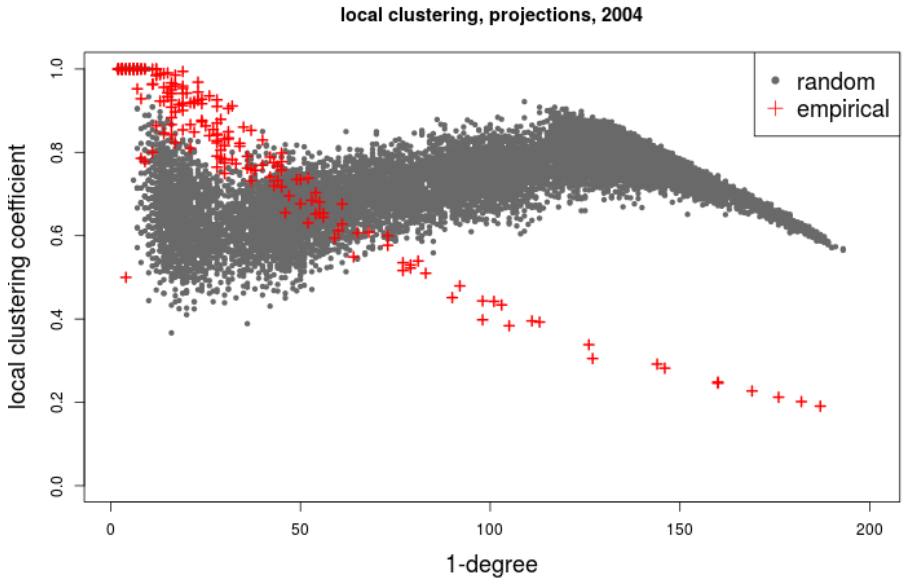

Fig. A.35 Random networks, year=2004: clustering in projections, banks.

A.6 Simulation results, year=2005

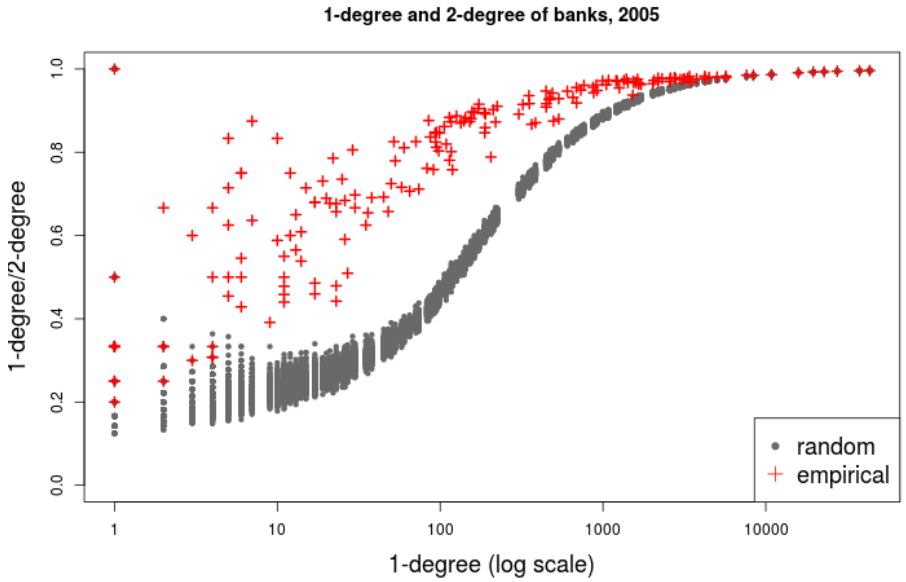

Fig. A.36 Random networks, year=2005: 1-degree and 2-degree, banks.

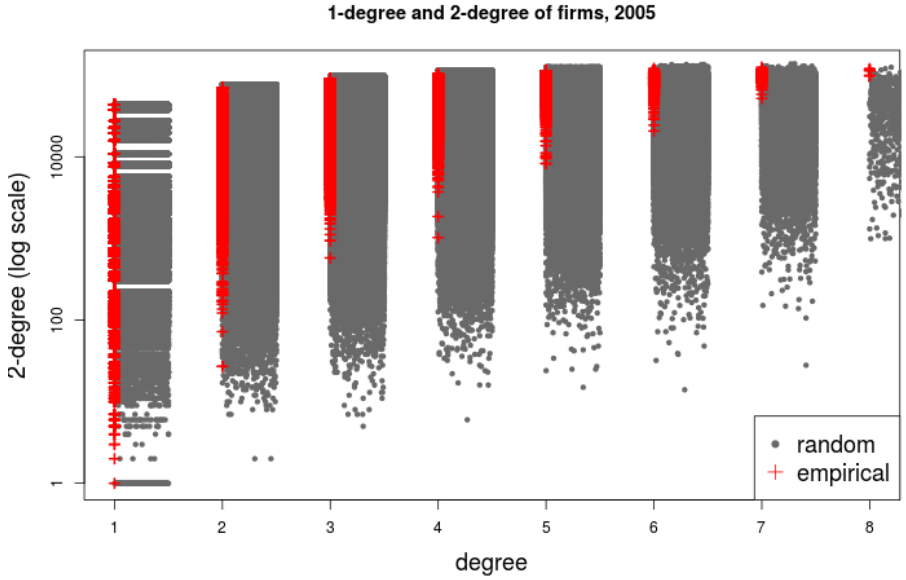

Fig. A.37 Random networks, year=2005: 1-degree and 2-degree, firms.

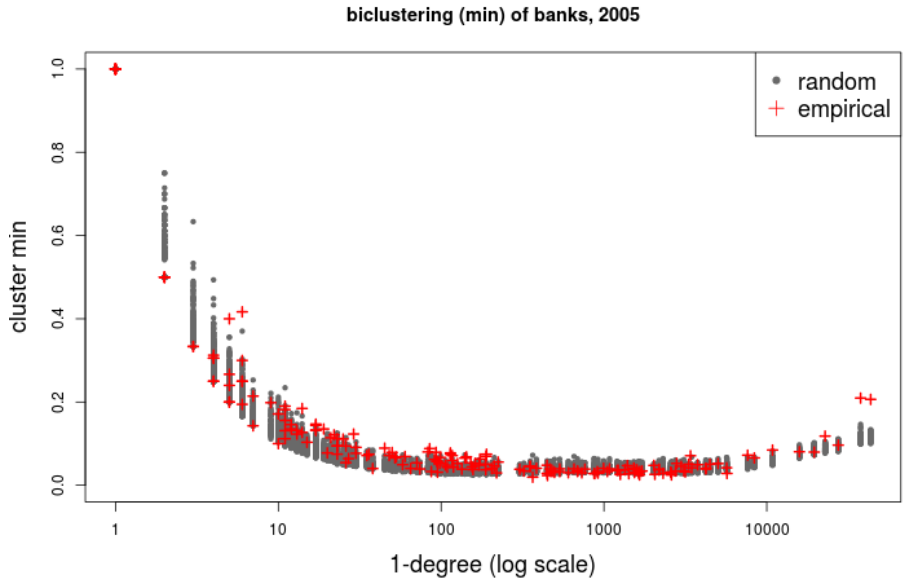

Fig. A.38 Random networks, year=2005: min clustering, banks.

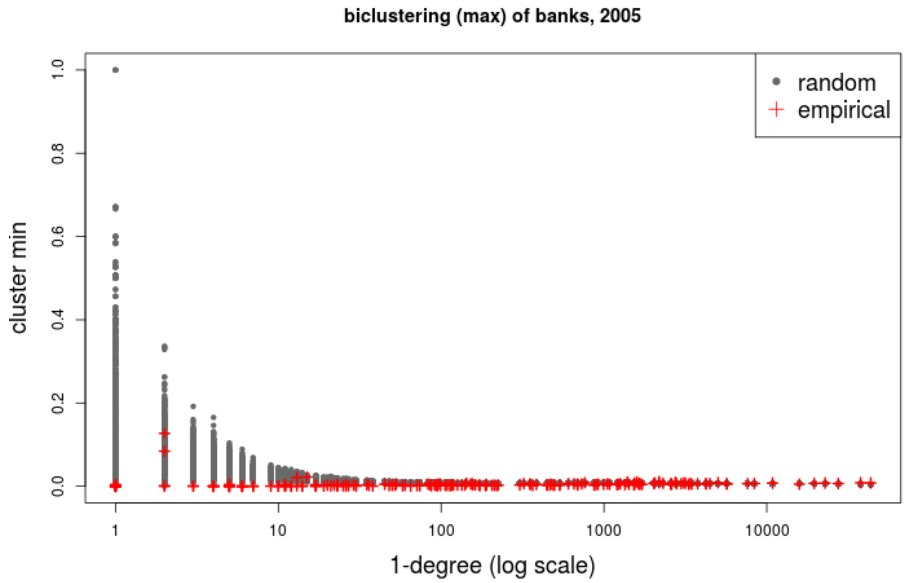

Fig. A.39 Random networks, year=2005: max clustering, banks.

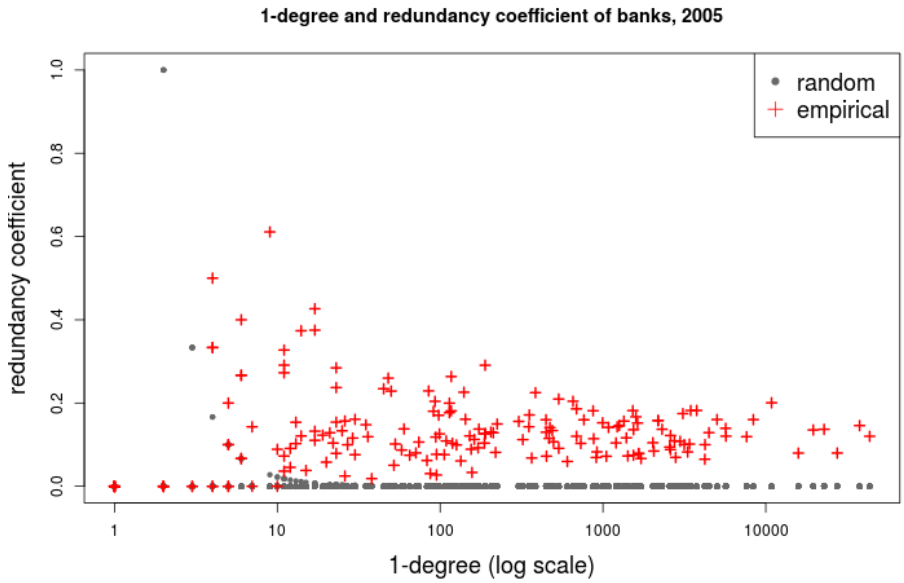

Fig. A.40 Random networks, year=2005: redundancy, banks.

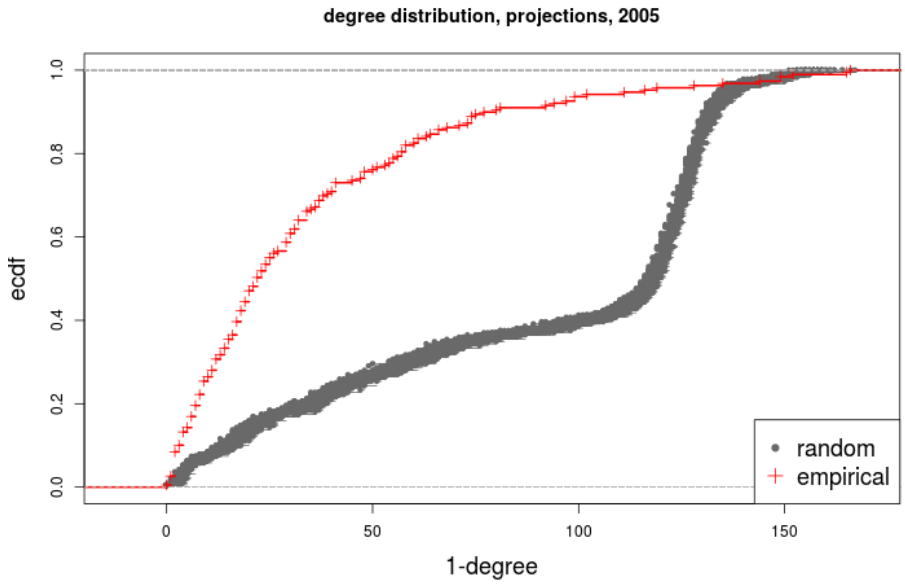

Fig. A.41 Random networks, year=2005: degree distribution of projections, banks.

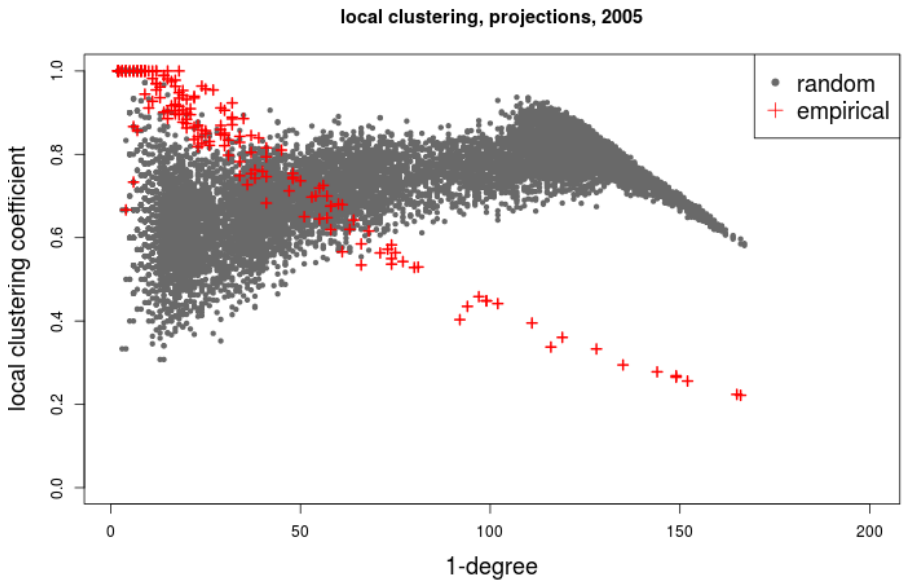

Fig. A.42 Random networks, year=2005: clustering in projections, banks.

A.7 Simulation results, year=2006

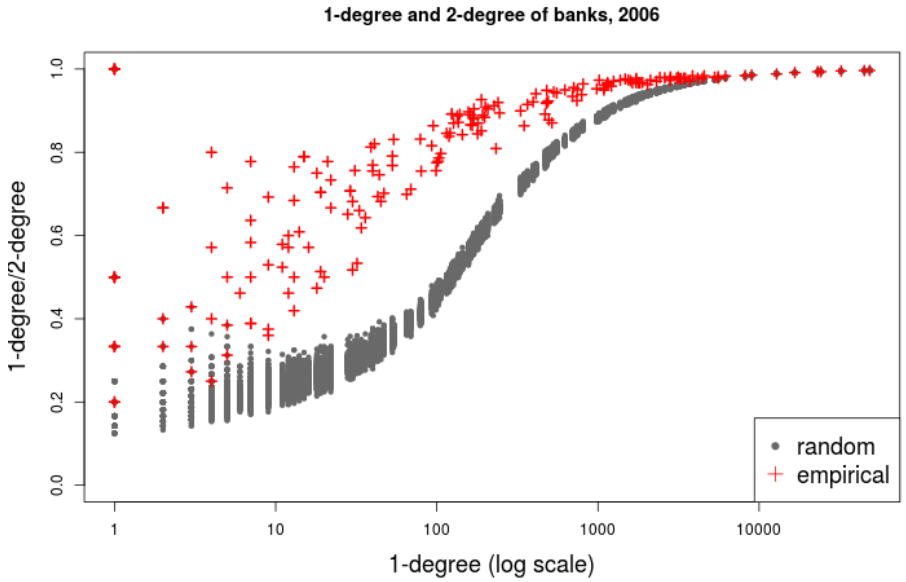

Fig. A.43 Random networks, year=2006: 1-degree and 2-degree, banks.

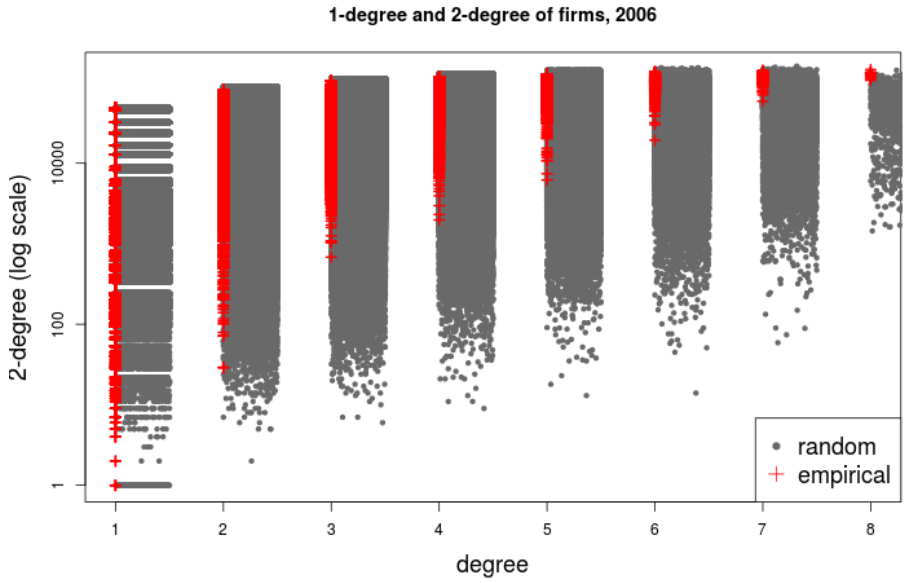

Fig. A.44 Random networks, year=2006: 1-degree and 2-degree, firms.

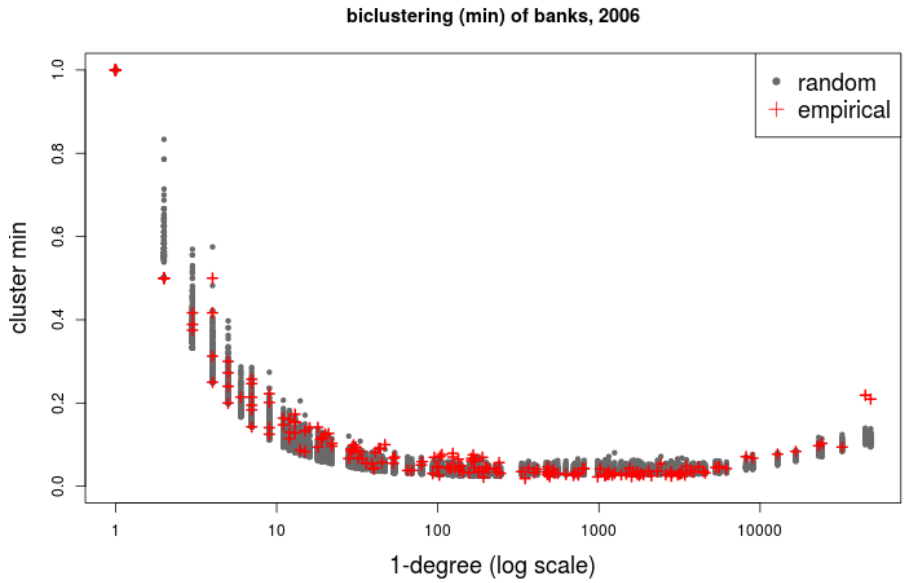

Fig. A.45 Random networks, year=2006: min clustering, banks.

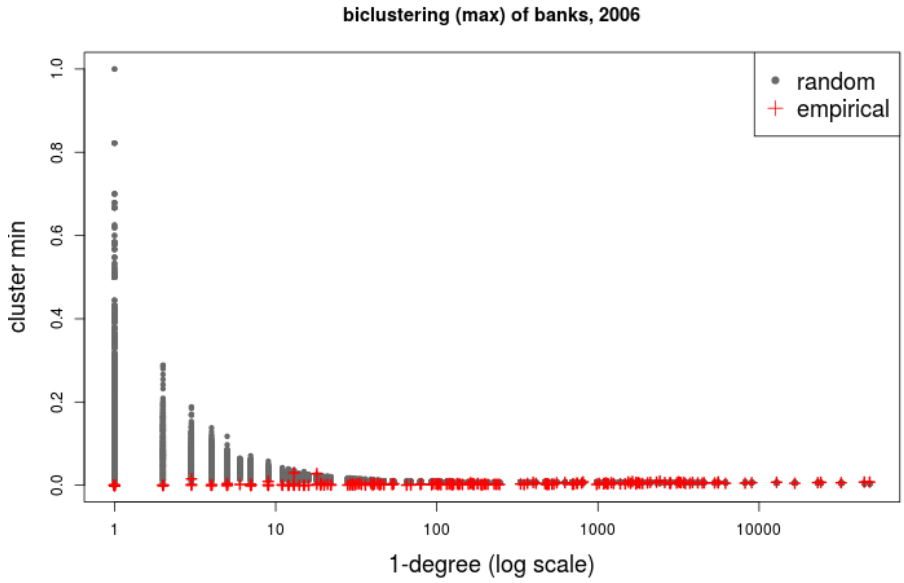

Fig. A.46 Random networks, year=2006: max clustering, banks.

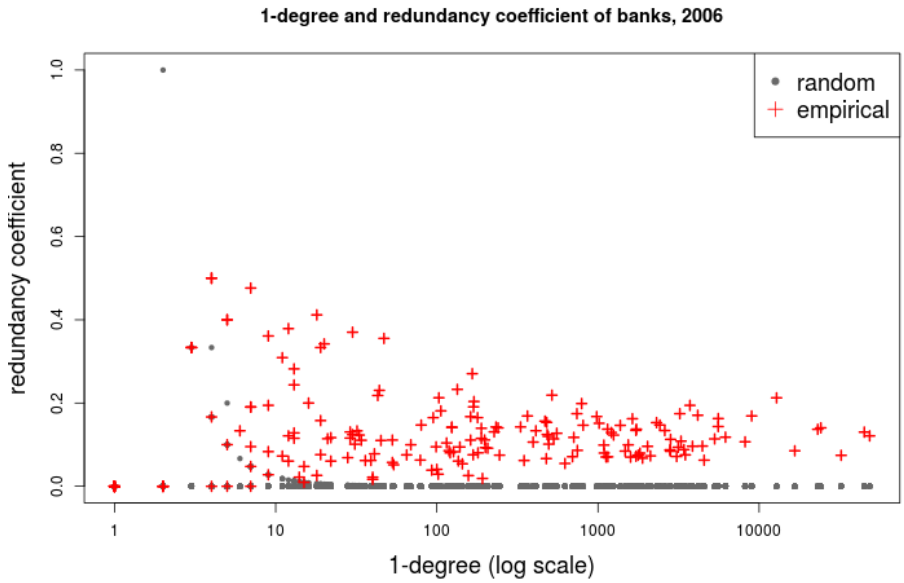

Fig. A.47 Random networks, year=2006: redundancy, banks.

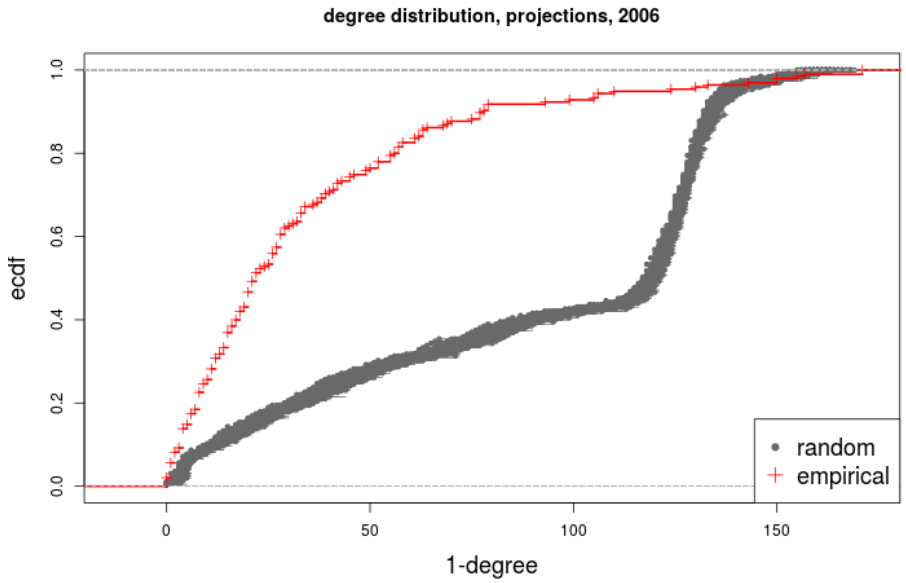

Fig. A.48 Random networks, year=2006: degree distribution of projections, banks.

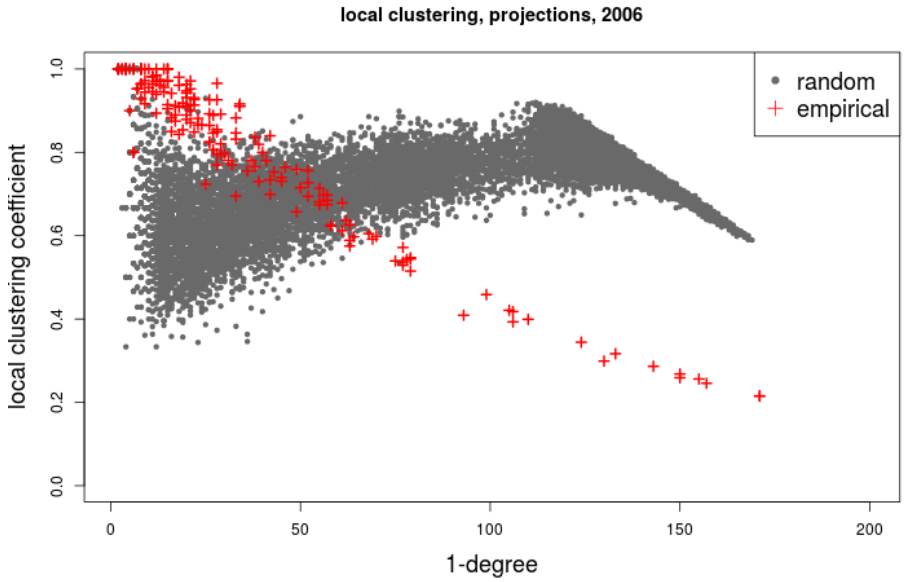

Fig. A.49 Random networks, year=2006: clustering in projections, banks.

A.8 Simulation results, year=2007

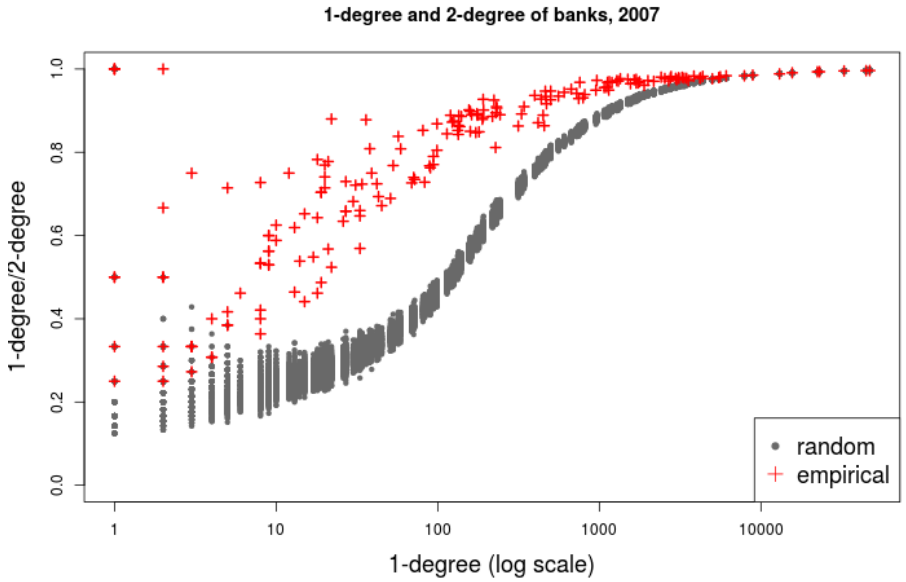

Fig. A.50 Random networks, year=2007: 1-degree and 2-degree, banks.

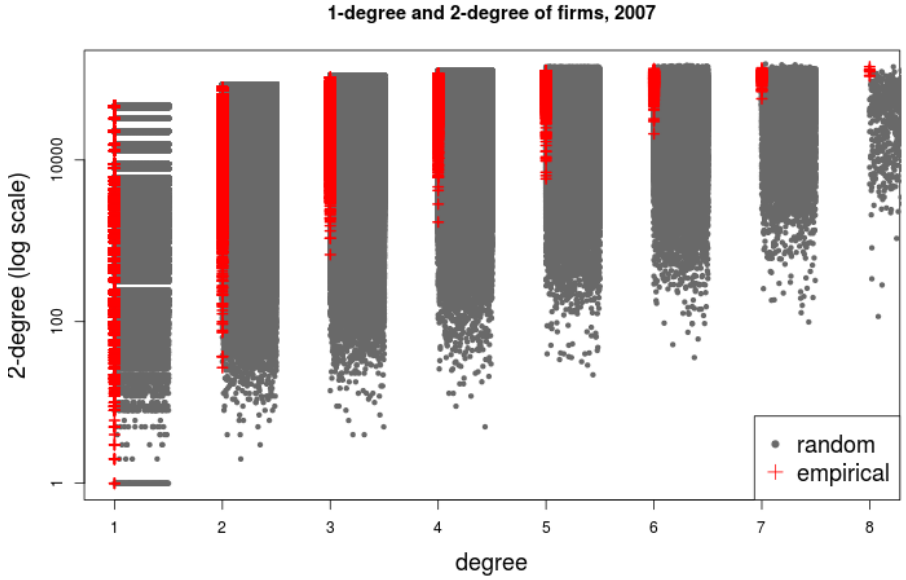

Fig. A.51 Random networks, year=2007: 1-degree and 2-degree, firms.

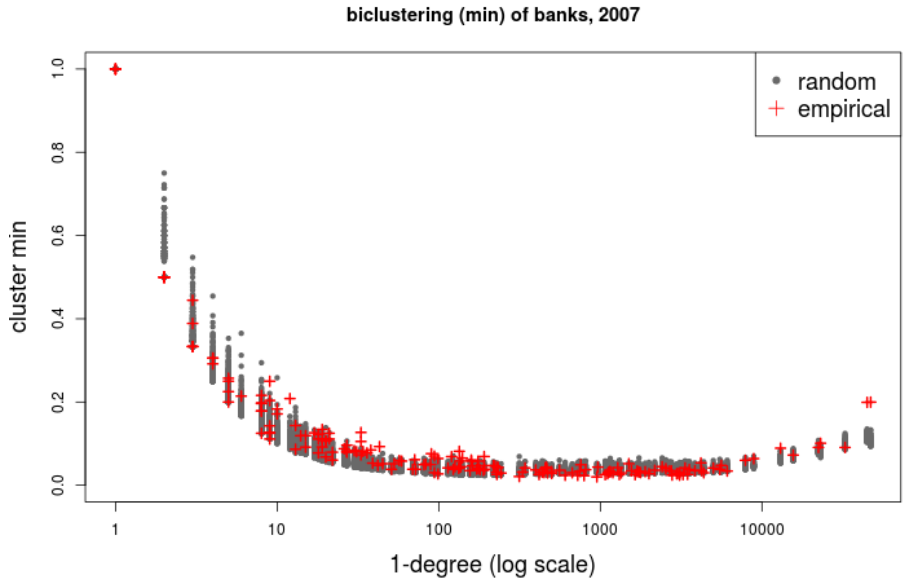

Fig. A.52 Random networks, year=2007: min clustering, banks.

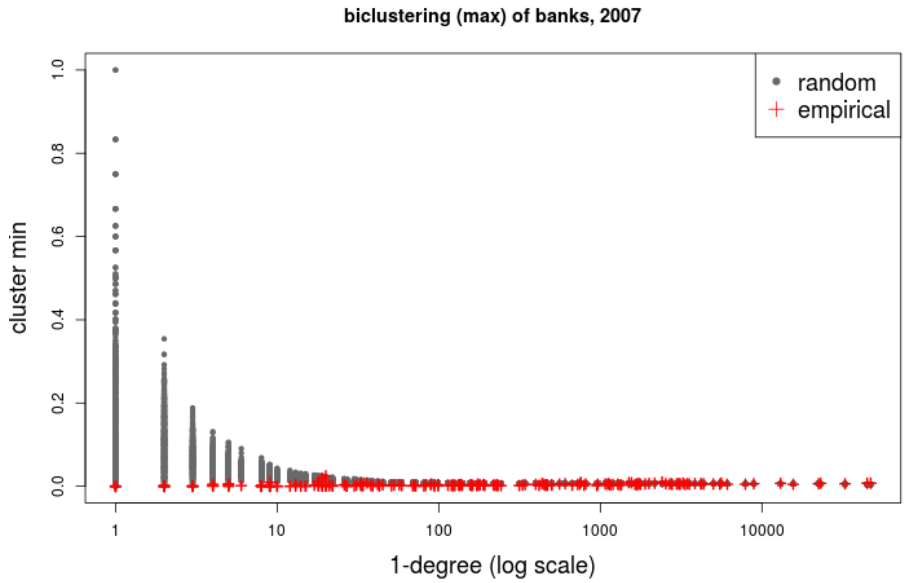

Fig. A.53 Random networks, year=2007: max clustering, banks.

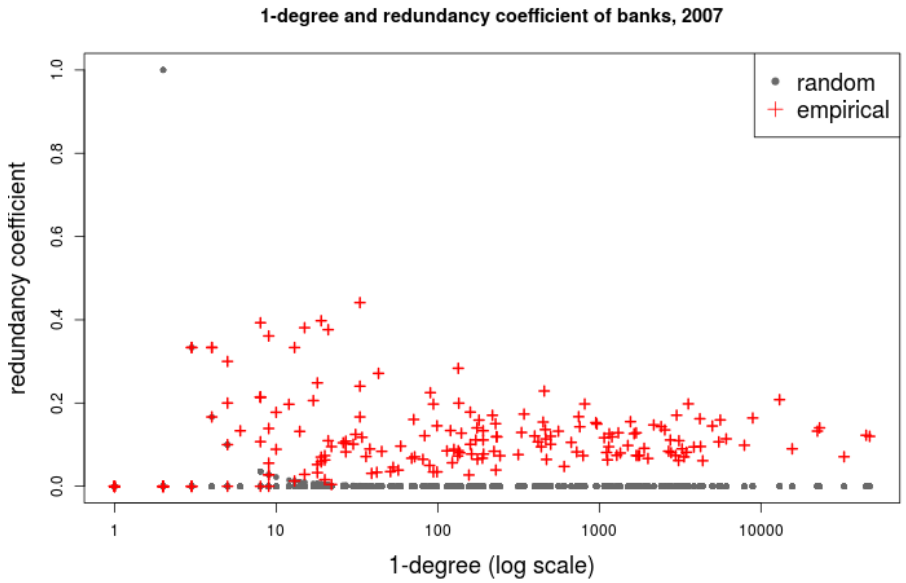

Fig. A.54 Random networks, year=2007: redundancy, banks.

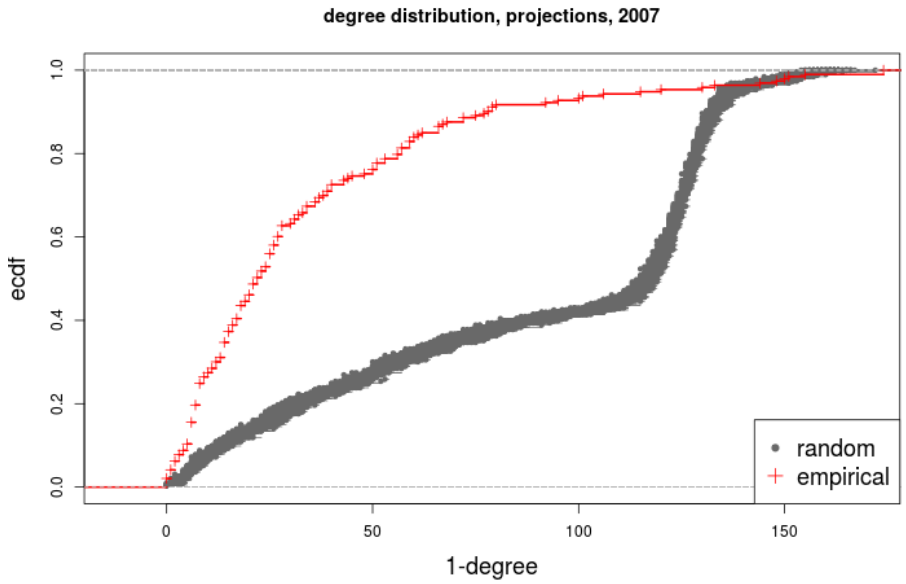

Fig. A.55 Random networks, year=2007: degree distribution of projections, banks.

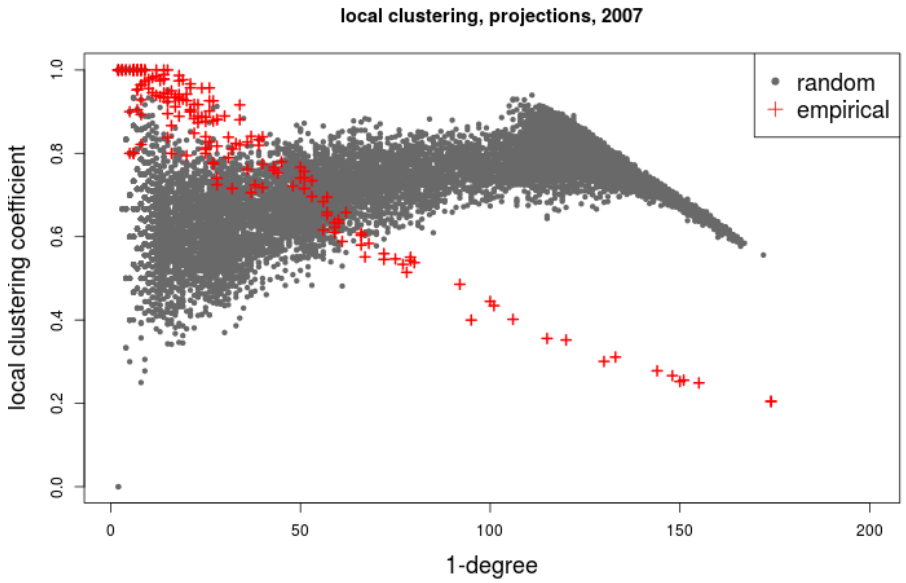

Fig. A.56 Random networks, year=2007: clustering in projections, banks.

Declaration

I hereby affirm that I have completed my doctoral thesis entitled, "Financial System Stability" entirely on my own and unassisted, and that I have specially marked all of the quotes I have used from other authors as well as these passages in my work that are extremely close to the thoughts presented by other authors, and listed the sources in accordance with the regulations I have been given.

Christian Freund

June 2017